FATIGUE IMPACTS ON HDPE PIPE MATERIAL PROPERTIES

by

MARJAN SHAHROKH ESFAHANI

Presented to the Faculty of the Graduate School of

The University of Texas at Arlington in Partial Fulfillment

of the Requirements

for the Degree of

DOCTOR OF PHILOSOPHY

THE UNIVERSITY OF TEXAS AT ARLINGTON

December 2017

Acknowledgements

First, I would like to express my sincere gratitude and appreciation to my Ph.D. advisor, Dr. Mohammad Najafi, for all his supports and guidance during my studies. I was blessed to have his recommendations and valuable knowledge which helped me to accomplish my research goals.

Special thanks to my supervising committee, Dr. Chien-Pai Han, Dr. Sharareh Kermanshachi and Dr. Nur Yazdani for their support and advice.

I would like to thanks Mr. Harvey Svetlik, P.E., Georg Fischer-Central Plastics for providing technical information and pipe samples used in this dissertation.

Thanks to the HTS Piping Company who helped me to make the samples and perform tensile tests, especially Mr. Eastwood, Ms. Khamla and Mr. Carnilo. Also thanks to Mr. David Yan from material science and engineering lab at UTA for helping me to perform SEM tests.

I would like to thank all of my friends and fellow students at the Department of Civil Engineering of UTA and CUIRE lab who assisted me during this project.

And, most importantly, I wish to express my special and warmest thanks to my dear family who have always supported me without any expectation.

November 8, 2017

Abstract

FATIGUE IMPACTS ON HDPE PIPE MATERIAL PROPERTIES

Marjan Shahrokh Esfahani, Ph.D.

The University of Texas at Arlington, 2017

Supervising Professor: Mohammad Najafi

During a pipe's life cycle, failures occur due to numerous factors such as age, loading conditions, environmental conditions, installation quality, manufacturing procedures, operation and maintenance strategies and so on. Frequent pressure surges or fluctuations in a piping system may cause a fatigue failure as fatigue is one of the most important issues in water pipes due to water hammer impacts. Application of buried high density polyethylene (HDPE) water pipelines has significantly increased in recent years, and PE4710 is a new member of HDPE family. So, there is not yet enough information about PE4710 long-term performance. Due to lack of enough information on resistance of large diameter HDPE pipes under transient pressures, this research focuses on post-fatigue mechanical properties of a large diameter DR 17 (16 in.) high density polyethylene (HDPE) 4710 pipe under cyclic loading. This work consists of two parts: First, experimental work which included the fatigue tests on an HDPE pipe sample for

2,000,000 cycles. Second, tensile tests on the dogbone specimens cut from the fatigue tested HDPE pipe and a new pipe sample from the same manufacturer were performed to compare material properties. Scanning Electron Microscopy (SEM) tests were done to visually show the impacts of fatigue on the molecular structure of the HDPE pipe. Finite Element Modeling (FEM) of tensile tests validated material properties and were used to investigate the effects of different stress amplitudes on the HDPE pipe. The findings of this experimental study showed that after two million cycles of internal water pressure of 125 psi to 188 psi, rupture strain and tensile strength of PE4710 increased about 15% and 2% respectively, while yield strain reduced by approximately 20%. The circumferential location of dogbone specimens from the pipe sample did not have any effects on the results, but longitudinal location of specimens had impacts on fatigue mechanical properties of samples. Sections near butt-fused joint showed more reduction in yield strain and less increase in tensile strength than end sections near the end supports. The SEM test results showed initiation of micro-cracks in longitudinal direction of the pipe. Using finite element analysis, a new equation using Stress Amplitude vs. No. of Cycles (S-N) curve for PE4710 was developed for PE4710. FEA results showed that current equations to predict fatigue life of PE4710 pipes may overestimate its fatigue life, but more numerical studies are required to confirm this conclusion.

List of Abbreviations and Acronyms

AC: Asbestos-cement

AO: Anti-Oxidant

ASCE: American Society of Civil Engineers

ASTM: American Society for Testing and Materials

AWWA: American Water Works Association

BCCP: Bar-wrapped Concrete Cylinder Pipe

BFP: Back Flow Pressure

CB: Control Board

CIP: Cast Iron Pipe

CP: Concrete Pipe

CTOD: Crack Tip Opening Displacement

CUIRE: Center for Underground Infrastructure Research and Engineering

DI: Ductile Iron

DIP: Ductile Iron Pipe

DR: Dimension Ratio

EPFM: Elastic Plastic Fracture Mechanics

ESCR: Environmental Stress Cracking Resistance

FC: Fiber Cement

FEM: Finite Element Modeling

FRP: Fiber Reinforced Plastic

HCF: High Cycle Fatigue

HDPE: High Density Polyethylene

HP: Horsepower

ICI: Imperial Chemical Company

ISO: International Organization for Standardization

LCB: Long Chain Branching

LCF: Low Cycle Fatigue

LDPE: Low Density Polyethylene

LEFM: Linear Elastic Fracture Mechanics

LLDPE: Linear Low Density Polyethylene

MDPE: Medium Density Polyethylene

MW: Molecular Weight

MWD: Molecular Weight Distribution

PC: Pressure Class

PCCP: Pre-stressed Concrete Cylinder

PE: Polyethylene

PPI: Plastic Pipe Institute

PVC: Polyvinyl Chloride

RCP: Reinforced Concrete Pipe

SCB: Short Chain Branching

SCG: Slow Crack Growth

SEM: Scanning Electron Microscopy

SP: Steel Pipe

TMF: Thermal Mechanical Fatigue

VCP: Vitrified Clay Pipe

WRF: Water Research Foundation

List of Definitions

C3D8: A three dimensional element with 8 nodes.

Charpy: A standardized high strain rate test which defines the amount of energy absorption by the material during the fracture process.

Cold Drawing: A phenomenon happens when a thermoplastic polymer is subjected to a continuous stress above its yield point.

PC or Pressure Class: Maximum anticipated, sustained operating pressure applied to the pipe exclusive of transient pressures.

Reptation: Thermal motion of a long linear entangled macro-molecule in polymer melt.

S-N Curve: Graph of magnitudes of stresses (S) vs. the logarithmic scale of cycles to failure (N) for a given material.

USDFLD: A subroutine in ABAQUS to define the values of field variables directly at the integration points of elements. The field variable values can be functions of element variables such as stress or strain.

Table of Contents

List of Illustrations

List of Tables

Chapter 1 INTRODUCTION

HISTORY OF WATER DISTRIBUTION

The main objective of any municipality and water utility is efficient and cost-effective delivery of high quality and hygienic water to the public. Every water distribution network includes pumps, pipes, junctions, tanks, reservoirs, and valves. For water delivery, pumps and gravity systems are used to convey water from a reservoir by a group of pipelines. According to Austin (2011), pipe a network is designed to deliver sufficient quality water under a desirable pressure.

According to Clark (2012), water usage is classified as:

- Domestic or Urban
- Agricultural
- Industrial

The primary task of municipal water distribution systems is to provide water to residential, industrial, and commercial areas. While the delivered water must be drinkable, it is also used for other purposes such as toilet flushing, showering, landscaping or industrial usages. Drinking water must be certified based on the standard for drinking water system components – health effects, NSF International Standard/American National Standard (NSF/ANSI 61 standard) (Austin; 2011).

Early civilizations were built near the rivers such as Sindhu, Tigris and Euphrates, Yellow and Nile which indicates the knowledge of water distribution system has a long history (Cech; 2005). Use of ceramic pipes to distribute water from the ruins of Harappa and Mohenjo-daro was confirmed by archaeologists (Bhave and Gupta; 2006). During the 6th century B.C., Ephesus in Anatolia or Asia Minor (currently located in Turkey) was reestablished by the Romans (Cech; 2005). “Water for the Great Fountain

was diverted from a dam at Marnss and conveyed to the city by a 3.75-mile system consisting of one large and two smaller clay pipelines" (Mays; 2000).

The first city to operate a functional water supply system in the United States was in 1795 in Boston. Wooden pipes made from a tree trunk used to convey water from Jamaica Pond to Boston by a private water supplier (Wallace, Floyd Associates; 1984). The Moravian community of Bethlehem, Pennsylvania, installed bore logs to draw water from their water source during 1652. The water was delivered by a network of pipes built on bored logs which provided service to the entire community of Bethlehem by 1754. Horse-driven pumps were used to pump water from a spring (Mays; 2000). In 1817 the first cast iron pipe was used to deliver water to citizens of Philadelphia (Bhave and Gupta; 2006).

BACKGROUND OF PIPELINE SYSTEMS

"Water is the basis of life on earth and the foundation of all civilizations" (Cech; 2005). Pipeline makes water available to use. Pipelines have a long history. Pipes were used in ancient times till now. They have been modified extensively to be more efficient in the modern era. The Egyptians used clay pipes for drainage system in 4000 B.C. The Romans used lead pipes in aqueduct system during 400 B.C., (Liu; 2003). During the 18th century, a breakthrough occurred in pipeline technology with invention of the cast iron pipe. Cast iron pipes dominated water pipe materials until the 19th century when steel pipes were invented. Steel pipes gained popularity because of their increased wall strength.

According to Liu (2003), comparing to roads, railways and air transportation, pipes are the most neglected and least appreciated means of transportation because of being buried underground. Pipeline infrastructure in general and water pipes specifically play an important role in the economy and security of each nation.

The majority of pipelines are laid to convey fluids or gases such as water, sewage, natural gas, crude oil, gasoline, jet fuel, etc., from treatment plants and refineries to residential and commercial buildings in various distances (Liu; 2003).

CLASSIFICATION OF PIPES

Table 1-1 presents a summary of classifications of pipes according to Mays (2000). Pipes can be classified based on:

- The nature of applications (commodity transported in pipeline like gas, water or sewage).
- Environment of applications (offshore, inland or mountain pipelines).
- Burial or support's type (underground, elevated or underwater).

Material's type (cast iron pipe (CIP), Polyvinyl Chloride (PVC), High Density Polyethylene （HDPE), steel pipe (SP), ductile iron pipe (DIP), vitrified clay pipe (VCP) or concrete pipe (CP)).

According to Najafi (2010), pipes can be classified as semi-rigid, semi-flexible or intermediate. Intermediate are a type of pipe, which share partial characteristic of two other types. Table 1-2 presents pipe materials classifications as rigid or flexible. Rigid pipes are resistant to bending in both longitudinal and circumferential directions and they do not have deformation under the load. Flexible pipes are capable of deforming without any damage to the pipe. According to Najafi (2010), flexible pipes are capable of being deformed more than 2 percent of their diameter size without failure. Strength and stiffness are used to characterize properties of pipes as rigid and flexible.

Table 1-1 Classifications of Pipelines based on Application, Mays (2000)

Classifications	Applications
Commodity Transported	Water, Sewer, Natural Gas, Oil, Product, Solid Pipelines
Environment	Offshore, Inland, In-plant, Mountain, Space Pipeline
Type of Burial or Support	Underground, Elevated, Aboveground, Underwater
Pipe Material	Steel, Cast-iron, Ductile Iron, Plastic (PVC, HDPE, etc.), Concrete, Others (Clay, PCP)

Table 1-2 Classification of Pipes based on Material, Najafi (2010)

Rigid Pipes	Flexible Pipes
Concrete (CP)	Steel (SP)
Vitrified Clay (VCP)	Ductile Iron (DIP)
Pre-stressed Concrete Cylinder (PCCP)	Polyvinyl Chloride (PVC)
Reinforced Concrete (RCP)	High Density Polyethylene (HDPE)
Bar-wrapped Concrete Cylinder (BCCP)	Fiber Reinforced Plastic (FRP)
Asbestos-cement (AC)	-
Fiber Cement (FC)	-

Table 1-3 presents classification of pipes based on being metallic or nonmetallic. Metallic (or mixture of metals) pipes are conductive and classified as metallic pipes. If materials other than metals are used to manufacturing pipes, such as concrete or plastics, pipes are non-conductive and classified as non-metallic pipes (Mays; 2000 and Liu; 2002).

Table 1-3 Classification of Pipes based on Metallic and Non-Metallic, Liu (2002)

Metallic Pipes	Non-metallic Pipes
Steel Pipe, Cast-iron Pipe, Ductile Iron Pipe, Stainless Steel Pipes, Copper Pipe	Concrete Pipe (PCCP, RCCP), Plastic Pipe (PVC, PE), Vitrified Clay Pipe, Asbestos-Cement Pipe

Polyethylene discovery was in 1933, and manufacturing of these pipes was during the 1940s (Storm and Rasmussen; 2011), but the application of HDPE pipes in the water distribution was approved by AWWA in 1980 and installation of HDPE pipes started the same year (Frank et al.; 2009).

POLYETHYLENE PIPES

Usage of High Density Polyethylene (HDPE) pipe for conveying and distributing gas and water is significantly increased recently. The HDPE water pipes, like any other pipe, are subjected to internal and external pressures as well as processes of deterioration such as creep, fatigue damage and crack growth (Divyashree; 2014). Despite of their durable structure, the pipe design and analysis should consider their working conditions, such as cyclic loading to the pipe (fluctuations in internal pressure) with a considerable stress ratio; and accumulation of energy in the water under pressure, which manifests in the form of elastic strain energy (Cheng; 2008). This accumulated energy initiates and develops crack growth in various ways, such as brittle, semi-brittle and ductile failures; and defects during manufacturing process and installation. “Stress cracking” is almost the most dangerous failure that may occur in a pipe (Cheng; 2008). Polyethylene pipes are capable of resisting static loading as well as periodic and cyclic loading. The periodic and cyclic loadings have constant, random or intermittent frequencies and can be cause material creep. Therefore, fatigue strength is an important parameter in the design process. Additionally, Divyashree et al. (2015) stated that fatigue testing of a large diameter HDPE pipe was ranked with high priority during the WRF’s project workshops with water utilities and other pipe professionals.

Fatigue is a phenomenon which occurs in structures subjected to time-dependent loading and deteriorates material ability to withstand applied loads that are below the

elastic limit. Experimental observations by Pugno et al. (2006), Molent et al. (2006) and Schijve et al. (2005) indicated that at low stress levels (high-cycle fatigue), a considerable percentage of the usable fatigue life is consumed by the crack initiation period, while at high stress levels (low-cycle fatigue), fatigue cracks initiate in the early cycles.

According to Zhou et al. (1996) plastic pipes used for gas and water distribution are increasingly the subject of many studies that emphasize different behavior aspects of service lifetime. In order to develop engineering and lifetime design, many tests such as fatigue, creep and environmental stress cracking (ESC) are performed although this information is not still sufficient in the literature (Li and Qi; 2014). The purpose of dynamic fatigue tests is to specify the endurance limit of polyethylene resins subjected to periodic loading, quantitatively. The endurance limit is the maximum stress amplitude which can be supported for an infinite number of cycles without failure of specimen (Li and Qi; 2014). Loading type and pattern differentiate long-term fatigue testing methods. Graphs of magnitudes of stresses (S) vs. the logarithmic scale of cycles to failure (N) (S-N curves) are the most useful and common method to describe the fatigue behavior, for practical use and design (Kawai and Itoh; 2014).

Analysis of history of crack growth shows when crack initiates, there is a log-linear relationship between the crack size and the lifetime. Also, when plotted in a log–log scale, a linear relationship exists between the crack growth rate and the crack length or the stress intensity factor range in mode I (ΔK_I).

In the literature, many studies are performed on fatigue crack growth. Pinter et al. (2006), Favier et al (2002) and Ward et al. (1990) performed accelerated fatigue tests on circumferentially notched HDPE bars. A comparative study on crack propagation in HDPE under fatigue and creep loading is presented by Kasakevich et al. (1990). Their study is focused on the interaction between creep and fatigue and discusses the validity

of fatigue as an accelerated laboratory test for long-term field failure under creep conditions.

According to Parsons et al. (2000), the correlation between creep and fatigue strengths indicated that creep resistance of Medium Density Polyethylene (MDPE) was much more than HDPE and HDPE pipes were much less sensitive to strain rate in fatigue. Reynolds et al. (1993) studied the mechanisms of failure for externally notched sections of polyethylene pipe under pressure. They confirmed that localized shear deformation is origin of branching fracture features.

Kiass et al. (2005) conducted an experimental investigation to establish the distribution of mechanical properties throughout a HDPE gas pipe wall. The mechanical properties varied within the pipe wall which indicates the complexity of hierarchical structure in HDPE. This approach contributed in understanding of the long-term behavior of pipe and associated brittle failure.

Majority of studies on fatigue of HDPE consider the crack propagation and assume that stress concentration and crack already occurred. But in most parts of pipes fatigue may occur without any previously initiated crack. In this case, fatigue generates accumulated damage in material, which leads either to nucleation of crack or to large deformation, dependent on the level of stress. In fact, the total lifetime of pipe would be the sum of damage and propagation stages (Lin and Argon; 1994). Fatigue damage represents more than 90% of the overall fatigue lifetime of pipe in many cases (Khelif et al.; 2008). When stress variation is moderate or low, the crack propagation time is much less than the damage time (Khelif et al.; 2008).

In searching the literature, no experimental work was found for HDPE after-fatigue analysis to evaluate the fatigue damage on HDPE material. Material property after fatigue was recommended by industry professional and utilities during a workshop for a

Water Research Foundation project (Divyashree et al.; 2015). In this dissertation, the main focus is on the experimental study of after-fatigue analysis of HDPE pipe's material as well as a numerical study on the effect of stress amplitude on the number of cycles that PE4710 pipes can withstand before failure.

Background of HDPE

Because of higher hydrostatic design stress, advanced PE4710 is utilized in water pipe applications with the following designation codes:

- Base resin density – 1st digit in the code
- Slow crack growth (SCG) – 2nd digit in the code
- Hydrostatic design stress (HDS) – 3rd and 4th digits in the code (Divyashree; 2014)

According to ASTM standard specification D 3350, the pipe material designation codes for other PE materials are (Divyashree; 2014):

1. PE 3408 is a polyethylene (the PE abbreviation is according to ASTM D1600) with a density cell class of 3 and a slow crack growth (SCG) cell class of 4 (according to ASTM D3350). It has an 800 psi maximum recommended Hydrostatic Design Stress (HDS) for water at 73°F (23°C).
2. PE 3608 is a polyethylene (the PE abbreviation is according to ASTM D1600) with a density cell class of 3 and a slow crack growth (SCG) cell class of 6 （according to ASTM D3350). It has an 800 psi maximum recommended Hydrostatic Design Stress (HDS) for water at 73°F (23°C).
3. PE 4710 is a polyethylene (the PE abbreviation is according to ASTM D1600) with a density cell class of 4 and a slow crack growth (SCG) cell class of 7 (according to ASTM D3350). It has a 1000 psi maximum recommended

Hydrostatic Design Stress (HDS) for water at 73°F (23°C).

Table 1-4 summarizes the differences between PE3408, PE3608 and PE4710.

Table 1-4 Differences Between PE3408, PE3608 and PE4710, Divyashree (2014)

<table>
<tr><th colspan="2">PE 3408 and PE 3608</th><th>PE4710</th></tr>
<tr><td colspan="2">The resin is classifies as class 3.</td><td>The resin is classifies as class 4.</td></tr>
<tr><td colspan="2">Base resin density of PE3408 is 0.941 – 0.947 g/cc</td><td>Base resin density of PE3408 is 0.947 – 0.955 g/cc</td></tr>
<tr><td>The slow crack growth for Class 4 is at least 10 hours</td><td>The slow crack growth for Class 6 is at least 100 hours</td><td>The slow crack growth for Class 7 is at least 500 hours</td></tr>
<tr><td colspan="2">Hydrostatic design stress (HDS) is 800 psi</td><td>Hydrostatic design stress (HDS) is 1000 psi</td></tr>
<tr><td colspan="2">Pressure Class for PE3408 and PE3608 is lower for specified DR. The flow capacity is less.</td><td>Pressure Class is higher for specified DR when compared to PE3408 & PE3608. The flow capacity increases.</td></tr>
</table>

RESEARCH OBJECTIVES

The objectives of this dissertation are:

- To evaluate the impact of fatigue on mechanical properties of PE4710 pipe material.
- To develop a new equation for stresses (S) vs. the logarithmic scale of cycles to failure (N) (S-N curves) of PE4710.

The ultimate objective of this dissertation is to have a better understanding of fatigue life of HDPE water pipelines. Using the S-N curve developed with this dissertation, fatigue life of PE4710 pipes can be estimated more accurately.

RESEARCH NEEDS

According to “Report Card from America’s Drinking Water Infrastructure” (ASCE, 2017), there is approximately 240,000 water main breaks per year in the United States due to the poor conditions of the U.S. infrastructure. Water utilities in the United States

lose 40 billion liters out of 160 billion liters (10.5 billion gallons out of 42.3 billion gallons) of processed water everyday due to leaks and breaks (Divyashree; 2014). Approximately $1.2 billion was spent on water rehabilitation in the U.S. in 2006 (Najafi; 2013) and this cost could reach to more than $1 trillion during the next decades (AWWA, 2013). Also, according to ASCE (2013), the existing drinking water pipeline is near the end of its useful life.

The most critical elements of a water supply system are large diameter transmission mains. If a failure occurs, in addition to extended service interruptions and property damages, it causes disruption to the social life. Replacement of deteriorated large diameter water pipelines may be necessary since due to capacity concerns and structural integrity of large diameter pipes, rehabilitation by relining of a deteriorated water main may not be feasible. High density polyethylene (HDPE) pipes with high flexibility and durability, large diameter (16-in. and larger), thick walls (with lower DRs) are manufactured recently taking advantages of development in polymer science (Divyashree; 2014). Since PE4710 is relatively a new material, studies are required to assess the suitability of current design approaches (Jana; 2012, Divyashree; 2014).

According to PPI (2012), development of additional cyclic fatigue data provides justification for increasing the allowable repetitive surge pressures and provides additional experimental support of the design approach. Also, four workshops and a survey were conducted by Divyashree et al. (2015) at the Center for Underground Infrastructure Research and Education (CUIRE) and results of a utility survey showed, as of 2013, 63% of PE4710 pipes in use are less than 5 years old. In the survey, water utilities suggested fatigue testing on 16 in. or larger diameter HDPE pipe since no testing was performed prior to that, also they recommended the fatigue-tested piece should be tested for material properties and compared with material testing of a new identical pipe.

In addition, since infrastructure projects, including pipelines, are usually designed using limit-state-design procedure due to the potential of this method for a safer and lower cost design (Zhang and Moore, 1997), a clear understanding of serviceability, stability, performance limitations and durability of HDPE pipe is required for limit-state-design method. But there are still many difficulties related to time dependent properties of HDPE, as well as impact of its loading history which means there is a gap in information and research studies about the non-linear time dependent behavior of HDPE pipes. Predictability of performance of a pipe in service requires knowledge of the mechanical properties of the HDPE resin and knowledge of the profile geometry (Gabriel, 2016) but there is not enough information about impact of fatigue on HDPE mechanical properties and profile geometry. This dissertation focuses on the after fatigue mechanical properties of HDPE pipes, as one of the main concerns of water utilities, as well as the effect of stress amplitude on the number of cycles the pipe can withstand (S-N curve) of PE4710.

CONTRIBUTIONS TO THE BODY OF KNOWLEDGE

The followings are the main contributions of this research:

1. Providing an estimation of the amount of degradation of material properties of PE4710 pipe due to cyclic internal water pressure of 1.5 time of its pressure class.
2. Developing a new equation for S-N curve of PE4710.

Both above mentioned findings will contribute to predict more accurate design life of HDPE water pipes.

SCOPE

The scope of this research includes experimental study on mechanical properties of HDPE specimens cut from a pipe sample after successfully passing two million cycles of internal water pressure ranges between 125 psi (pressure class) to 188 psi (1.5 times

pressure class). The same pipe sample went through additional 50,000 cycles of twice its pressure class. AWWA C906 defines working pressure as "the maximum anticipated, sustained operating pressure applied to the pipe exclusive of transient pressures." Experimental part of this dissertation includes:

1. Tensile test on 6 new HDPE dogbone specimens.
2. Tensile tests on 32 HDPE dogbone specimens cut from fatigue-tested pipe.
3. Scanning Electron Microscopy (SEM) test on new and fatigue-tested specimens.

The numerical part of this dissertation includes applying different cyclic loadings to a 15-ft long HDPE pipe to check the effects of stress amplitude on the number of cycles that pipe can withstand before failure and develop a new S-N curve.

METHODOLOGY

To achieve the objectives of this research, in addition to a comprehensive literature review, a testing concept was developed to determine the performance of a PE4710 pipe sample with recurring surges for two million cycles ranging between 125 psi and 188 psi (1.5 times Pressure Class, PC) for a 16-in., 15-ft long, DR 17, HDPE pipe. After successfully passing two million cycles of internal water pressure, dogbone shaped specimens were cut from fatigue-tested pipe. Tensile tests based on ASTM D638 were conducted on dogbone shaped specimens to perform fracture analysis of HDPE samples and to experimentally evaluate the impact of fatigue on HDPE pipes. In addition to tensile experiment, a corresponding numerical simulation was modeled by ABAQUS 6.14-3 software.

Another objective of this dissertation was to numerically simulate the behavior of HDPE subjected to cyclic loading with FEM code ABAQUS 6.14-3, to analyze impact of stress amplitude on HDPE pipe. For this purpose, different FE models under different Von Misses stresses were analyzed to check the effect of stress (σ) on fatigue behavior

of HDPE pipe and present the number of cycles pipe could successfully pass before failure. This dissertation is a preliminary step towards understanding the PE4710 pipe performance after fatigue for larger pipe size diameters.

An overview of the methodology to accomplish the objectives of this research is presented below.

- Conduct an extensive literature search.
- Conduct an experimental study to understand the fatigue performance of the HDPE pipe under two million cycles of internal water pressure of 125 psi to 188 psi.
- Perform tensile tests based on ASTM D638 and SEM test on new dogbone shaped HDPE specimens to evaluate mechanical behavior of HDPE and to determine the material parameters for further numerical study.
- Perform tensile tests based on ASTM D638 and SEM test on dogbone shaped specimens of already fatigue tested pipe to evaluate material properties of HDPE after two million cycles of internal water pressure ranges between 125 psi to 188 psi.
- Conduct Finite Element (FE) modeling and analysis of HDPE pipe to develop a new equation for S-N relation of PE4710.
- Draw conclusions from analysis of results.

The methodology of this research is illustrated in Figure 1-1.

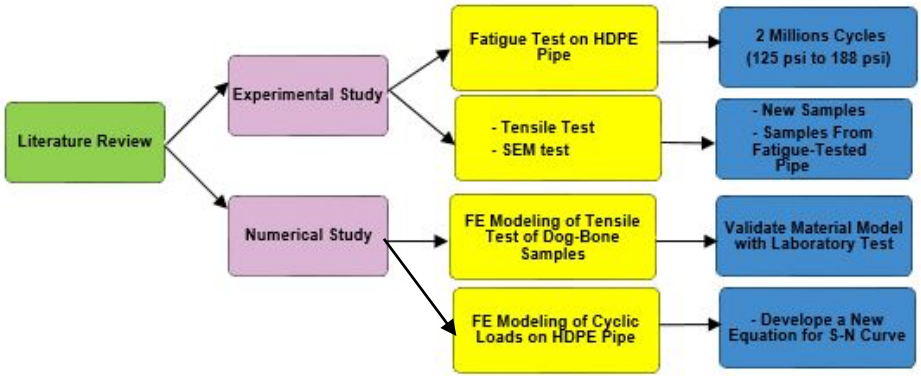

Figure 1-1 Research Methodology

HYPOTHESES

It is expected that this research will show that mechanical properties of HDPE, e.g., strain at rupture, yield strain and tensile stress, degrade approximately 20% after going under 2 million cycles of internal water pressure (considering 50 surges per day will result to approximately 100 years (Divyashree; 2014)) ranging between 125 psi to 188 psi. The FE modeling results will indicate that current equations for S-N curve of PE4710 provided by Petroff (2013) and EPRI (2013) overestimate fatigue life of this material.

STRUCTURE OF THIS THESIS

Chapter 1 presents a brief background on the pipeline history and polyethylene pipes as well as problem statement, contribution of this study to the body of knowledge, scope of the work and research methodology.

Chapter 2 provides a comprehensive literature study on background of HDPE material.

Chapter 3 covers the background and literature review on fatigue.

Chapter 4 presents the experimental part of the research including methods and results of fatigue test on HDPE pipe, tensile test on HDPE dogbone specimens cut from

fatigue-tested pipe and scanning electron microscopic (SEM) test accompanied with discussions.

Chapter 5 presents FE modeling and analysis of tensile test and cyclic loading of HDPE pipe using ABAQUS 6.14-3, as well as results and discussions.

Finally, Chapter 6 includes conclusions and recommendations for the future studies.

CHAPTER SUMMARY

The drinking water infrastructure in the North America requires a durable and reliable water transmission pipe material. Thus, it is important to study pipe performance, so that water utilities can benefit from cost-effective and efficient pipe installations and longer pipe design life. All pipe materials deteriorate overtime and every pipe has unique properties with advantages and limitations. During a pipe's life cycle, failures occur due to numerous factors such as age, loading conditions, environmental conditions, installation quality, manufacturing procedures, operation and maintenance strategies and so on. Since application of HDPE pipes in the water pipeline industry has been significantly increased in recent years and there is not enough study available about their long-term performance, more research in this area is required.

Chapter 2 INTRODUCTION AND BACKGROUND OF PE MATERIAL

INTRODUCTION

HDPE pipes are widely used to convey water, gas and all other types of liquids. Due to its lighter weight, leak-free joints, flexibility, simple installation and reduced breaks due to freezing, HDPE pipes are preferred over metal pipes.

HDPE pipes typically have lower cost and are corrosion resistant. Previous chapter provided an introduction for this dissertation and some general information about different classification of pipes, polyethylene pipes and water distribution. In this chapter, a brief overview of HDPE background, material properties, its application in water pipeline systems, advantages and limitations and its manufacturing process are presented.

BACKGROUND

According to PPI (2008), “High Density Polyethylene (HDPE) was first invented in England in 1933 by Imperial Chemical Company (ICI). The early polymerization processes used high-pressure (14,000 to 44,000 psi) autoclave reactors and temperatures of 200˚F to 600˚F. It was produced in a free radical chain reaction by combining ethylene gas under high pressure with peroxide or a trace amount of oxygen. Later in the 1950’s, polyethylene (PE) with low pressure was introduced. Density of polyethylene varies between 0.935 to 0.941 g/cc (58.37 to 58.74 pcf) for medium density polyethylene, and 0.941 to 0.945 g/cc (58.74 to 58.99 pcf) for high density polyethylene. Industry practice has shown that base resin densities are in the range of 0.936 to 0.945 g/cc (58.43 to 58.99 pcf). The polyethylene pipes with higher density, such as 0.952 g/cc (59.43 pcf), in combination with higher molecular weight and bimodal molecular weight distribution are known for higher levels of performance under International Organization for Standardization (ISO) standards for PE piping outside North America.”

According to AWWA (2006), “Polyethylene (PE) is a semi crystalline polymer composed of long, chain-like molecules of varying lengths and numbers of side branches.” This definition means that the structure of polyethylene is made of many parts (monomers) are joined together to build the whole (polymer). High density polyethylene is structurally stronger comparing to two other types of PE (i.e., LDPE & MDPE). Its durability is determined by the molecular weight. Increasing molecular weight improves the long-term strength, toughness, ductility, and fatigue endurance. Also, high density polyethylene (HDPE) has 65% crystallinity which is more than MDPE and LDPE. Increasing crystallinity leads to increasing stiffness, modulus, and chemical resistance, and decreasing permeability, elongation at failure, and flexibility decreases (Koerner; 2012).

According to Najafi et al. (2005), “PE pipes in North America are classified into three groups, based on density and crystallinity, which is an indicator of the tensile strength. The higher the crystallinity, results in greater hardness, stiffness, tensile strength, and density. ASTM classifies Type I as a low-density PE (LDPE), Type II as a medium density PE (MDPE), and Type III as a high density PE (HDPE). HDPE displays the highest stiffness whereas LDPE is the most flexible.”

MOLECULAR PROPERTIES OF POLYETHYLENE

Microstructure

According to Ward (1971) polyethylene is made up of repeating basic units of (-CH_2–CH_2 -) to form chemically simple polymer. It has crystalline and amorphous phases which build a semi-crystalline polymer. Structural integrity of polyethylene is provided by the ordered crystalline lamellae and elastic properties are provided by the random amorphous parts. Polyethylene is one of the most widely used polymers worldwide due to its semi-crystalline nature.

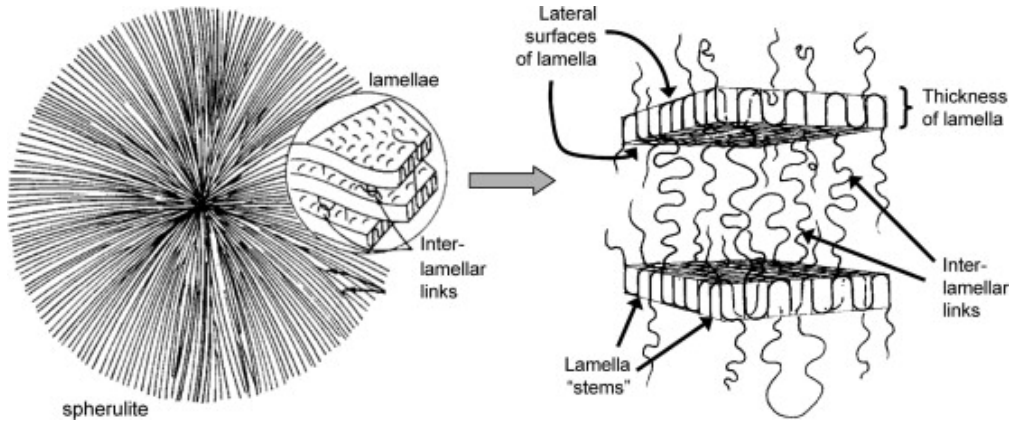

Figure 2-1 Schematic Illustration of Spherulite, Lamella and Amorphous Phase Structures

Cheng et al. (2011)

Single crystals of polyethylene can be obtained with nearly one hundred percent crystallinity in dilute solutions (Keller; 2007). Polyethylene is normally crystallized from a melt in practical applications. According to Keith et al. (1959) “melt-crystallized polyethylene has a spherulite morphology, where lamellae made up of spherulites are embedded in a matrix of amorphous material.” Figure 2-1 illustrates the thin flat lamellae form spherulites. Based on Keller (1959) “the structure of lamella generally consists of regular chain-folding arrangements with the molecular chains (or “stems”) perpendicularly aligned to the lateral lamellar surfaces” as shown in Figures 2-1 and 2-2 (a). Crystals with lateral direction dimensions (1-50 μm or 39.3-1,968 μin.) of much larger than their thickness (2-25 nm or 78.7-984 nin.) is caused by the regular chain-folding growth of a lamella (Keller, 1957, Fischer, 1957, Till, 1957, Lin et al. 1994 and Cheng 2008). Another type of lamella structure was proposed by Flory and Yoon (1978) in addition to the chain folding model. In their model an arrangement is formed by a growing crystal which feeds on whatever chains are available, as shown in Figure 2-2 (b). A study by Keller (1957) and Lin et al. (1994) indicated that melt-crystallized polyethylene consists of both types of previously explained crystalline structures. The regularly folded chain model is more

extensively used than the non- regularly folded chain model in studies on polyethylene. Currently, regular chain folding model is the base of most of the studies on polyethylene fracture.

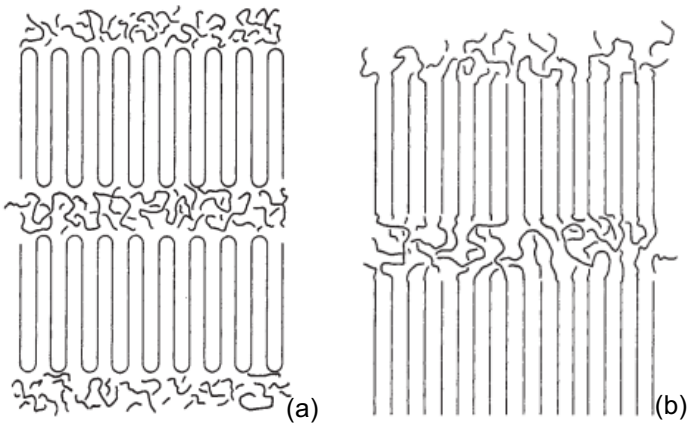

Figure 2-2 Structure of Lamella (a) Regularly folded model for a semi-crystalline polymer and (b) Extensively inter-wined molecules for a semi-crystalline polymer

Flory et al. (1978)

For the amorphous phase of polyethylene, there are three types of inter-crystalline material. The first type, cilia, begins as a crystalline chain and ends as an amorphous chain. The second type begins and ends in a lamella with its mid-section in the amorphous phase, thus forming a loose loop. The third type consists of inter-lamellar links that connect two adjacent lamellae. There are two types of inter- lamellar links; the first are *tie-molecules* that are chains crystallized in two or more lamellae at the same time. The second type of inter-lamellar links consists of physical chain entanglements that can be made up by the entanglements of cilia, loose loops and even tie-molecules.

Types of Polyethylene

Various types of polyethylene all are made up of the same basic repeating unit (-CH_2 – CH_2-). However, they have different properties and applications because of differences in their structure. Molecular weight (MW), molecular weight distribution

(MWD), density, percentage crystallinity and degree of long chain and short chain branching are the main reasons that differentiate the various types of polyethylene.

The main factors which affect process-ability and mechanical properties of polyethylene are molecular weights and molecular weight distribution. Shorter chains that act as “lubricant” make the process of MWD material easier. Chains in polyethylene can be linear or branched. Usage of comonomer (like 1-hexene) can introduce short chain branching into polyethylene. Short chain branches can affect crystallinity and density of semi-crystalline polymer with interfering with the formation of lamellae (Hosoda et al.; 1990). According to ASTM Standards (D1693, D5397), polyethylene can be classified in four density categories, as shown in Table 2-1. Linear low density polyethylene (LLDPE) and HDPE have a lamellar and spherulitic morphology. According to Lu et al. (1995) increase in crystallinity increases density of polyethylene, hence the stiffness and tensile yield strength of the material increase. In pipe applications, due to the high strength of the material, high density polyethylene (HDPE) is the preferred choice (Scheirs et al.; 1996).

Table 2-1 Classification of Polyethylene Based on Density, Scheirs et al. (1996)

PE Type	**Density (lb./in.^{3})**
Low	0.0328 – 0.0334
Medium	0.0335 – 0.0339
High	0.034 – 0.0346
High density homo-polymer	0.0347 and above

Branch Structures

Material density and other properties of polyethylene are affected by branching in chains (e.g., rheological properties). There are two types of branching, short chain branching and long chain branching. Short chain branching (SCB) is formed mostly due to introduction of comonomer, and long chain branching (LCB) is formed from side

reactions during polymerization. As illustrated in Figure 2-3, HDPE is generally linear with low SCB content. LLDPE has more SCB content than HDPE. Low density polyethylene (LDPE) has both high short chain branching and long chain branching contents. LLDPE and LDPE with higher SCB content have lower density. Type of catalyst used during the polymerization process controls short chain branch distribution (SCBD) of polyethylene.

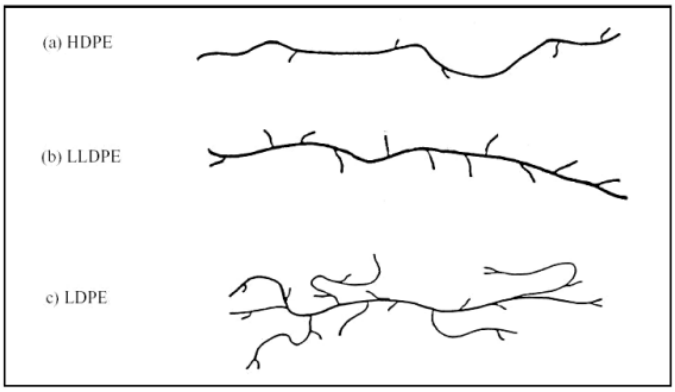

Figure 2-3 Polyethylene's Branch Structures, Elvers et al. (1992)

Chain Movement and Viscoelasticity

Polyethylene is a viscoelastic material, with both solid-like and liquid-like properties. Changes in temperature moves chains which leads to change in mechanical behavior of polyethylene. In Figure 2-4, changes in the storage modulus (E') of polyethylene with changes in temperature are illustrated. Polyethylene behaves more like a rigid solid with high E' values at temperature lower than the glass transition temperature (T_g) because only local movement of the polymer backbone and bending of side chains are possible. Larger scale chain movements in the amorphous phase is possible at temperature above T_g which leads polyethylene behaves more liquid-like and the E' value decreases. Crystalline lamellae inside the polyethylene matrix start to melt at the melting temperature T_m which is typically 120° to 180°C (248° to 356°F) (Cheng; 2008), large scale chain slippage occurs and the E' value significantly reduces (Menard; 1999).

Polyethylene loses its structural integrity and becomes a viscous melt at temperature higher than the T_m.

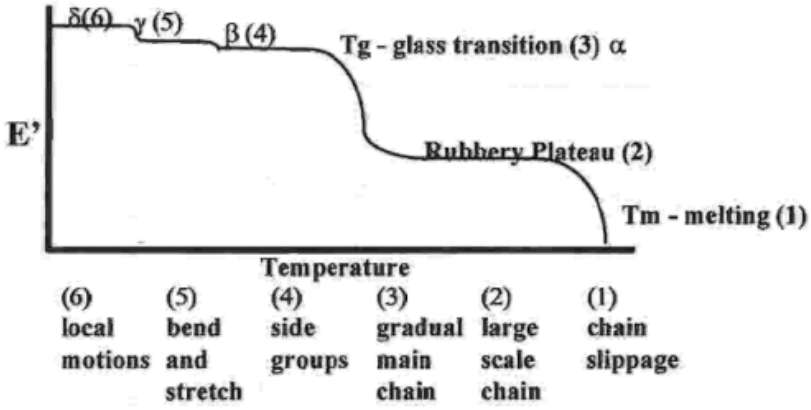

Figure 2-4 Stages of Thermal Transition of Polyethylene, Menrad (1999)

Creep of polymer chains influences many mechanical properties of polyethylene in temperatures above T_g (the solid state) shown in Figure 2-4. The type of chain motion in PE solid is the same as that of chain motion in the melt, although chain movements in solid state can take a long time because of restrictions from the crystalline phase and lower chain energy. Brochard et al. (1986) used tube model to explain the movement (relaxation) of polymer chains in the melt. In tube model, polymer chains move by reptation, which is a thermal motion of a long linear entangled macro-molecule in polymer melt (Cheng; 2008), and primitive-path fluctuations. De Gennes (1971) first proposed reptation for the movement of a single long polymer chain. In reptation, the long chain moves in a like a sliding motion along its own contour confined in an imaginary tube as illustrated in Figure 2-5. That section disappears as the chain moves out of a section of the tube. Chain can move back and forth along the tube in both ways due to not anchoring the chain at either end. Figure 2-6 illustrates the reptation movement in a

straight imaginary tube. The tube can bend and twist in various directions in reality (Doi et al.; 1986).

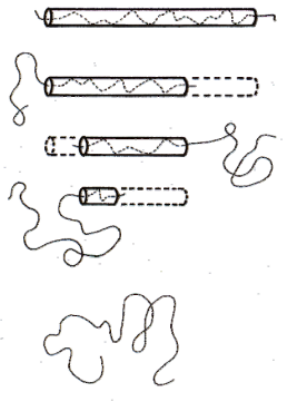

Figure 2-5 Polymer Chain's Reptation, Graessley et al. (1982)

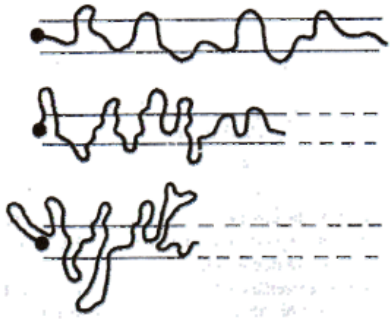

Figure 2-6 Primitive Path Fluctuations, Graessley et al. (1982)

De Gennes (1975) and Doi et al. (1980) proposed movement by primitive-path fluctuations for a polymer chain tethered at one end (e.g., a branch). The free end of the chain in primitive-path fluctuations randomly pulls away from the end of the imaginary tube. Then it re-relaxes into a new tube of lower energy. Resulting chain movement of both reptation and primitive-path fluctuation is called double reptation. Chain segments in the interior of the chain in a long polymer chain relax by reptation, but because of being faster than single reputation, the chain ends relax by primitive-path fluctuation. With

increasing MW of the polymer, the chain length increases and the contribution to overall relaxation time by chain ends reduces (Larson; 1999). The contribution of primitive-path fluctuation in high MW polymer chains becomes too small and can be ignored. Reptation of long chains dominates the relaxation time of polymer, this is the reason that rheological properties of polymer are strongly influenced by the longest chains in the system (Ferry; 1980).

MECHANICAL BEHAVIOR OF POLYETHYLENE

Ductile Failure

Ductile failure usually happens in a short period of time at high stress levels. Ductile tensile failure results in observation of visible deformation (necking) in the polymer sample. Semi-crystalline nature of polyethylene influences its tensile ductile behavior. Figures 2-7 and 2-8, illustrate the stress-strain curve for tensile ductile deformation and what occurs at the micro scale within the polyethylene matrix (material), respectively. At the beginning, before the yield point, there is not any visible deformation in the material and rigid crystalline lamellae carry the load. With increasing strain, stress increases as well and yield occurs. During the yield point and strain hardening, the load remains at almost constant level. Combination of amorphous phase rearranging itself and crystal lamellae slipping each other create deformation in this region, but still each individual crystal itself is intact. With increasing stress-strain values, orientation of the crystalline and the amorphous phases in the direction of drawing increases, as shown in Figure 2-7, then occurrence of strain hardening is observed.

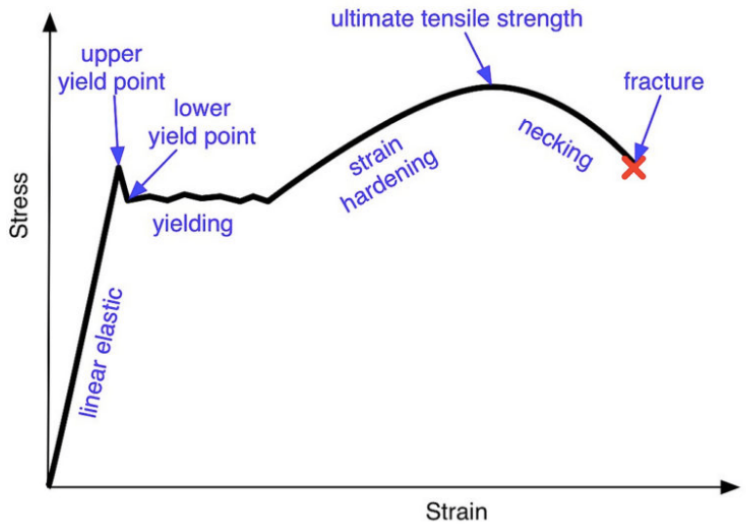

Figure 2-7 Typical Stress-Strain Curve for Tensile Ductile Deformation, Menrad (1999)

The amorphous phase reaches its full extension during strain hardening. Further deformation of the polymer in this stage is due to breaking and unfolding of lamellae. Under the scanning electron microscope (SEM), it is observed that the breaking of lamellae into smaller chunks leads to the characteristic rough fibrous surface of ductile failure (Lustiger et al.; 1983). Ultimate failure occurs as stress continues to increase with increasing strain and the material breaks (Alvarado-Contreras; 2007).

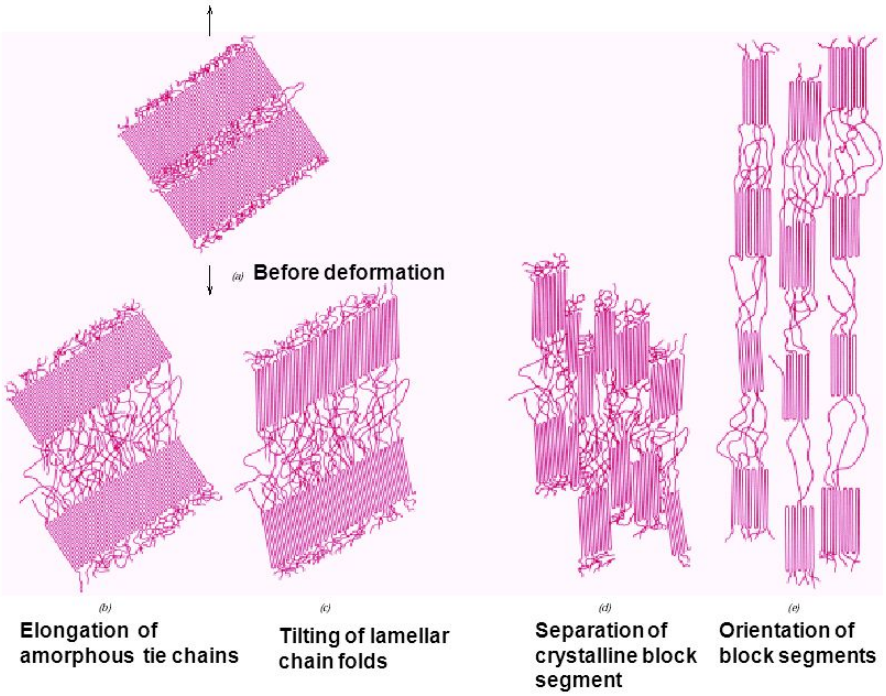

Figure 2-8 Deformation of Semi-Crystalline Polymer, Graessley et al. (1982)

Brittle Failure

Comparing to ductile failure, brittle failure of polymers is a quick break with little material deformation. The fracture surface appears smooth to the naked eye but SEM shows that the surface actually consists of short random pullouts (Lustiger et al.; 1983). Brittle failure occurs with applied low stress over a long period of time. As shown in Figure 2-9, in the first steps of brittle fracture, stress makes the amorphous materials to stretch. The inter-lamellar links under stress start to relax and untangle from each other due to the longer time period until the number of remaining linkages becomes very small. After stretching the few remaining inter-lamellar links to their limit, they are not able to pull apart lamellae, so, a brittle fracture of the polymer occurs, as illustrated in Figure 2-9.

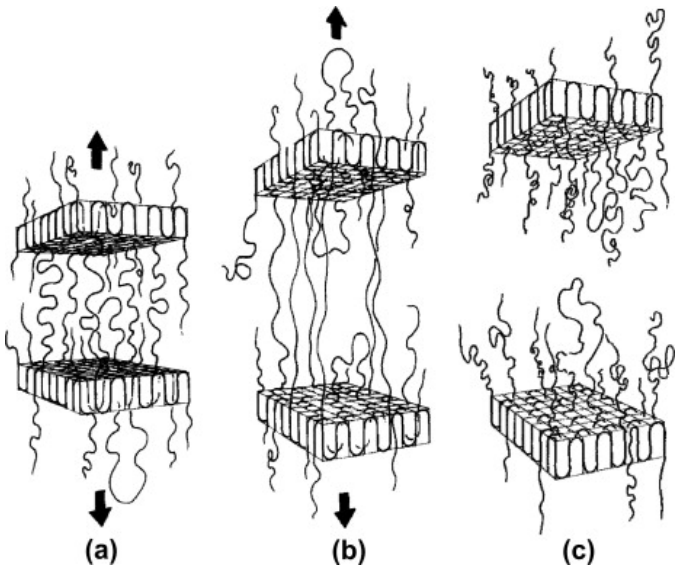

Figure 2-9 Different Stages of Brittle Fracture: (a) Lamella starts to pull away, (b) Tight stretching of tie-molecules and (c) Clean break of lamellae, Cheng et al. (2011)

Strain Hardening

According to Ward (1971) strain hardening is observed in fully drawn and cold-drawing polymers. Cold drawing is a phenomenon happens when a thermoplastic polymer is subjected to a continuous stress above its yield point (Nicholson; 2017). Molecular alignment of polymer chains leads to increasing strength of the material in the reason of increasing stress during strain hardening. This alignment of chain can be seen as a form of strain-induced crystallization (Ward; 1971). Increasing crystallinity increases tensile strength of polyethylene.

With stretching the amorphous phase of polyethylene to its limiting extensibility, strain hardening occurs (Allison et al.; 1966). Number of load-bearing junction points in the system affect the extensibility of a polymer network. These junction points contain cross-links and chain entanglements in cross-linked polymer. The network junction points consist of physical entanglements and crystalline structures in semi-crystalline polymer, such as high density polyethylene. However, where the drawing ratio is high, the junction

points formed from crystalline structures are temporary in cold-drawing cases. Intense morphology reorganization occurs in semi-crystalline polymers and the crystalline structure is destroyed in high strain deformations like strain hardening (Hay et al.; 1965, Peterlin; 1965 and Geil; 1964). Therefore, junction point role falls on physical chain entanglements alone. Hence, the number of chain entanglements influences strain hardening behavior of polyethylene considerably.

Environmental Stress Cracking

When exposed to an aggressive environment, such as soapy water, environmental stress cracking (ESC) occurs in the polymer (Cheng; 2008). In pipe networks and other polymer structure applications ESC is a frequent problem (Brostow et al.; 1986). In most cases, ESC fracture in characterized by clean cracks which indicates a brittle fracture mechanism. Any cracking of polymer due to subjecting to an aggressive environment, such as degradation of polymer due to exposure to UV light which ultimately leads to failure of the material, can be called environmental stress cracking. ESC commonly is known as stress cracking of polymer because of an active environment without any chemical change of the material; hence, a purely physical process. Some examples of aggressive environments for polyethylene are polar solvents such as alcohols, silicone oils and even emulsified water.

Stress cracking of polyethylene needs a very long time in normal conditions. Lagarón *et al.* (1999) conducted experiments on the impact of an active environment on the polyethylene structure. They indicated that surfactants, decrease the free surface energy of the fibrils and prevent the fibrils from packing into a dense structure, thus craze stabilization. Finally, cracks were formed and polymer is failed. Ward *et al*. (1991) studied how Igepal (a common surfactant) facilitates slow crack growth (SCG). They proposed that the long Igepal molecules align themselves with tie-molecules in the fibrils. It leads to

reducing the frictional stress as tie-molecules disentangle from crystals. The environmental stress cracking resistance (ESCR) of the polymer reduces as tie-molecules become untangled easier. It is generally accepted that acceleration in slow crack growth of polyethylene is because an active environment acts as 'lubrication' for chain disentanglement (Ward et al.; 1991 and Scheirs; 2000).

Study by Ward et al. (1991) indicated that diffusional limitations of the active ingredient controls the initial rate of ESC. When diffusion of the aggressive agent is restricted, the ESCR of polyethylene can be increased.

HDPE PIPE MANUFACTURING

Most of the material properties of HDPE pipes are affected by HDPE resins. The latest research on HDPE resins has resulted in development of PE4710. Extrusion process is used to manufacturing HDPE pipes. Properties of HDPE can be impacted by extrusion process (Park et al.; 1987). Residual stresses in HDPE pipe has been subject of many studies of HDPE. Longitudinal direction of the liner with crack growth from the outer surface through the liner thickness is highly affected by residual stresses. This points that one of the factors that have led to pipe cracking in the field could be residual stress (Hsuan and McGrath; 1999). A solution to the residual stress problems in HDPE pipe is annealing (Bhatnagar and Broutman; 1985). According to Bonds (2000) the accuracy of manufacturers in extrusion of pipe is not exact enough and it limits the pressure class of HDPE pipe. Based on PPI (2008) extrusion of pipes include heat, melt, mix, and convey the material to the die, to shape a pipe section. Figure 2-10 illustrates the typical HDPE pipe extrusion line.

Paul et al. (2005) introduced a high density polyethylene resins made in the loop-slurry process (single-reactor). They used a catalyst of chromium on modified alumino-phosphate. A unique structure that is suitable for high performance pipe applications was

developed using his process. The performance requirements of PE4710 specifications is satisfied with pipes made from these ethylene l-hexane copolymers. Since high density polyethylene pipes are widely used for conveying and distribution of natural gas, Chevron Phillips Chemical Company has developed a catalyst and polymerization system capable of producing PE4710 resin in a single reactor from a single catalyst (Paul et al.; 2005).

Paul et al. (2005) concluded that these polyethylene resins have enough resistance to rapid crack propagation as indicated by the Charpy (a standardized high strain rate test which defines the amount of energy absorption by the material during the fracture process (Meyers and Kumar; 1998)) results (see ASTM F1554 - 07ae1) while they have a wide molecular weight distribution. The new multimodal, high density polyethylene resins is made of chromium/alumino-phosphate catalysts.

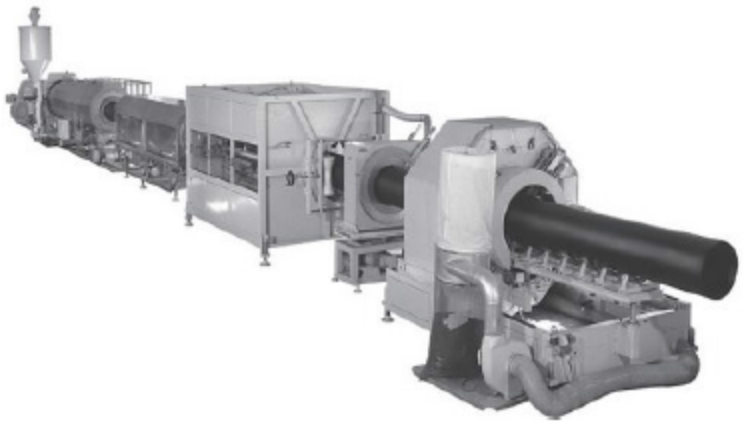

Figure 2-10 Typical Extrusion Line of HDPE Pipe, PPI Handbook of Polyethylene Pipe (2008)

HDPE PIPE STRUCTURAL PROPERTIES

The PE pipe has a viscoelastic nature which is a complex combination of elastic-like and fluid-like elements. Figure 2-11 illustrates the small elastic strain which is followed by a time-dependent strain. With increase in time, the strain increases as well.

After some time, the strain reduces with increase in time which is related to fatigue resistance of surges in the pipe (PPI handbook of polyethylene pipe; 2008).

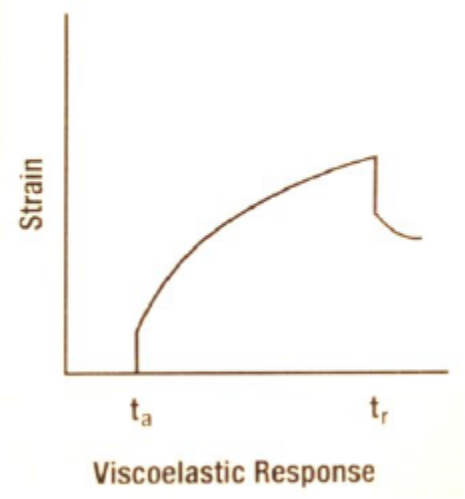

Figure 2-11 Viscoelastic Response of HDPE, Donald et al. (2011)

Leakage

Donald et al. (2011) presented a “Chambers Report” regarding three stages of failures Figure 2-12 illustrates a schematic creep rupture curve produced by Donald et al. (2011). According to Donald et al. (2011), “The stage I failure involves a purely mechanical failure mechanism due to ductile overload of the material failure mechanism. Stage I failures on pipe testing manifest as ductile bursting of the pipe with yielding of the material. Stage II failure also involves a mechanical failure mechanism but manifests itself as non-ductile slit or pinhole cracks in the pipe wall permitting leakage from the pipe. Stage III failure also manifests itself as leakage from non-ductile cracking of the pipe wall but it is not purely mechanical. Stage III failure occurs at lower stresses that Stage II failure and requires some minimum level of oxidative degradation of the HDPE pipe material.”

A high cost for many water networks, which often overlooked is water loss through holes and cracks in the pipe material. Ambrose et al. (2008) estimated cost of leakage based on two models as:

- Background leakage, which happens in the joints of the pipes and perforations.
- Leakage from burst failures, which can be longitudinal splits or circumferential breaks.

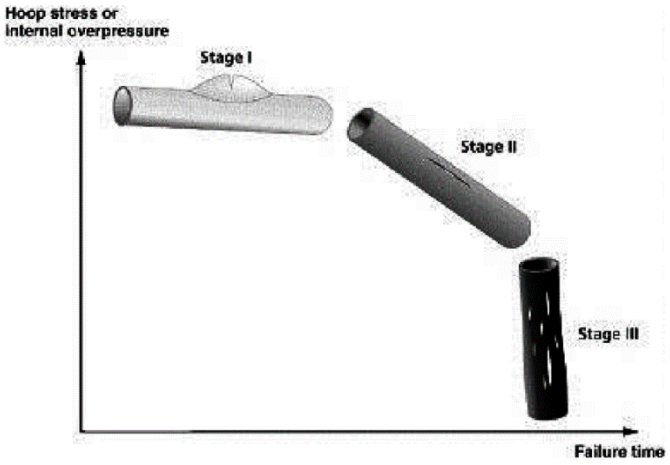

Figure 2-12 Stages of Failure of HDPE Pipe, Donald et al. (2011)

Leakage cost simulation by Ambrose et al. (2008) on PE, PVC/DI, DI and mixed pipe material for a medium network of 100,000 costumers indicated that PE has the lowest leakage cost. According to American Water Works Association (AWWA) Manual M36, the main water lines have the largest leaks which can reach up to 1,000 GPM (AWWA, 1999). AWWA mentions the cost for leak detection can be added up to $800 per mile of main water lines (in 1999 dollars). This cost will be added to the cost of leaking water, treating water and repair of the leak (Rubeiz; 2004).

When using the bell and spigot type joints associated with some piping products such as PVC or ductile iron, leak points exist every 10-ft to 20-ft. For municipal

applications, fused joints in HDPE pipes eliminate that potential leaks. Therefore, the PE pipe allowable water leakage is zero compared to the water leakage rates of 10% or greater associated with other piping products (PPI, 2008). This significantly decreases the cost associated with leakage.

Fatigue Resistance

For fatigue damage to thermoplastic materials, three primary models exist, depending on the load type (Oliphant et al.; 2012);

- Self-heating with induced localized melting,
- Cumulative damage model, and
- Crack propagation model which is accelerated by cyclic loading. This model is divided into:
    - Pure fatigue and,
    - Combined creep and fatigue.

Oliphant (2012) found resistance of PE4710 materials based on available data. He found an approach for both repetitive fatigue resistance and occasional surge resistance of PE4710 and PVC. He concluded that PE has significantly higher fatigue resistance over PVC piping material.

Jeremy (1990) studied the fatigue response of PVC and PE pipes. He concluded that fluctuating internal pressures induces fatigue stresses in pipes and fittings and the final wave pattern quantifies the fatigue damage that pipe systems sustain in service. The results also indicated that fatigue response of un-plasticized PVC (UPVC) pipe was correctly defined, whereas at elevated temperature PE pipes failed at fittings and joints. Figure 2-13 illustrates the different cyclic loading profiles.

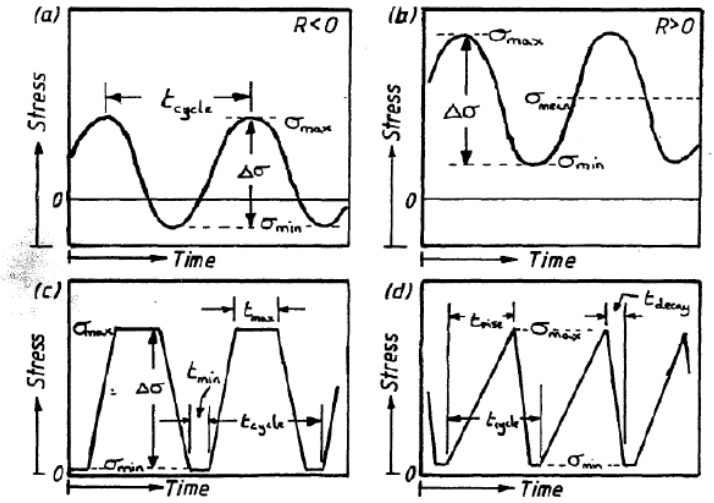

Figure 2-13 Schematic Illustration of Different Periodic Loading Patterns;

(a) & (b) Sinusoidal, (c) Trapezoidal and (d) Saw-tooth, Jeremy (1990)

A study of literature indicates that butt fused joints are capable of carrying high surge fatigue stresses at 68-73˚F (20/23˚C) and have the best projected fatigue lifetimes (Donald and Dale; 2011).

Velocity in HDPE Pipe

Petroff (2013) studied the impact of flow velocity on surge pressure. He concluded that with increasing the velocity, lower dimension ratio (DR) (thicker wall) pipes may be required to withstand the surge pressure. AWWA-WRF “Guidance Manual for Maintaining Distribution System Water Quality” recommends “a velocity of 5 fps or greater to remove biofilm, promote scouring and removal of loose deposits, and to reduce disinfection.” 5 fps is the safe upper limit even though some of the utilities extend up to 8 fps (Fleming et al.; 2006).

Elevated Temperature

Peak elevated temperature 140°-176°F (60-80°C) influences the geo-membranes service life. Acceleration of depletion of geo-membranes antioxidant and degradation of

polymer reduce the service life of high density polyethylene geo-membranes. Jafari et al. (2014) studied possible temperature requirements for landfills. They present an explanation of the approximate service life of HDPE geo-membranes based on 50% reduction in tensile strength at break in various temperatures. Table 2-2 presents service life of HDPE geo-membranes. With maintaining the temperature at 68˚F (20°C) the life of HDPE increases to 565-900 years (Jafari et al.; 2014). With increasing temperature, the service life reduces. Figure 2-14 illustrates the effect of temperature on tensile stress-strain curves of HDPE material.

Table 2-2 Effect of Elevated Temperature on Service Life of HDPE Geomembranes

Jafari et al. (2014)

Temperature		Service Life (years)	Temperature		Service Life (years)
°F	°C		°F	°C	
68	20	565-900	104	40	80-120
86	30	205-315	122	50	35-50
95	35	130-190	140	60	15-20

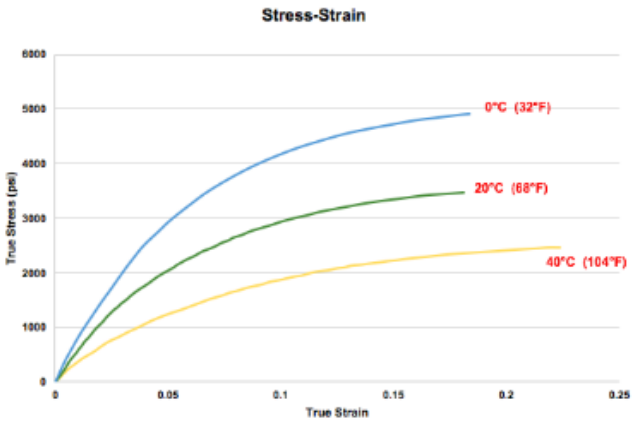

Figure 2-14 Effect of Elevated Temperature on Tensile Behavior of HDPE

Provided by Georg Fischer-Central Plastics Company

Thermal Expansion

Zheng et al (2012) investigated the effect of soil load combined with effect of temperature on HDPE pipe with introduction of thermal expansion. Using ABAQUS software, the variation between stress and deflection was studied. The result indicated that pipe temperature has a significant effect on performance of buried HDPE pipe, and thermal stresses was much higher than stresses induced by soil load. Hence, deflection of pipe due to soil load is prevented by thermal expansion, which protect HDPE pipe in application. Temperature changes cause expansion and contraction of HDPE pipes. Expansion and contraction coefficients should be considered in the piping system. The coefficient of thermal expansion for HDPE pipe is approximately $67*10^{-6}$ in. /in. /°F (PPI hand book of Polyethylene, 2008).

Oxidation

Donald et al. (2009) investigated oxidation in HDPE pipe. Chlorinated water, disinfectants such as chlorine, chlorine dioxide and chloramines leads to oxidative degradation of polyethylene pipe failure. According to research by major utilities in France, HDPE pipe oxidation and failure are associated with factors such as disinfectant type, average service temperature, disinfectant concentration and pressure (Haager et al.; 2006). Three failure stages of oxidation degradation of HDPE pipes are:

1. In stage I, flowing water which contains chemical disinfectants washes finite supply of anti-oxidants in the HDPE pipe.
2. The water disinfectants oxidants degrade pipe inner surface polymer when the protective anti-oxidants (AO) package is exhausted or depleted. In stage II, molecular weight is reduced and mechanical properties of the surface polymer is diminished.

3. In severe degradation of inner surface, cracks are developed. By internal pressure and other sources of pipe wall stress cracks will propagate through the pipe wall. Then non-ductile failure of the HDPE pipe occurs in stage III.

Permeability

Water Research Foundation (WRF) (2008) has reported “Impact of Hydrocarbon on PE/PVC Pipes and Pipe Gaskets” which is susceptible to permeation of organic compounds. Water utilities require to maintain high standards for water quality and protect water from contamination. In 2009, Plastic Pipe Institute (PPI) commented that while the overall effect of hydrocarbons is very small, measures must be taken to restrict the of hydrocarbon permeation effect. Plastics Pipe Institute presented three methods of addressing permeation of hydrocarbons:

1. The pipe to be surrounded with good clean soil of Class I or Class II materials,
2. The pipe to be sleeved in areas where active hydrocarbon contamination exists, and
3. The pipe to be rerouted around the contaminated plume.

Ong et al. (2008) suggested replacing HDPE water pipes in contaminated areas. Plastic Pipe Institute (PPI) states that in water mains permeation is not an issue, as there is not any water stagnation. According to PPI (2008), the WRF report is not applicable since they did not consider the effect of temperature on rate of permeation as their study was conducted in temperature of 73˚ F. However, based on PPI handbook of polyethylene pipe (2008), increase in density will reduce permeability.

Seismic Resistance

A severe earthquake occurred in Awaji (Kobe), Japan, in 1995. Table 2.3 presents the failure rates of water pipes.

Table 2-3 Failure Rates of Water Pipes in Kobe Earthquake, Rubiez (2009)

Type of Pipe	Water Pipe Damage/Km (Damage/mile)
PE	0.00 (0)
Steel	0.437 (0.26)
DCIP	0.488 (0.303)
PVC	1.43 (0.88)
CIP	1.508 (0.937)
AC	1.782 (1.107)

Compared to other pipe materials, HDPE pipe performed “very well with few failures” (Rubeiz; 2009). Three recent earthquakes have indicated that main areas of occurrence of total earthquake damage to water systems, and thus, water outages to customers, are zones of in firm ground with smaller diameter distribution pipes. In 2012, seismic-resistant design was used for approximately 75% of new water pipes installed in Japan while in California less than 1% of new water pipes use seismic resistant design. HDPE pipes (including either butt fused joints or electro-welded with clamped joints) show excellent earthquake performance in common distribution pipes and service laterals (diameter of under 1 in. to 8 in.), as observed in three recent earthquakes (WRF; 2012).

PE pipe is well suited for installation in dynamic soil environment and in areas prone to earthquake due to its toughness, ductility and flexibility combined with other special properties, such as its leak-free fully restrained heat fused joints. Table 2-4 presents the vulnerability to ground deformation for various pipe materials and shows that compared to other commonly used water pipe materials, PE pipe with fused joint has low vulnerability to ground deformation.

Table 2-4 Water Pipeline Materials, Standards and Ground Deformation's Vulnerability, AWWA (2010)

Material Type and Diameter	AWWA Standard	Joint Type
Low Vulnerability to Ground Deformation[1]		
Ductile iron	C100s series	Bell and spigot, rubber gasket, restrained
Polyethylene	C906	Fused
Steel	C200 series	Arc welded
Steel	No designation	Riveted
Steel	C200 series	Bell and spigot, rubber gasket, restrained
Low to Moderate Vulnerability to Ground Deformation[1]		
Concrete cylinder	C300, C303	Bell and spigot, restrained
Ductile iron	C100s series	Bell and spigot, rubber gasket, unrestrained
Polyvinyl chloride	C900, C905	Bell and spigot, restrained
Moderate Vulnerability to Ground Deformation[1]		
Cast iron>8-in (203-mm) diameter	No designation	Bell and spigot, rubber gasket
Polyvinyl chloride	C900, C905	Bell and spigot, unrestrained
Steel	C200 series	Bell and spigot, rubber gasket, unrestrained
Moderate to High Vulnerability to Ground Deformation[1]		
Concrete cylinder	C300, C303	Bell and spigot, unrestrained
Steel	No designation	Gas welded
High Vulnerability to Ground Deformation[1]		
Cast iron	No designation	Bell and spigot, leaded or mortared

[1] Resistance of a pipe to ground movements due to seismic and dynamic loads

HDPE MATERIAL PROPERTIES

Table 2-5 presents typical physical, mechanical and thermal properties of HDPE.

Table 2-5 Typical Engineering Properties of High Density Polyethylene, Cheng (2008)

Property	ASTM Test Method	Unit	Value
Physical			
Density	D-792	lbs/in.^{3}	0.0336 to 0.0349
Water absorption	D-570	%	0.01 to 0.03
Mechanical			
Tensile strength at break	D638	psi	3,200 to 4,500
Elongation at break	D638	%	10 to 1200%
Tensile yield strength	D638	psi	3,400 to 4,800
Elongation at yield	D638	%	15 to 40
Modulus of elasticity	D638	psi	60,000 to 160, 000
Flexural modulus	D-790	psi	145,000 to 225,000
Compressive strength	D695	psi	2,700 to 3,600
Thermal			
Melt point	D3417	°F	259-267
Coefficient of linear thermal expansion	D696	in./in. °F	0.000059 to 0.000120

ADVANTAGES OF HDPE PIPES

HDPE pipe is a perfect choice for piping systems due to its physical and performance. HDPE pipe is specified and approved in various standards, i.e., AWWA C901, AWWA C906, NSF 14, NSF 61 and ASTM International D3035. Some distinctive advantages of HDPE pipe that provide important benefits for water applications are listed below (PPI handbook of polyethylene pipe; 2008).

Corrosion Resistance

One of the most important and costliest problems of metal piping systems is corrosion. Hydraulic efficiency of pipe is affected by corrosion which can happen inside or outside of the pipe. To help slow rust and pitting which is inevitable at metal pipes treated water is used. Cathodic protection which is very costly, plastic coating, or sleeving can also be implemented to extend the service life of metallic pipes (Divyashree; 2014).

HDPE pipe does not rust, rot or corrode. It is biological growth resistant. HDPE pipe is chemical resistant and in aggressive chemical environments, is the material of choice. HDPE has an extended service life and is long term cost savings.

Fatigue Resistance

HDPE pipe is flexible and ductile. It is fatigue resistant. HDPE is designed to withstand the occasional and recurring surge events that commonly happens in water distribution systems. Compared to other types of plastic piping, fatigue resistance of HDPE pipes allow utilizing a thinner wall (Divyashree; 2014).

Extended Service Life

HDPE pipe is a durable material which is suitable for pipeline systems. Depending on application, with proper design and installation of HDPE, it is estimated to have the service life of 50 to 100 years (Khelif et al.; 2008).

Leak-Free Joints

Bell and spigot or mechanical type joints are the main type of joints used in traditional infrastructure piping and all have a specified leakage factor. Leaking pipes cost cities money and water, this precious resources is lost as well. Heat fusion joints used in HDPE pipes produce permanent leak free joints (Divyashree; 2014).

Fusion Joints

Heat fusion welds can be used to join HDPE pipes. In heat fusion, after heating two HDPE surfaces, they are brought together to form a permanent, monolithic, leak-free system (Najafi and Gokhale; 2005).

Adaptability

Stab or mechanical fittings can be used to join HDPE pipes. Dependent on the size of the pipe and its application, different types of fittings can be used. Using various

types of joints and fittings makes transition of HDPE pipe to and from non-HDPE piping systems so easy (Hsuan and McGrath; 1999).

Trenchless Installation

Open-cut method of pipe installation causes disruption in traffic and environment while trenchless technology is an environmentally friendly method (Najafi and Gokhale; 2005). However, both open-cut and trenchless technology can be used to install HDPE pipes.

HDPE pipe is flexible and in combination with its high tensile strength and abrasion resistance, it is a perfect option for being installed using trenchless technology. Leak free HDPE pipe installed using trenchless method is cost effective than non-plastic pipes installed using traditional open-cut method.

Eco-Friendly

HDPE is known for being environment-friendly. According to Bell and Cave (2011):

- Manufacturing HDPE requires less energy compared to non-plastic pipes.
- Being lightweight has made its transportation much more cost effective compared to metal pipes.
- Being flexible and capability of utilizing heat fusion joints in HDPE pipes has made it to need less fittings compared to other piping materials.
- Physical characteristics of HDPE help to utilize smaller diameters of pipes which means less disruption in ground when using trenchless installation compared to other fusible products.
- Heat fusion joints of HDPE pipe has made perfect leak free connections.
- Hazardous levels of toxins is not emitted by HDPE during different steps of its production and application.

- HDPE pipe is recyclable.

HDPE PIPE LIMITATIONS

While in the literature many benefits of HDPE pipes are listed, some major limitations are also described as follow:

One of the major limitations of HDPE pipes is permeation. According to PPI (2009) “If any ground contamination due to existence of hydrocarbons are found, then the pipe should be rerouted around the contaminated plume, or surround the pipe with good clean soil of class I or class II materials to allow the hydrocarbon that may have contacted the pipe’s wall to dissipate into the atmosphere.”

Oxidation is another problem with HDPE pipes. Water disinfectants such as chlorine, chlorine dioxide and chloramines induce oxidative degradation in polyethylene pipe (Donald and Dale; 2009).

Also, HDPE has poor weathering resistance and temperature capability. When temperature reaches to near or below freezing, stiffness of PE pipe increases while resistance to impact damage decreases. HDPE requires more time for handling and installation procedures that bend and flex the pipe in colder situations. Pipe should be prevented of being dropped or impacted by handling equipment or other things which strike the pipe forcefully. Pipe surface can become slippery in inclement weather condition and walking on the pipe should be prevented (PPI handbook of polyethylene pipe; 2008).

Limitations of HDPE pipes may include, environmental stress cracking, its high flexibility results in encountering problems in retaining joints restraints (unless inserting stiffener into the pipe before attaching the restraints) and requirements for skilled labor and special equipment to perform butt-fusion joints (Divyashree et al.; 2015). Table 2-6 summarizes advantages and limitations of HDPE pipes.

Table 2-6 Advantages and Limitations of HDPE Pipes, Najafi and Gokhale (2005)

Advantages	Limitations
Resistant to both internal and external corrosion	May be subject to environmental stress cracking
Butt-fused joints effectively create a continues joint less conduit	Lower Hydrostatic Design Basis than other thermoplastic material, require thicker walls, which results in smaller flow area
Abrasion resistant not when used in sewer applications.	Skilled labor and special equipment required for butt-fusion
High ductility, flexibility and toughness.	Chemical burial properties resist most ground contamination, unless excessively exposed.
Lightweight in smaller diameters.	Cost/Benefit Ratio is different from other thermoplastic pipes of same pressure capacity
High flow coefficient, low frictional resistance to fluid flow.	Cannot be located unless buried with metallic wire or tape, except by Ground Penetrating Radar.
Highly resistance to rupture by impact, even at very low temperatures.	Sensitive to temperature differentials, resulting in measurable expansion and contraction unless constrained by soil friction.
Resists shatter-type or rapid crack-propagation failure.	High flexibility causes problems in retaining joints restraints, unless stiffener is inserted into pipe prior to attachment of restraints.
Does not easily crack under expansive forces of freezing water.	Degradation owing to ultraviolet light exposure has been seen in some HDPE pipes of low carbon black content.

PE PIPING SYSTEMS OVERVIEW

Polyethylene (PE) is one of the most used thermoplastic materials after its development in 1933 (Oliphant et al.; 2012). New resins made for PE are suitable for different applications in gas, sanitary and drinking water pipelines, and a wide range of other applications (PPI Manual for Water Application; 2009).

PE Water Service Lines Sizes, Pressures, and Specifications

Typical nominal diameter of PE pipe or tubing in water service lines are 1⁄2 in. to 3 in. in accordance with AWWA C901-17, ASTM D2239, ASTM D3035 and ASTM

D2737, and rated pressure is 80 to 250 psi. This water service pipelines can be joined to another types of pipes or fittings (Oliphant et al.; 2012)

CHAPTER SUMMARY

HDPE is a semi-crystalline polymeric material with crystalline and amorphous phases. Structural integrity of polyethylene is provided by crystalline lamellae and elastic properties of polyethylene is provided by amorphous parts. The semi-crystalline nature of polyethylene has made it one of the most used polymers in the world.

Polyethylene (PE) can be classified as Low Density (LD), Medium Density (MD) and High Density (HD). Due to structural differences, they show different properties and applications. Main properties which distinguish different types of PE are molecular weight (MW), molecular weight distribution (MWD), density, percentage crystallinity and degree of long chain branching and short chain branching.

The PE pipe is a viscoelastic material which makes it a complex combination of elastic-like and fluid-like elements. Resins in HDPE material are responsible for most of its material properties.

Corrosion resistance, fatigue resistance, leak free-joints and extended service life are some of the benefits of HDPE pipes. Permeation, oxidation and poor weathering resistance are HDPE pipe limitations.

Chapter 3 FATIGUE FAILURE

INTRODUCTION

In the previous chapter an overview and background of the PE material, its mechanical and structural properties and use of HDPE in the water piping systems was provided. In this chapter, an introduction to the fatigue phenomena, background of fracture and some general information and literature review about fatigue of HDPE are presented.

FATIGUE

Fatigue is a progressive, localized, permanent structural change. According to Boyer (1986), fatigue is fluctuating stresses and strains that may result in cracks or fracture after a sufficient number of fluctuations. The process of fatigue consists of three stages: 1) Initial fatigue damage leading to crack initiation, 2) Progressive cyclic growth of a crack (crack propagation) and 3) Final, sudden fracture of the remaining cross section (PPI; 2012).

Boyer (1986) mentioned stress level, cyclic wave form, fatigue environment and metallurgical condition of the material are the effective factors on the fatigue behavior. There are three different types of fatigue: high cycle fatigue (HCF), low cycle fatigue (LCF) and thermal mechanical fatigue (TMF). The main difference between HCF and LCF is the region of the stress strain curve where the repetitive application of load (and resultant deformation or strain) is occurring.

High Cycle Fatigue (HCF) has low amplitude high frequency elastic strains. An example would be repeated bending applied on an airfoil. One source of this bending occurs as a compressor or turbine blade passes behind a stator vane. High velocity gas pressure bend the blade when it comes into the gas path. Blade loading frequency is

changed by rotor speed's change. When the excitation matches the resonant frequency of blade, the vibration amplitude significantly increases.

In High Cycle Fatigue (HCF), hundreds of cycles of loading are applied on the sample per second. This cyclic loading amplitude leads to strains that remain in the elastic part of the stress strain curve. There would not be any permanent deformation since only elastic strain has taken place. The sample can withstand millions of cycles but finally failure occurs due to HCF.

Low Cycle Fatigue (LCF) has high amplitude low frequency plastic strains. Permanent deformation means elastic strain limit is exceeded and the plastic region is crossed. Only a low number of cycles can be tolerated with sample before failure due to LCF. In areas of stress concentration of the turbine blade these large strain occurs. Holes, curves and notches are the portions of a sample where the local stress level is increased to the point of plastic strains occurrence.

In Thermal Mechanical Fatigue (TMF), large changes of temperature leads to significant thermal expansion and contraction and hence considerable strain excursions. Mechanical strains associated with centrifugal loads of change in engine reinforces or counters this strains. Combination of these two makes material degradation due to TMF. It may happen in turbine blades, vanes and other hot section components.

FRACTURE MECHANICS

There are two types of reason for most failures:

1. Negligence during design, construction, or operation of the structure (Peacock; 2000).
2. Application of a new design or material, which produces an unexpected (and undesirable) result (peacock; 2000).

While because of many advantages of polymers over metal their application in structures is rapidly increasing, but another kinds of fractures will occur in polymers. The PE material is mostly utilized in the water and natural gas transportation system. One important advantage of PE material is that it is possible to perform maintenance on a small part of the pipeline and it is not necessary to shut down the whole system; using a clamping tool to the PE pipe, the small area can be shut down. While the operation of pinch clamping saves money, it will make fracture problem (Hsuan et al.; 2005). Figures 3-1 and 3-2 show the typical surfaces of fractured PE pipe.

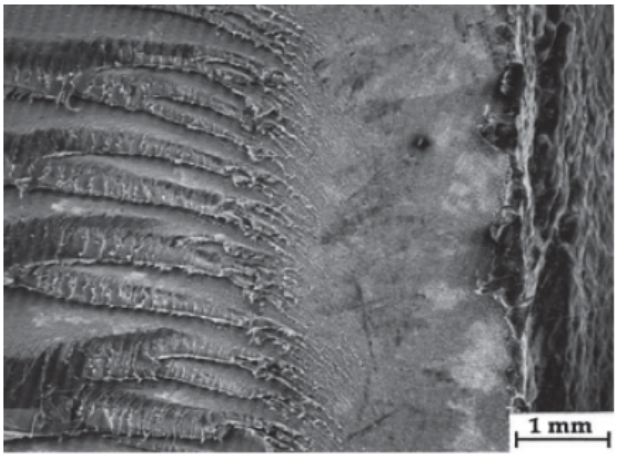

Figure 3-1 Fracture Surface of a PE Pipe, Hsuan et al. (2005)

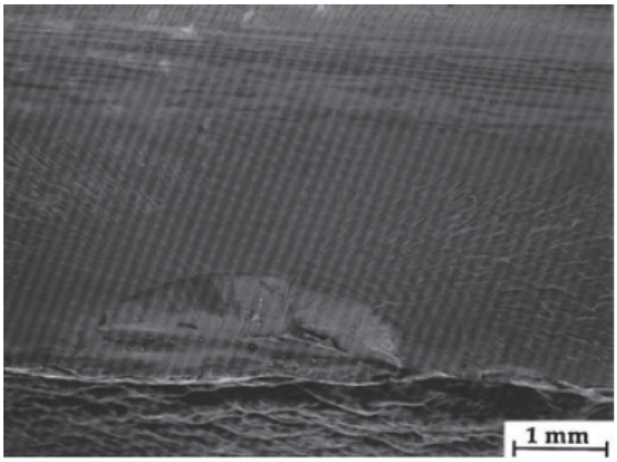

Figure 3-2 Thumbnail Crack Produced in a PE Pipe, Hsuan et al. (2005)

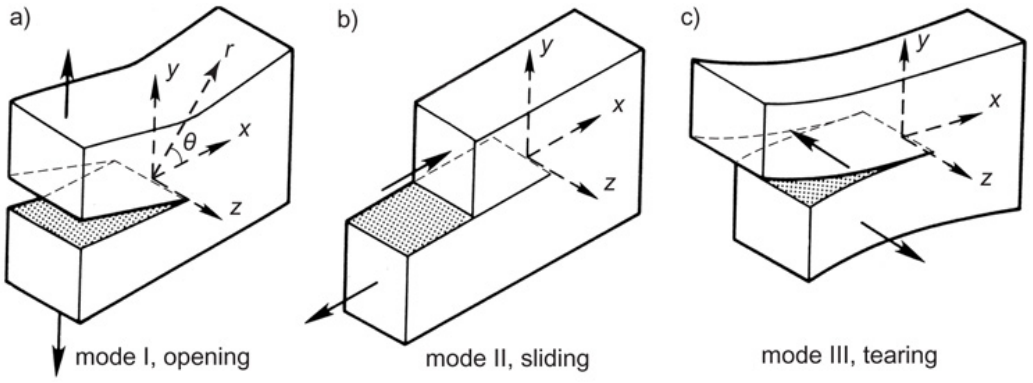

Figure 3-3 Different Modes of Fracture, (a) Mode I, (b) Mode II, (c) Mode III, Kanninen and Popelar (1985)

Three types of loading which a crack can experience, as Figure 3-3 illustrates, include:

Mode I fracture – Opening mode (a tensile stress normal to the plane of the crack). The load is applied normal to the crack plane and open the crack.

Mode II fracture – Sliding mode (a shear stress acting parallel to the plane of the crack and perpendicular to the crack front), corresponds to in-plane shear loading and tends to slide one crack face with respect to the other.

Mode III fracture – Tearing mode (shear stress acting parallel to the plane of the crack and parallel to the crack front). It is associated with a pure shear condition, typical of a round bar loaded in torsion.

Linear Elastic Fracture Mechanics (LEFM)

Linear Elastic Fracture Mechanics (LEFM) is a common method to analyze fracture behavior of materials, since the fracture property is narrowed to the stage of fracture initiation. By comparing applied K (the driving force) to a critical K (critical force), the fracture behavior of a linear elastic structure is defined.

The closed form expressions for stress in body can be determined when applying external forces on the crack configurations and making isotropic linear elastic material behavior assumption. Figure 3-4 shows a polar coordinate axis with the origin at the crack tip.

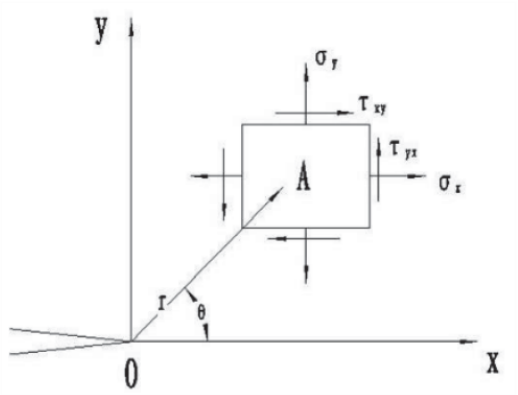

Figure 3-4 Polar Coordinate Axis with the Origin at the Crack Tip, Liang (2007)

According to Li and Qi (2014) the stress field in any linear elastic cracked body is given by Equation 3-1.

$$\sigma_{ij} = \left(\frac{k}{\sqrt{r}}\right) f_{ij}(\theta) + \sum_{m=0}^{\infty} A_m r^{\frac{m}{2}} g_{ij}^{(m)}(\theta) \qquad \text{Equation 3-1}$$

σ_{ij} is stress tensor,

r and θ can be found in Figure 3-5,

k is the constant and,

f_{ij} is dimensional function of θ in the leading term.

The stress intensity factor can be given to express the mode of loading, so the stress on the crack tip in an isotropic linear elastic material can be written as Equations 3-2, 3-3 and 3-4, presented below (Li and Qi; 2014).

$$\lim_{r\to 0} \sigma_{ij}^{(I)} = \frac{K_I}{\sqrt{2\pi r}} f_{ij}^{(I)}(\theta) \text{ Mode I} \qquad \text{Equation 3-2}$$

$$\lim_{r\to 0} \sigma_{ij}^{(II)} = \frac{K_I}{\sqrt{2\pi r}} f_{ij}^{(II)}(\theta) \text{ Mode II} \qquad \text{Equation 3-3}$$

$$\lim_{r\to 0}\sigma_{ij}^{(III)} = \frac{K_I}{\sqrt{2\pi r}} f_{ij}^{(III)}(\theta) \text{ Mode III} \qquad \text{Equation 3-4}$$

In a mixed-mode problem the principles of linear superposition can be written as the following format in Equation 3-5 (Li and Qi; 2014).

$$\sigma_{ij}^{(total)} = \sigma_{ij}^{(I)} + \sigma_{ij}^{(II)} + \sigma_{ij}^{(III)} \qquad \text{Equation 3-5}$$

Although stress intensity solution can be given in different forms, the stress intensity factor K can be related to the crack through the appropriate correction as shown in Equation 3-6.

$$K_{I,II,III} = Y\sigma\sqrt{\pi\alpha} \qquad \text{Equation 3-6}$$

Where the characteristic stress is σ; α is the characteristic crack dimension and Y is the dimensionless constant which depends on the geometry and the mode of loading. For the linear elastic material, due to the linearity, stresses, and the stress intensity factor will become additive as the loading is consistent. That is (Li and Qi; 2014):

$$K_I^{Total} = K_I^{(A)} + K_I^{(B)} + K_I^{(C)} \qquad \text{Equation 3-7}$$

Elastic Plastic Fracture Mechanics

Linear Elastic Fracture Mechanics (LEFM) can be utilized to determine material properties when material shows time independent plastic deformation. Since when plastic zone occurs the LEFM cannot be operated, a simple plastic zone correction to the stress intensity factor was provided by Irwin (1957). The other correction methods are suggested by Barenblatt (1959) and then Dugdale (1960).

For materials which show time-independent, non-linear behavior, the elastic plastic fracture mechanism (EPFM) is applied. Two elastic-plastic parameters which can be utilized to determine the fracture condition are the crack tip opening displacement

(CTOD) and J contour integral. Although there are limits to the applicability of J and CTOD, these limits are less restrictive than validity requirement of LEFM.

Crack Tip Opening Displacement

According to Liang (2007) and Peacock (2000), Wells introduced the crack tip displacement theory and an approximate analysis to relate CTOD to the stress intensity factor in the limit of small-scale yielding. Figure 3-5 shows a crack with a small plastic area. Irwin (1957) presented another method to solve CTOD by solving for the displacement at the physical crack tip (Callister; 2007, Hodgkinson; 2000, Wetzel et al.; 2006 and Kfouri; 1996).

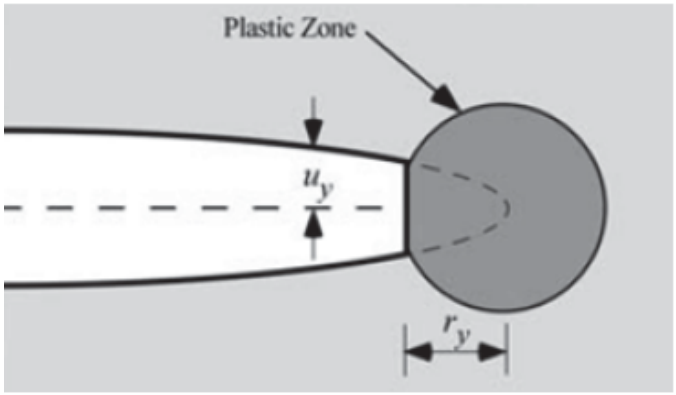

Figure 3-5 A Crack with a Small Plastic Area, Callister et al. (2007)

In Wells theory, the CTOD can be written as the following format:

$$\delta = \frac{4}{\pi} * \frac{K_I^2}{\sigma_{YS}} * \frac{1}{E} \qquad \text{Equation 3-8}$$

δ is the CTOD. As $\frac{\delta}{\sigma_{YS}} \rightarrow 0$, Equation 8 can be rewritten as Equation 3-9.

$$\delta = \frac{K_I^2}{E * \sigma_{YS}} \qquad \text{Equation 3-9}$$

There are different definitions of CTOD. Two popular definitions are the displacement at the original crack tip and the 90°intercept, as illustrated in Figure 3-6. If the crack blunts in a semi circled, these two definitions will be equivalent.

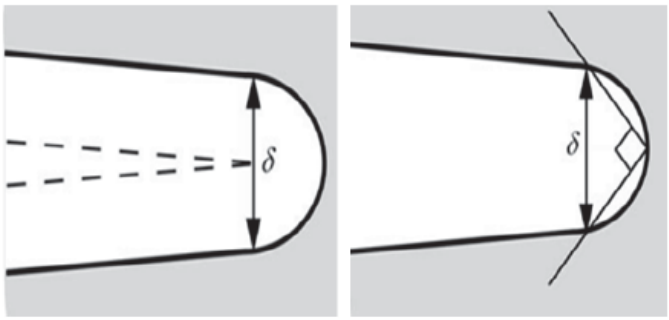

Figure 3-6 Typical Crack Tip Opening Displacement, Callister (2007)

Modified hinge modal is the standard method for CTOD and the displacement can be expressed as the following format in Equation 3-10.

$$\delta = \delta_{el} + \delta_p = \frac{K_I^2}{m\sigma_{YS}E'} + \frac{r_p(W-a)V_p}{r_p(W-a)+a} \quad \text{Equation 3-10}$$

$\delta_{el}$is elastic component, $\delta_p$is the plastic component, r_p is plastic rotational factor and the typical value is 0.44.

Fracture Toughness

One important property of materials is fracture toughness (K_{IC}) which plays an important role in the material science and shows the ability of a cracked material to resist fracture (Yau et al.; 1980 and Malchev et al.; 2007).

The fracture toughness (K_{IC}) is measured by loading a deliberately cracked sample of length 2c or a surface crack of length c as shown in the Figure 3-7. Using the tensile stress and bending load at which the crack suddenly propagates, the fracture toughness (K_{IC}) can be calculated by Equations 3-11 and 3-12.

$$K_{IC} = Y_1\sigma * \sqrt{\pi c} \quad \text{Equation 3-11}$$

$$K_{IC} = Y_2 \frac{F}{bw} * \sqrt{\pi c}$$ Equation 3-12

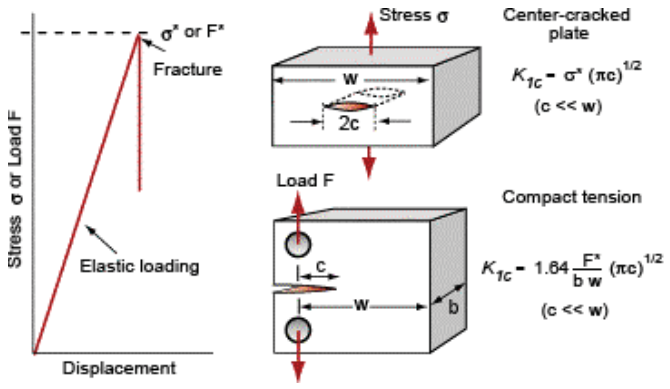

Figure 3-7 Calculation Relationship of Fracture Toughness, Callister (2007)

F is the bending load and σ is the tensile stress. Y_1 and Y_2 are geometric factors. E is Young's modulus and b and w are the beam thickness and depth, as illustrated in Figure 3-8. The fracture toughness can be well obtained followed the above method for material. For mullite-fiber composite, the fracture toughness is about 1.8–3.3 MPa.$m^{1/2}$ (Liang; 2007). Figure 3-8 shows the general relationship between fracture toughness and thickness.

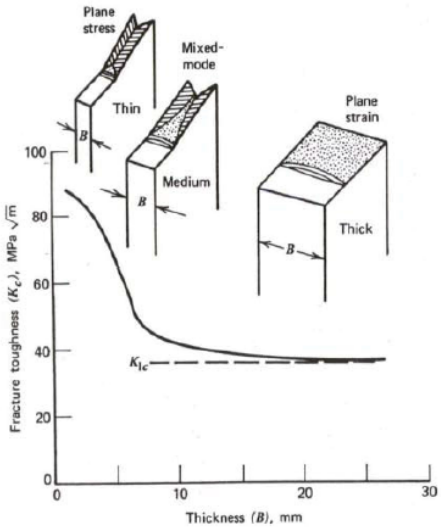

Figure 3-8 Relationship Between Fracture Toughness and Thickness, Bao et al. (2004)

From Figure 3-9, the thin parts have a high value of fracture toughness and with increasing the thickness, the K_c value will reduce and this type is called stress-strain mixed mode. In thick parts, the whole surface of fracture is flat and the fracture toughness will reach the minimum value of the asymptotic. In thin parts the plastic zone sizes at fracture are much larger than thick parts.

FUNDAMENTAL THEORY OF MECHANICAL PROPERTIES

To understand the nature of fatigue it is first necessary to consider some basic aspects of material behavior presented in this section.

Stress-Strain Curve

Tensile strength is one of the important mechanical properties of material. It is expressed as a stress, measured as force per unit area, as presented in Equation 3-13. In non-homogeneous materials, tensile strength can be presented as force per unit width. If the material deforms while stretching, the cross-sectional area may change but the area used in the calculation is the un-deformed cross-sectional area A_0.

$$\sigma = \frac{Force}{A_0} \qquad \text{Equation 3-13}$$

Strain is the change in length of the sample as shown in Figure 3-9. The strain commonly is expressed in one of two ways shown in Equations 3-14 and 3-15.

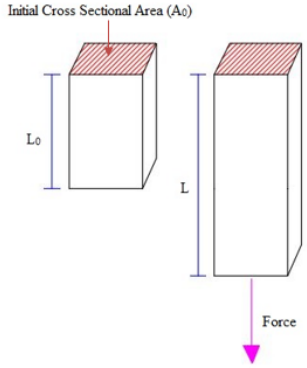

Figure 3-9 Elongation in direction of applied force

Elongation:

$$\varepsilon = \frac{L}{L_0} - 1 \qquad \text{Equation 3-14}$$

Extension ratio:

$$\alpha = \frac{L}{L_0} \qquad \text{Equation 3-15}$$

Figure 3-10 shows a typical stress - strain curve.

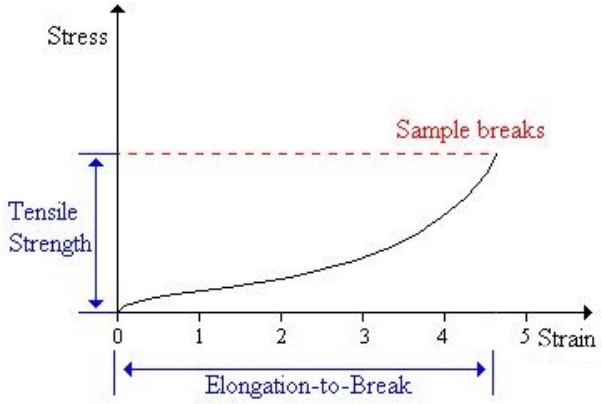

Figure 3-10 Typical Stress-Strain Curve, Li and Qi (2014)

Stress-strain behavior is best specified in tension. Degree of deformation is dependent on the applied stress magnitude. The strain is directly proportional to the stress at low stresses for most materials. It was first found by Hooke in 1678 and termed Hooke's law (Bao et al.; 2004).

Many materials show linear elastic behavior and controlled by linear stress-strain relationship. Linear stress-strain means loading a specimen elastically in tension which cause elongation, but after removing the load, it will return to its original shape and size. After the linear region, plastic deformations occur which means after unloading deformed specimen will not return to its original size and shape.

Young's Modulus

Young's modulus or modulus of elasticity is the proportion of stress to strain. It is used to characterize materials. Slope of the stress–strain curve at any point is the tangent modulus. Stress-strain curves often are not straight-lines, meaning that with change in the strain, the modulus changes. In this case the initial slope usually is used as the modulus which is illustrated in the Figure 3-11.

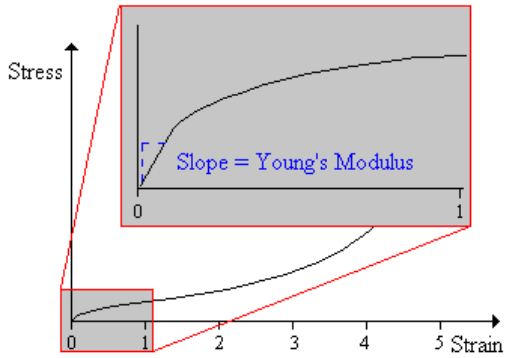

Figure 3-11 Graphical Definition of Young's Modulus, Li and Qi (2014)

In general, rigid materials have a high Young's modulus, and elastomers have low values.

Deformation of HDPE

An understanding of deformation mechanisms of polymers is important in order to be able to manage the mechanical characteristics of material. The deformation of the HDPE depends on many elements, for instance, the stress mode, speed and magnitude of the applied load. It contains the rearrangement of the molecules and change in the morphology, which is elastic (recoverable) at low stress levels. The shape of the stress versus strain curve shown in the Figure 3-12, it shows the details of deformation process.

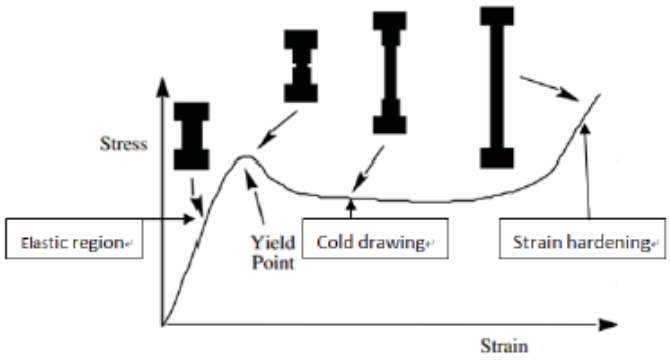

Figure 3-12 Typical Deformation Curve for Polymers, Li and Qi (2014)

In the elastic region, the deformation can be regarded as elastic and homogenous and it can be clearly seen in the Figure 3-13 (stage 1). The yield point which is the maximum in the stress-strain curve shows heterogeneous and plastic deformation. In the cold drawing stage, the neck grows along the specimen and it can be seen in Figure 3-13 (stage 2) next stage shows the segments separate from the lamellae but remain attached to each other by fiber chains (stage 3). In the hardening stage, it shows the fibrous material deform uniformly and finally reach break (stage 4).

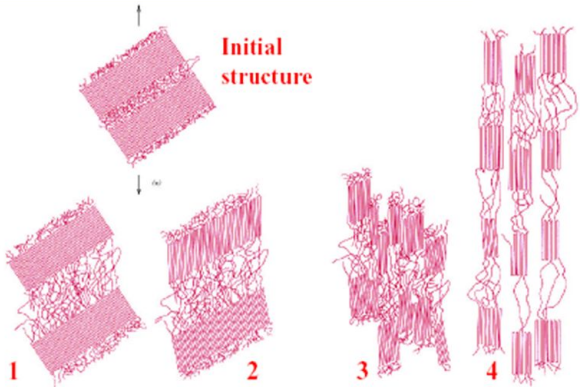

Figure 3-13 Typical Deformation of Polymers, Peacock (2000)

Figure 3-13 shows the processing of rearrangement of HDPE in tension test. Many elements like shear, compressive and flexural properties of HDPE are controlled by the same morphological characteristics that control the tensile properties (Peacock;

2000). In the above processing which represented are reversible and very different to the typical engineering materials such as steel or concrete.

FRACTURE OF PE PIPES

The phenomenon of fracture usually happens in our daily lives, for example, when a dish drops and breaks into several pieces. Metal and non-metal materials have extensively been used and utilizing polymer material has significantly increased in the last decades.

One of the failure causes of HDPE pipes is fatigue which is the result of pipes being subjected to cyclic loading of internal pressure and external loadings on buried pipes (Djebli et al.; 2014).

In the industry, the products should be tested under different types of loading before bringing it to the market. In those test, when the load exceeds the material's load bearing capacity, it fails by fracture (Hsuan et al.; 2005). Failure modes can be different but the sequence of failure is illustrated in Figure 3-14.

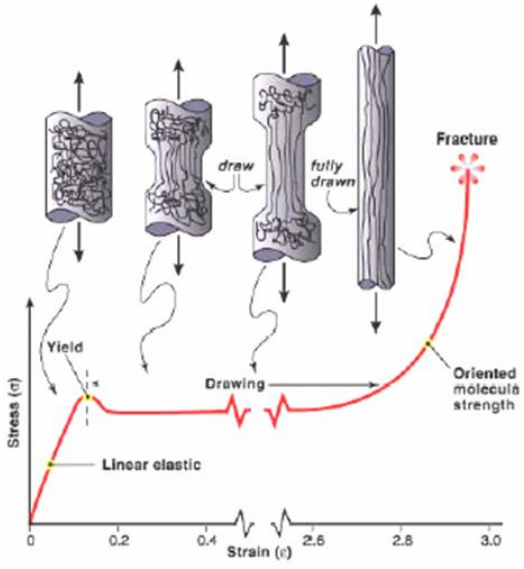

Figure 3-14 Typical Procedure of Failure of Plastics, Li and Qi (2014)

According to Barsoum et al. (2007) elasticity means a recoverable deformation in materials when the load is removed and plasticity is an unrecoverable deformation in the material when the load exceeds a certain limit. This plastic deformation remains stable until the reaching the ultimate tensile strength. Continuing loading the material after reaching the peak load leads to an unstable deformation and then fracture occurs.

FATIGUE OF PE PIPES

The PE design practices for preventing pressure surge fatigue failures in water pipe have a long history. These practices were developed based on the older generation PE materials. Since this time there has been considerable evolution in the performance of PE pipe and the introduction of a new classification of high performance PE4710 materials. With the introduction of these materials, questions have been raised around the suitability of the current design practices.

Bowman (1990) discusses the fatigue failure in polyvinyl chloride (PVC), MDPE and HDPE pipes. They cycled at a rate of 1-cycle per second from a base pressure of 58 psi to a range of peak pressures. They produced an S-N plot of their findings. Bowman compared his results to the tests run by Vinson (1981) and Hucks (1972) and concluded that all of the data were in agreement.

Marshall et al. (1998) studied the effects of “surge and fatigue” on different types of pipes in the UK. They looked at different types of failures for PE (polyethylene) and PVC pipes. As part of their research they derived an S-N curve. They concluded, “All types of PVC apparently have similar fatigue characteristics.”

Dusunceli et al. (2010) conducted a series of experimental work were performed to explore on mechanical response of HDPE at uniaxial cyclic and loading-unloading tensile deformation. It was observed that strain accumulation on cyclic loading increases

with increasing number of cycle. Figure 3-15 shows uniaxial cyclic stress-strain curve of HDPE.

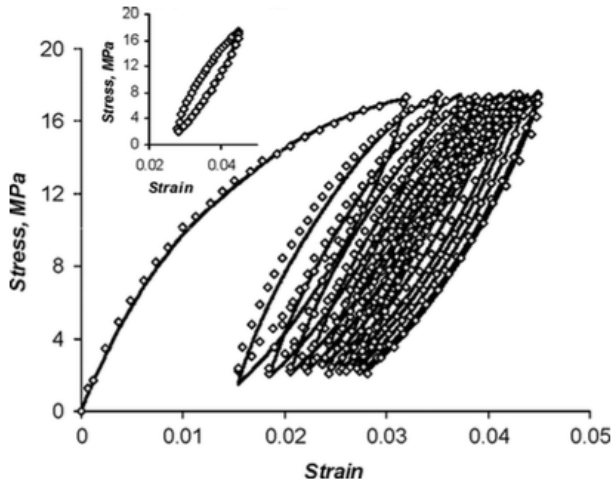

Figure 3-15 Uniaxial cyclic stress-strain diagram of HDPE,

Hizoum and Belouettar (2011)

Jeffrey et al. (2004) performed a fatigue study (cyclic test) on 6 in. diameter PVC pipe with thickness of 0.17 in and water pressure fluctuation of 40 psi. The pipe failed at 3.3 million cycles. These tests indicated that stress amplitude primarily influences the fatigue of PVC more than mean stress for lower peak stresses. They developed a new S-N fatigue diagram that is more accurate than all previous methods. Figure 3-16 illustrates S-N curves provided by Jeffrey (2004) and previous developed S-N curves by Moser (2001) and Bowman (1990). Another study by Folkman et al. (2013) focused on the effects of pressure fluctuation on failure rates of PVC pipes. They concluded that the fatigue damage is insignificant when pressure fluctuations are limited to 20 psi.

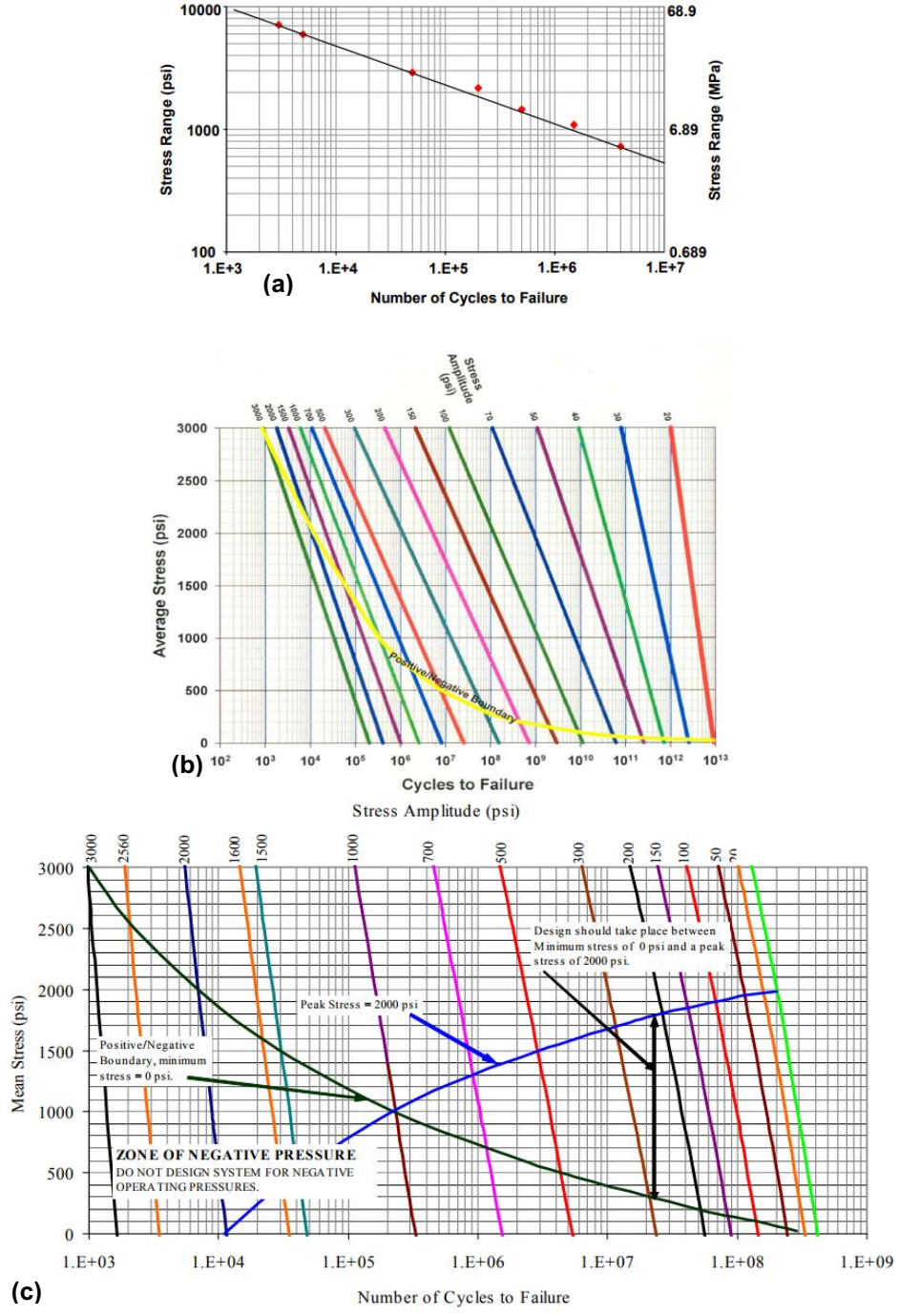

Figure 3-16 Developed S-N Curves by (a) Bowman (1990), (b) Moser (2004) and, (C) Jeffrey (2004), Jeffrey (2004)

Experimental analysis performed by Djebli et al. (2014) for determining the fatigue strength of PE-100 for pipes, under constant and cyclic axial loadings. Findings of the research showed that fatigue strength of HDPE grade PE-100 pipes depends on the pipe stress and HDPE exhibits a cyclic softening behavior in cyclic loading. Also, they established the relationships between stress and number of cycles (S-N curve) at test frequency of 2 Hz.

According to Khelif et al. (2008) Fatigue lifetime of HDPE structures such as pipes is recognized to show a large scatter. They compared median rank, the maximum likelihood and the Kolmogorov-Smirnov fitting for the estimation of Weibull parameters. They found that whether the three-parameter distributions of Weibull and lognormal types are suitable for lifetime prediction, the two-parameter Weibull is more conservative for probabilistic fatigue design.

PRESSURE SURGES IN PIPELINE SYSTEMS

"Rattling Pipes" occurs when turning on and off water systems within the house. Pressure surges in piping systems are common and can be destructive. The typical cause of this rattling or “Water Hammer” is caused by valve operation, entrapped air in the line and sometimes pumps operations. The effect of any one of these events can be effectively multiplied many times by the geometry of a piping system if the pressure wave is allowed to reflect, or bounce, back and forth within the system. Frequent pressure surges or fluctuations in a piping system will cause a fatigue failure (Jung et al.; 2011).

Surges are the result of a rapid change in liquid velocity within a pipeline which causes the stored energy in the flowing fluid to be converted to pressure energy, caused for example by rapid valve closure or a pump tripping (Mcpherson et al.; 2011). They are a short term event (on the order of seconds) that results in either an initial rapid increase or decrease in pressure above or below the steady state pressure. The resulting pressure

wave travels down the pipeline at the speed of sound traveling in the transport fluid (which for water piping systems is the speed of sound in water) until it hits a barrier and is reflected back. The resulting pressure changes, commonly referred to as transients, hydraulic surges, hydraulic transients, and water hammer, are an important consideration in the design of water transmission and distribution systems (Jung et al.; 2011).

Surges are characterized with two design approach paths; One deals with the instant (short term) impacts of the pressure surge (occasional surges) and the other deals with the effect of recurring surges (repetitive surges) (Mcpherson et al.; 2011).

Peak pressure surges created by incidents separate from normal operations of the pipe (e.g., tripping of pumps due to power outage) are occasional pressure surges. Peak pressure surges created by normal operation of pipe are recurring pressure surges (e.g., turned off and on of pumps, opening and closing of valves) and occur more than once per day (Mcpherson et al.; 2011).

According to Mcpherson et al. (2011) in short-term impact of pressure surges, these factors should be considered:

1. Upsurges (increase of pressure):
    - When pipe is over pressurized damage or rupture of pipes can happen.
    - Different components of the system can be damaged (gasket blowout, pump damage, etc.)
2. Down-surges (pressure decreases):
    - Collapse of pipe
    - Infiltration of groundwater (at leakage points such as joints)

Basics of Surge

The common reason to induce surges is a quick change in the velocity of the fluid in the pipe, which can be created by valves operating, pump start-up and shut-down,

air venting, fluid column separation, and other operations (Mcpherson et al.; 2011 and Jung et al.; 2011). In the flowing water, the kinetic energy converts to a pressure wave. This wave moves with a constant speed through the length of the pipe until facing a boundary or barrier. Interference of reflected waves which return back down the pipeline, with the incident wave, produces reinforced peaks which can have greater amplitude than the incident wave (Mcpherson et al.; 2011).

The Joukowsky equation helps to a basic understanding of the potential peak pressures in surge events. This equation defines the relationship between different factors affecting pressure surge event as presented by Equation 3-16 (Jana; 2012).

$$P_s = a\left(\frac{\Delta V}{2.31g}\right) \qquad \text{Equation 3-16}$$

where, P_s is surge (psi), ΔV is change in velocity (ft/s), g is acceleration due to gravity (32 ft/s^2) and a is wave velocity (ft/s).

For water pipelines, the wave velocity can be evaluated by the known fluid properties and the piping material modulus, as expressed in Equation 3-17.

$$a = \frac{4660}{\left((1+\left(\frac{K_{bulk}}{E_d}\right)*(DR-2)\right)^{\frac{1}{2}}} \qquad \text{Equation 3-17}$$

Where, a is wave velocity (ft/s), K_{bulk} is fluid bulk modulus (300,000 psi for water at 73°F) and E_d is dynamic instantaneous effective modulus of pipe material (normally 150,000 psi at 73°F for PE). Higher modulus materials which are stiffer have proportionately higher surge velocities (Jana; 2012).

Another effective parameter in surge analysis is the critical time. Critical time is the required time for incident pressure wave to reflect and return to the source. If the duration of the incident event is shorter than the critical time is longer, destructive interference at the source will not happen and the full pressure surge will occur. If the

duration of the incident event is longer than critical time, then some decrease in the full pressure surge happens (Jana; 2012). Using Equation 3-18 the critical time can be calculated.

$$T_{CR} = \frac{2L}{a}$$ Equation 3-18

Where, T_{CR} is critical time (seconds), L is distance through pipeline length that pressure wave moves before being reflected by barrier (ft) and a is wave velocity (fps).

Water Velocity Changes and Pressure Surge Loads

The only unknown in the Joukowsky equation to define pressure surge of a determined pipe is ΔV, the change in velocity. Change in velocity is dependent to specific design of the pipeline system, the certain event that induces a change in velocity, and the velocity of water flow. Fully stopped flow is the maximum change that can happen in velocity (so ΔV will be the same as the water flow velocity) (Jana; 2012).

Since a single surge event may result to failure, for design purposes the resistance to peak surges should be based on the maximum design velocity for the pipeline. UK IGN 4-37-029 for guidance on design of PE and PVC pipelines in the UK recommends “for identification of the peak surge, the worst case anticipated event (e.g., emergency trip of all pumps) should be considered.”

There are not any standard design velocities for pipeline systems. Utilities usually based on the requirements of a specific system determine maximum design velocities for the normal operation of the systems and fire flow (Jana; 2012).

A typical limit for normal operations recommended by AWWA operator training documents is 5 ft/s but higher velocity expected during “fire flow conditions.” AWWA Research Foundation Guidance Manual for Maintaining Distribution System Water Quality, suggests “a velocity of 5 ft/s or greater to remove biofilm, promote scouring and

removal of loose deposits, and to reduce disinfection demand and a velocity of 12 ft/s for removing sand from siphons."

Pressure Upsurges

With an idea of the maximum flow velocity changes that can be anticipated in water piping systems, the resistance of PE4710 piping to the potential pressure surges resulting from a sudden flow stoppage at these velocities can be considered (Jung et al.; 2011).

According to design against surge and fatigue conditions for thermoplastic pipes (1999) thermoplastics like PE in fast loading rates, e.g., a surge event with the rapid pressure rise, show higher strength and stiffness. Therefore, PE material resist better the higher stress levels produced by surge at higher pressure rates due to increase in material strength with higher loading rates (Design against surge and fatigue conditions for thermoplastic pipes; 1999). Bowman (1998) mentioned pressure surge events on thermoplastic piping systems usually happen at a rate of 14.5 to 145 psi/sec. The short term strength of PE at these loading rates is significantly greater than the long term strength utilized in Pressure Class (PC) design.

Surge Allowance for PE4710

The US (AWWA standards; 2006 and 2008), UK (Design against surge and fatigue conditions for thermoplastic pipes; 1999) and Australian (Industry guidelines: polyethylene pressure pipes design for dynamic stresses; 2010) guidelines of PE pipes consider peak surge events for design. It should be considered that these different guidelines are based on different design stresses dependent on the long-term strength rating practices of each region. Table 3-1 presents the applicable design stresses based on each guideline. PE design stress used in the AWWA (2006 and 2008) is 16% lower than design stress used in the UK and Australia (based on PE100 materials). Table 3-2

presents the maximum allowable short term stresses for PE4710/PE100 based on the US, UK and Australian design approaches.

Table 3-1 Design Stresses Based on the US, UK and Australian Standards, Jana (2012)

Material	**Design Stress (psi)**		
	US	UK	Australia
PE4710/PE100	1,000	1,160	1,160

Table 3-2 Allowable Upsurges Based on the US, UK and Australian Standards, Jana (2012)

Material	**Maximum Short Term Surge Stress (psi)**		
	US	UK	Australia
PE4710/PE100	2,000	2,320	1,450

Pressure Down-surges

Pressure down-surges are an important phenomenon in pipe (Jung et al.; 2011). Sub-atmospheric pressure down-surges can collapse pipelines (as has already occurred in steel pipes) or they can result to entrance of groundwater which can contaminate drinking water into the piping system (Fleming et al.; 2006). Design of pressure pipelines prevents sub-atmospheric pressures but yet there is chances of occurrence of this phenomenon, so a well understanding of its impact on the piping system is required (Fleming et al.; 2006).

According to AWWA (2006) PE4710 is resistant to collapse at full vacuum and butt fusion joints prevents entrance of groundwater into the PE pipes.

CYCLIC LOADING IN PIPELINE SYSTEMS

Another important factor to define the potential damage to the pipeline system is the total number of pressure surges over the lifetime of a pipe. The effect of repetitive or cyclic loads on piping materials is known as fatigue. For some materials, fatigue

performance is considerably below the static pressure long-term material strength, and hence, considering the effect of cyclic loading in design of pipes is vital (AWWA; 2002).

Cyclic Loading in PE4710

Dependent on the type of loading, primary models for fatigue damage of thermoplastic materials are suggested as follow (Bowman; 1990):

- Self-heating with induced localized melting;
- A cumulative damage model;
- A crack propagation model with acceleration by cyclic loading, which may be further subdivided into:
- Pure fatigue
- Combined creep and fatigue

According to Bowman (1990) “self-heating with induced localized melting can be discarded in water pipelines because of the high thermal heat sink of the water and soil and the relatively low surge frequencies.”

Accelerated Crack Initiation and Propagation by Cyclic Loading

Many plastics will transition to a macroscopically brittle failure mode, with very different failure morphology and failure arithmetic with reducing the peak load and increasing the number of cycles to fail. Macroscopically brittle failures are a product of initiation of crack followed by its propagation (Lu et al.; 1990, Schapery; 1975, Lu et al.; 1986). This mechanism in cyclic loadings results to fatigue weakness (Zhou et al.; 1992, Balika et al.; 2007 and Reynolds et al.; 1993).

Initiation and propagation of cracks depend on different factors including the number of cycles, the loading rate, the peak stress, and the stress amplitude. Crack propagation is accelerated by cyclic loading. Fatigue failures can occur in couple of

weeks to months for some materials even when the peak cyclic stress is less than 50% of the long-term creep-rupture stress (Balika et al.; 2007).

Some other materials can withstand much larger number of cycles with a higher fraction of their long-term creep-rupture stress (Marshal at al.; 1998, Design against surge and fatigue conditions for thermoplastic pipes; 1999).

Dependent on the resistance of material to initiation and propagation of cracks, brittle failures of pipe can occur due to being subjected to point loads, average stress combined with long times, or by fatigue from the cyclic system stress. Bowman (1990) suggests that “there may be an impact of both creep and fatigue on the long term strength of older generation PE materials under cyclic load.”

PE PIPE FATIGUE DESIGN PRACTICES

Currently, US PE pipe design practice for pressure and pressure surges is provided in AWWA C901-17, C906-15, M5521 and the Plastic Pipe Institute (PPI) handbook of polyethylene pipe (PPI; 2008 and 2012). The pipe pressure rating (Pressure Class (PC)) is determined utilizing the Recommended Hydrostatic Design Stress (HDS) and the standard ISO equation. For recurring surge events, the allowable peak surge pressure is limited to 1.5 times the PC. The number of acceptable recurring surges that are is not limited.

CHAPTER SUMMARY

The PE material is used in the water and natural gas transportation system in the world. The great advantage of PE is that maintenance can be performed on a section of the pipe without shutting down the whole system. By applying a clamping tool to the PE pipe, the local area can be closed; however, improper installation of electro fusion, tapping and connections may lead to fracture problems.

Fatigue is a progressive, localized, permanent structural change. It is fluctuating stresses and strains that may result in cracks or fracture after a sufficient number of fluctuations. The process of fatigue consists of three stages: 1) Initial fatigue damage leading to crack initiation, 2) Progressive cyclic growth of a crack (crack propagation) and 3) Final, sudden fracture of the remaining cross section.

Polymers are becoming more common in water piping applications due to their advantages over some other materials, such as their corrosion resistance and durability. However, polymers are prone to other types of fracture situations. Fatigue is the major cause of failure in plastic pipes.

Frequent pressure surges or fluctuations in a piping system will cause a fatigue failure. The PE design practices for preventing pressure surge fatigue failures in water pipe have a long history. These practices were developed based on the older generation PE materials. Since this time there has been considerable evolution in the performance of PE pipe and the introduction of a new classification of high performance PE4710 materials.

Chapter 4 EXPERIMENTAL STUDY

INTRODUCTION

Previous chapter provided a comprehensive review of fatigue and fracture in pipeline systems and mainly focused on PE pipes. This chapter will cover the experimental work to help in evaluating the effect of two million cycles of internal water pressure on HDPE pipe. This experimental study includes:

- Fatigue test on a HDPE pipe sample with 16-in. diameter, 15-ft length, DR 17 and a butt fused joint in the middle for 2 million cycles between 125 psi (pressure class) and 188 psi (1.5 times pressure class) and with additional 50,000 cycles up to twice its pressure class, conducted previously at CUIRE (Divyashree; 2014),
- Tensile tests on HDPE dogbone specimens cut from a new pipe and the pipe under fatigue test after passing two million cycles of internal water pressure, based on ASTM D-638 and,
- Scanning Electron Microscopy (SEM) on samples from the new pipe and fatigue-tested pipe.

FATIGUE TEST ON HDPE PIPE

High pressure cyclic loading fatigue test on a new HDPE pipes with a joint was conducted in the CUIRE Laboratory at the UT Arlington by Divyashree et al. (2015). This test determined whether a 16-in. diameter, 15-ft long HDPE (DR 17) with a butt fusion joint in middle can withstand cyclic loads that are 1.5 times higher than the long-term pressure rating of the pipe for an extended period of time (2 million cycles in this study). Dimension of the pipe are provided in Table 4-1. Figure 4-1 shows the HDPE pipe sample.

Table 4-1 Dimensions of HDPE Pipe, Divyashree (2014)

Diameter (in.)	**Length (in.)**	**Inlet/Outlet Pipe Diameter**		
		Valve	Inner Diameter (in.)	Outer Diameter (in.)
16	179.69	1/4	0.995	1.328

Figure 4-1 HDPE Pipe

PPI handbook of polyethylene pipe, is used to define maximum operating pressure. Pipe pressure class is calculated based on Equation 4-1.

$$PC = \frac{2*HDS}{(DR-1)} * SF_E * SF_T \qquad \text{Equation 4-1}$$

Where, PC is pressure class (psi), HDS is hydrostatic design stress which is 1000 psi for PLP water pipe at 73ºF, DR is dimension ratio (ratio of outer diameter to wall thickness), SF_E is environmental service factor which is equal to 1.0 for water and most sanitary sewer and SF_T is temperature service factor equal to 1.0 at 73ºF.

According to Equation 21, pressure class of the pipe in this research is 125 psi. Water pipes should also withstand the surge events. Pressure and surge events can reach up to 2 times of pressure class for occasional surge and up to 1.5 times pressure class for repeated surge. Table 4-2 presents the pressure class and associated working pressure.

Table 4-2 Pressure Class and Associated Working Pressure, Divyashree (2014)

Pressure Class (PC)	Dimension Ratio (DR)	Working Pressure (WP) (psi)	WP + Recurring surge (psi)	WP + occasional surge (psi)
200	11	200	300	400
160	13.5	160	240	320
125	17	125	188	250
100	21	100	150	200

Experiment Setup

The testing setup comprised of a 450-gallon water Reservoir Tank, a Multi-stage Centrifugal Pump (10 HP), a Data Acquisition System, a Control Board, several Pressure Transducers, a DC power supply, one specimen (16-in. diameter), and Control Valves including one Back-flow Pressure Valve, two Solenoid/Pressure Ball Valves, and two Butterfly Valves. A galvanized steel pipe system with pipe diameters of 1-in and 2-in connects the equipment. Before the test setup is completed, it was important to design the test parameters based on the PE4710 HDPE. The discharge, temperature, and head loss were calculated and accounted for.

Initial Project Start-up Procedure

- Power to pump should be off.
- Water filling hose to tank should be properly secured, so water will not flood.
- Reservoir should be full.
- Then ball valve connected to reservoir should be opened.
- The pump should be filled with water and bleed air from pump.
- The inlet valve should be opened to fill up the tank.
- The specimen pipe should be bled from air.
- The bleed valve should be closed until water comes out.
- Outlet solenoid valve should be opened using control board.

- The bypass valve should be partially opened on the inlet side.
- The gate valve on the outlet line, which is near reservoir, should be opened.
- Inlet solenoid valve should be closed.
- Then outlet solenoid valve should be closed.
- Bypass valve on inlet side should get closed.
- The pump should be turned on and backflow valve adjusted to 208 psi.
- Bypass valve should be adjusted, otherwise it takes too long to come to 188 psi.
- The control board should get adjusted and finally the procedure sheet should be checked for operation.

Routine Experiment Start-up

- That tank should be full.
- Control board switches should be plugged in.
- The pressure in Control board should be checked to be right.
- Roc-link software should be online.
- Power the pump.
- The hand operated valve should be opened to bleed the air.
- The cycle time and water temperature should be checked.

Equipment Details

Back-Flow Pressure (BFP) Valve

The back-flow pressure (BFP) control valve is used for two main reasons:

- During water hammer protecting the pump from excessive water pressure and,
- Control excessive pressures of the pump since the inlet control valve to the pipe is not able to sustain excessive pressures.

Figure 4-2 illustrates the back-flow pressure valve. While testing, the pump's head was approximately 480-ft (i.e., 208 psi) and the sample is designed to carry 188 psi at each cycle. So, the pressure is decreased to 188 psi by back-flow pressure control valve assimilating the water head from multi-stage pump and reducing the surge on the inlet valve.

Figure 4-2 Back-Flow Pressure Valve

Inlet and Outlet Solenoid Valves

Opening inlet valve induces pressure inside the specimen to reach 188 psi, and the pressure inside the sample is reduced to 125 psi by outlet solenoid valve reduces. Figure 4-3 shows inlet and outlet valves.

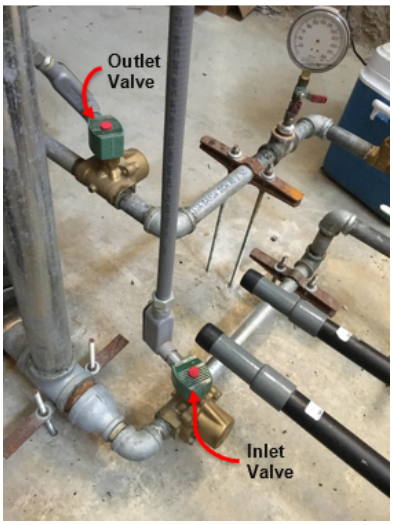

Figure 4-3 Inlet and Outlet Solenoid Valve

Control Board

Signalizing both inlet and outlet solenoid valves to open and close is performed by the Control Board (CB). Also, generation of the data using Roc-link software is done by CB. Figure 4-4 shows the control board and its components.

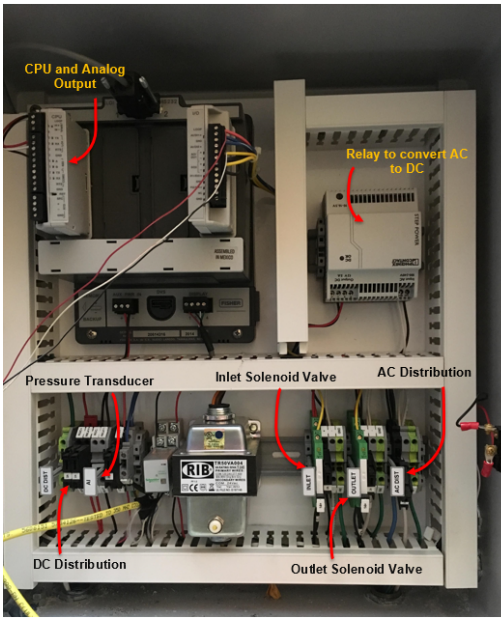

Figure 4-4 Control Board and Its Components

Pressure Transducer

Pressure transducer is used to convert water pressure in the pipe into an analog electrical signal and to regulate convert pressure inside the pipe (125 psi -188 psi).

Multi-Stage Centrifugal Pump

The pump used with this experiment had 10 horse power (HP) to provide input pressure to the solenoid valves. Based on head pressure of the pump and the inlet settings of solenoid valves, the backflow valve opens and closes. Figure 4-5 illustrates the multistage centrifugal pump.

Figure 4-5 Multi-Stage Centrifugal Pump (10 HP)

Other Project Equipment

Water Reservoir: It contains three inlet pipes at top and one outlet pipe at bottom, which is connected to the pump that is 10-ft below. Its dimension is 3-ft height and 42-in. diameter with 450 gallons capacity.

Butterfly Valve: For maintenance purposes, this valve is used to turn on and off the water flow into the pump. To prevent flooding of test area, it should get turned off when the pump is off.

Air Conditioning Unit (Cooler): It is used to maintain the water temperature at 70˚F-73˚F since water temperature impacts cycle time (i.e., with increasing water temperature, the duration to complete one cycle gradually increases). To keep water temperature and cycle duration constant, a cooler was installed.

Fatigue Testing Operation

To create a head pressure of 480-ft, the water from reservoir flow to the10-ft below the reservoir located pump. Pressure of 208 psi is put out by the pump and since the pipe can withstand pressure between 125 psi to 188 psi, a “backflow control valve” is used to back pressure the extra water from the pump to reservoir that is approximately 20 psi. With the control board, inlet and outlet solenoid valves are electrically operated to pressurize the specimen using 188 psi from the pump. The pressure transducer is connected to the end of pipe. A signal is sent to the control board, once the water wave pressure hits the transducer, to operate solenoid valves.

The pressure increases to 188 psi when the inlet valve opens, then the inlet valve closes. For about one second, this pressure impacts the pipe and then outlet valve opens and with decreasing the pressure to 125 psi, it closes. Now, water goes back to reservoir from outlet valve. This process repeated for 2 million cycles. The Control Board (CB) is connected to data logger to collect data from software. The air conditioner works to maintain temperature range between 70°F- 73°F. Figure 4-6 shows the saw-tooth loading pattern of the pipe while under fatigue test.

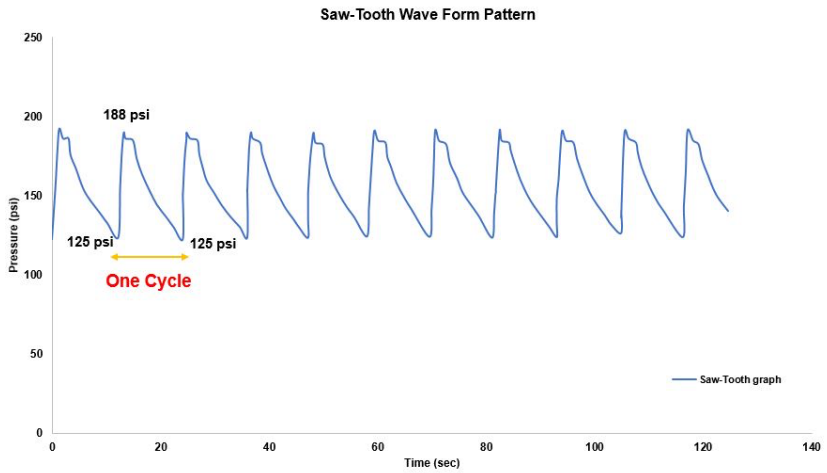

Figure 4-6 Fatigue Loading Pattern of the Pipe Sample

Fatigue Test Results

After about 6 months of testing, the pipe could successfully pass two million cycles of internal water pressure of 125 psi to 188 psi which is 1.5 times of its pressure class. Figure 4-7 shows the graph of deformation of pipe during testing versus time. As can be seen, after approximately 1.1 million cycles, pipe had about 0.27-in. circumferential expansion. Pipe diameter remained constant after 0.54-in. expansion with 1.7 million cycles of internal water pressure.

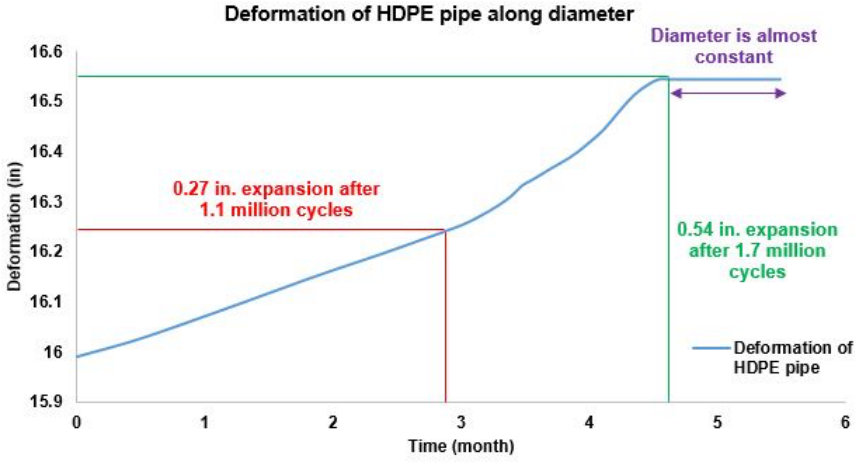

Figure 4-7 Diagram of Deformation vs. Time for Pipe Sample

Discussion

The pipe sample successfully passed 2 million cycles. As shown in Figure 4-7, until approximately 1.7 million cycles, the diameter of pipe remained constant which means higher stresses required to induce higher deformation in the pipe. It also indicates that PE4710 is durable and reliable enough to be used in water pipeline systems.

TENSILE TEST

Tensile tests are performed to measure the strength of material in terms of either the required stress to create large plastic deformation or the maximum tolerable stress of the material (ASM International; 2004). In this test, the specimen should be mounted in the testing machine, between top and bottom grips, and be subjected to tension force until fracture. The measure of deformation before fracture shows material's ductility, which is used in material specifications to assure quality and toughness of the material (ASM International; 2004).

Elastic properties also could be measure during tensile testing using special methods such as ultrasonic techniques. Tensile test's results are used to select appropriate materials for engineering applications, ensure quality and predict material's behavior under different loading conditions.

After successfully passing the fatigue tests, pipe was divided in different sections through its length and then each section is marked based on the angles from 0º to 360º to study the effect of longitudinal and circumferential location of each segment on the after fatigue properties. Figure 4-8 illustrates the marked pipe through its length and perimeter and after cutting each segment.

Figure 4-8 Longitudinal and Circumferential Marking of the Pipe Sample

To clarify the locations of first, middle and last sections of the pipe and also angle-marking definition Figures 4-9 and 4-10 are illustrated. Segments A, E, F, K and J are the selected sections of the pipe to be tested. Dogbone specimen type III came from angles 0º to 360º in 45º intervals (angles 0º, 45º, 90º, 135º, 180º, 225º, 270º and 315º) through pipe's perimeter, illustrated in Figure 4-11, to perform tensile test. For the middle segment (segment F), no sample could be tensile tested, since the responsible company to prepare the samples, destroyed the middle segment and enough samples could not be made.

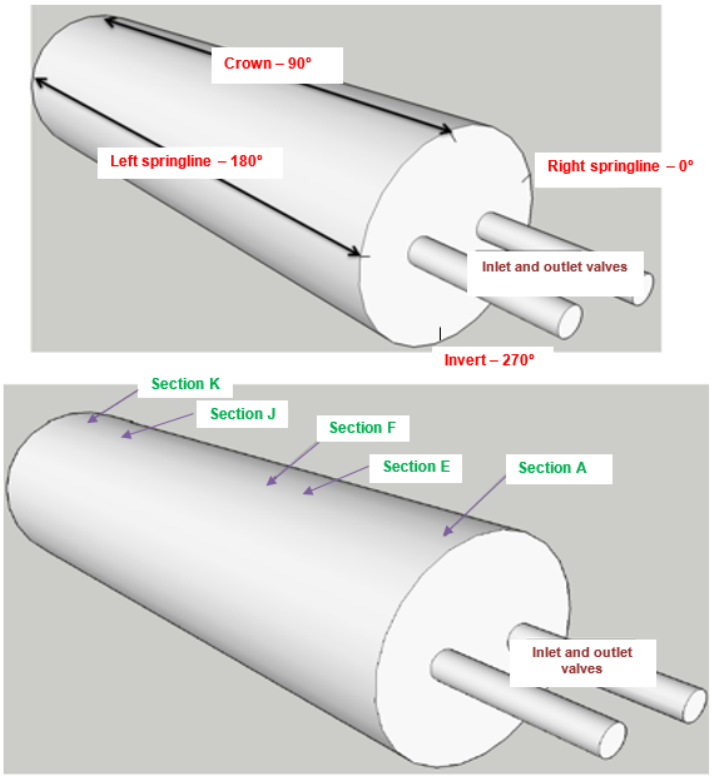

Figure 4-9 Schematic Design of Sections and Angles of the Pipe Sample

Figure 4-10 Schematic Drawing of Longitudinal Marking of the Pipe Sample

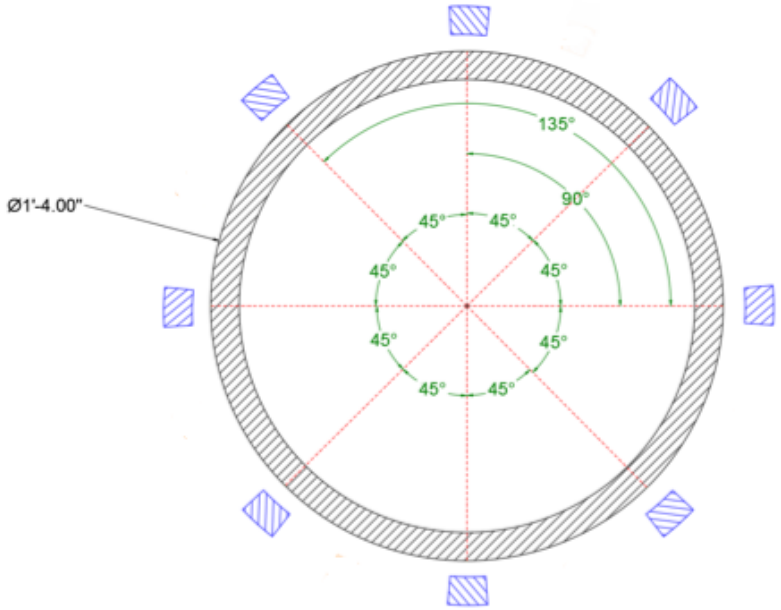

Figure 4-11 Circumferential Locations of Dogbone Specimens Type III

Specimens

A typical tensile test's specimen is shown in Figure 4-12. The gage length is the most important part of the specimen. Reduction of cross sectional area of gage section occurs relative to the remained specimen in gage length and localized deformation and failure will happen in that area.

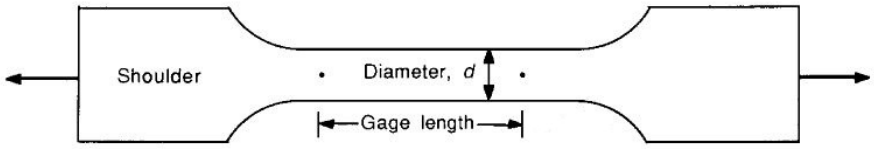

Figure 4-12 Typical Tensile Test Specimen, ASM International (2004)

Tensile test on plastic samples would be based on ASTM D-638. In this study sample type III is cut from the pipe and used for tensile testing. Figure 4-13 shows a schematic design of sample type III.

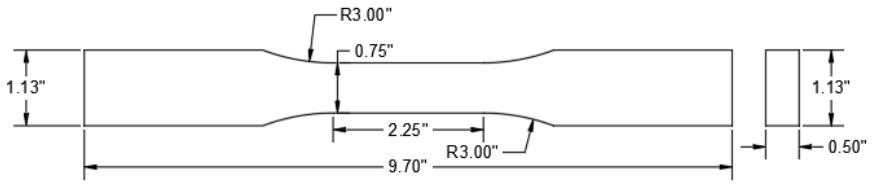

Figure 4-13 Dimensions of Dogbone Sample Type III

Figure 4-14 illustrates a picture of HDPE type III dogbone sample before tensile test.

Figure 4-14 Dogbone Specimen Type III Cut from Fatigue-Tested Pipe Sample

Specimens' numbering and exact dimensions, temperature and humidity are shown in Table A-1 and Table A-2 in the Appendix A. The number in each sample's ID shows the circumferential angle of the pipe's sample and the alphabet shows the longitudinal location of the segment; i.e., specimen ID "45-A" shows the sample was located at the angle 45º of the segment A (first segment) of the original pipe. More pictures of samples and testing are provided in Appendix A.

Testing Machine

Universal testing machines are the most common testing machines used for tensile tests. They can test materials under tension, compression or bending and show the outcome as stress-strain curves.

Based on the method of applying load, testing machines can be electromechanical or hydraulic.

An electromechanical machine is shown in Figure 4-15. It includes a variable-speed electric motor, a gear reduction system, and screws that move the crosshead up or down to create tension or compression.

A hydraulic testing machine is illustrated in Figure 4-16, which includes a single or dual-acting piston that moves up and down the crosshead.

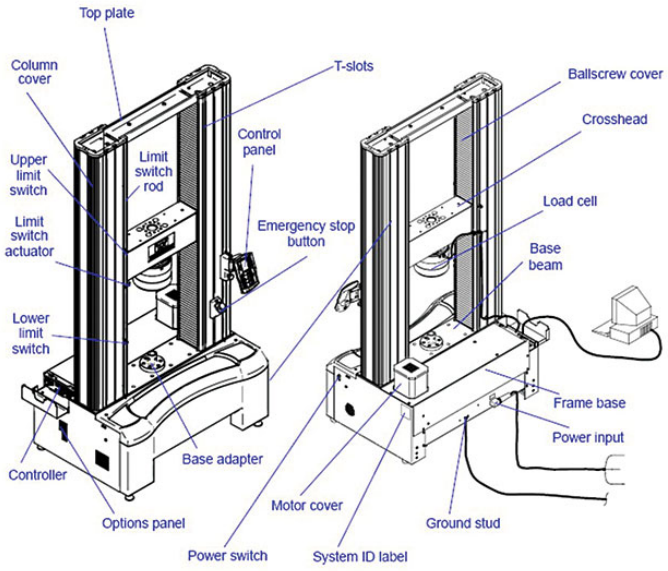

Figure 4-15 Components of a Electromechanical Universal Testing Machine, ASM International (2004)

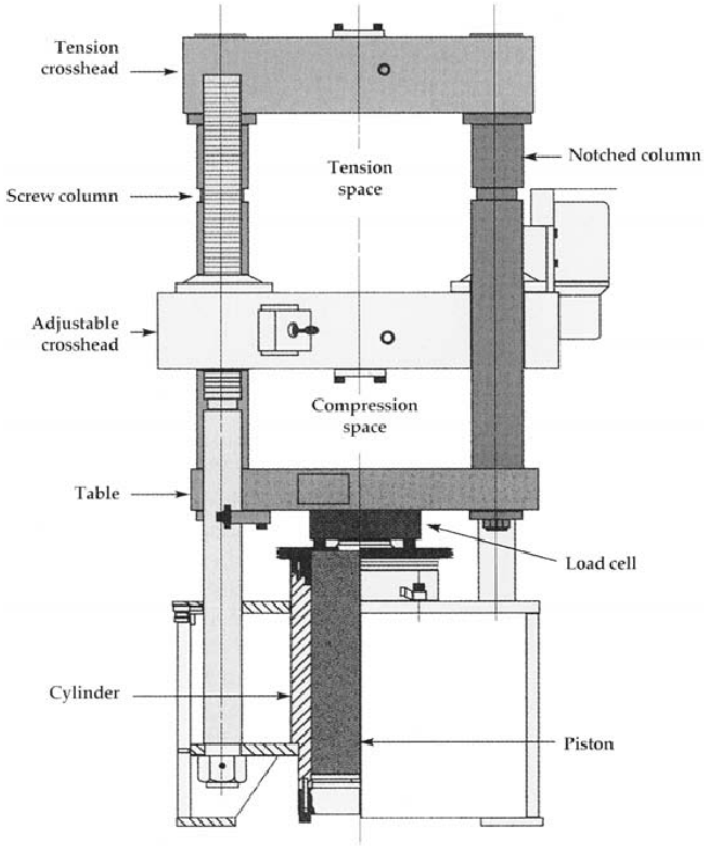

Figure 4-16 Hydraulic Universal Testing Machine and Its Components

ASM International (2004)

In terms of capability of performing wider range of test's speeds and longer displacements, electromechanical machines work much better that hydraulic ones but if the cost-effectiveness and applying higher loads are the main points, hydraulic machines would be the better option. In this study, testing machine INSTRON 4467 was used to perform tensile tests. Figure 4-17 shows the testing machine used for this dissertation.

Figure 4-17 Instron 4467 Testing Machine Used for this Dissertation

This tensile machine, has a pair of pneumatic gripper which is used to clamp the ends of specimen. In the operation process, the lower grip keeps stationary and the upper grip moves with the certain defined speed. The specimen is mounted between the grips and it the phenomenon of slipping can be avoided because of the clamp. The testing machine was connected to a data acquisition system and a desktop computer with software to collect the test data.

Tensile Test Performance

Tensile tests were performed on 38 dogbone specimens, based on ASTM D-638. Tests were performed at HTS piping company at Houston, on Tuesday, August 22nd 2017 and Wednesday, October 18th 2017. The temperature of the room ranges between 74º-76º F with humidity of 42-45%. The rate of tensile test was 2 in./min for all tests. Figures 4-18 shows how the specimen is mounted on the testing machine and Figure 4-19 and 4-

20 illustrate the pulling process of the HDPE dogbone specimen and rupture of specimen, respectively.

Figure 4-18 Placement of Dogbone Specimen in Testing Machine

Figure 4-19 Pulling the Specimen

Figure 4-20 Rupture of the Specimen

Stress-Strain Curve

Tensile strength is one of the important mechanical property of material and is defined as force per unit area or for some non-homogeneous materials. While stretching the samples, the cross-sectional area would change, so the area used in the calculation of stress is the original non-deformed cross-sectional area A_o. Also, strain is measured as changes in length of the samples.

After placing the sample in testing machine and applying tensile force, recording the tensile force as a function of elongation of gage length started. Using these data, testing load-deflection curve is produced. This load-deflection curve would be converted to engineering or nominal stress-strain curve using Equations 4-2 and 4-3.

$$\sigma = \frac{F}{A_0}$$ Equation 4-2

$$\varepsilon = \frac{\Delta L}{L_0}$$ Equation 4-3

Where F is applied tensile force (lb.), A_0 is initial cross section (in.^{2}), ΔL is elongation (in.) and L_0 is initial length (in.).

Once necking starts and developed, A_0 would not be the cross sectional area and it should be measured directly at the base of the neck. Because the true stress calculated, is the true stress at the base of the neck, the true strain should also be at the base of the neck. Thus the true stress and true strain can be calculated as Equations 4-4 and 4-5, respectively.

$$\sigma_{true} = \sigma_{nom}(1 + \varepsilon_{nom}) \quad \text{Equation 4-4}$$

$$\varepsilon_{true} = ln\,(1 + \varepsilon_{nom}) \quad \text{Equation 4-5}$$

Results of Tensile Test

Tensile tests were performed on the dogbone shaped new and fatigue-tested specimens. Results of the yield stress, yield strain and strain at rupture for each segment are presented. Of 38 samples tested, inappropriate results were discarded and 30 other remained approximately accurate results were presented and compared. Since there was not any difference between the results of different circumferential locations of dogbone specimens of each section cut from HDPE pipe sample after fatigue test (circumferential angle), the study focused mainly on the effect of longitudinal locations of specimens and comparison with new HDPE dogbone specimens. So, to prevent confusion, specimens called just as numbers 1 to 6 for each section.

Yield Strain

Table 4-3 and Figure 4-21 present the results of yield strain of each fatigue-tested section and new specimens as well as location of each section on the pipe sample.

Table 4-3 Results of Tensile Test on HDPE Dogbone Specimens, Yield Strain

Yield Strain (%)					
Specimen No.	**Section A**	**Section E**	**Section J**	**Section K**	**New**
1	22	18	21	21	25
2	20	17	19	20	23
3	19	16	18	19	22
4	18	16	17	17	21
5	18	15	16	16	21
6	17	14	14	16	20
Mean Value	19	16	17	18	22
Standard Deviation	1.6	1.3	2.2	1.9	1.6

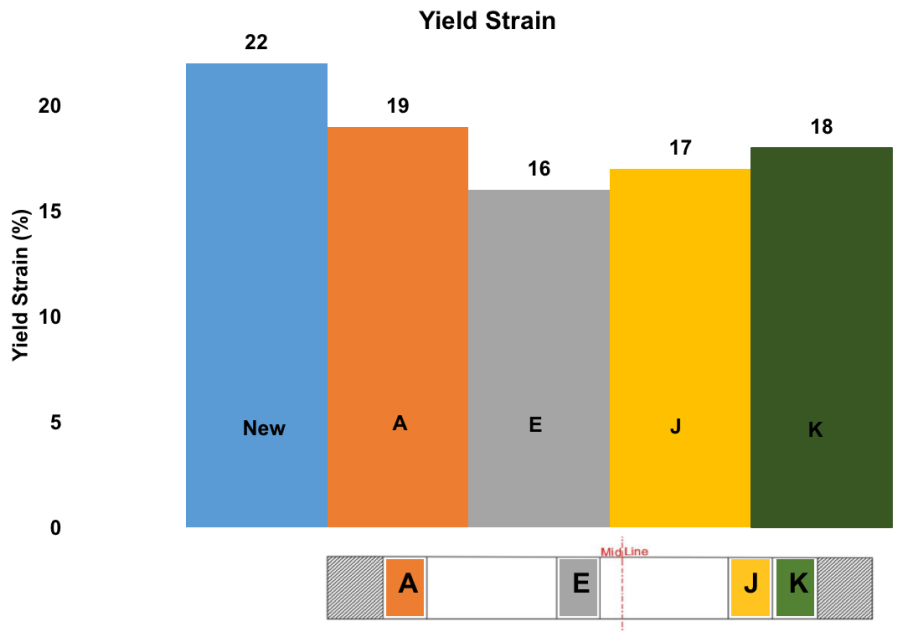

Figure 4-21 Yield Strain of New and Fatigue-Tested Dogbone Specimens

As can be seen from the graph above, yield strain in all segments (A, E, K and J) is decreased comparing to the new HDPE samples. Comparison of mean value of yield strains of sections A, E, J and K with new samples show approximately 14%, 27%, 23% and 18% reduction in yield strain after fatigue test comparing to new specimens, respectively.

Also, results indicated that end sections A and K, have slightly larger yield strain comparing to other two sections, E and J.

Tensile Strength

Tensile strength of specimens cut from various sections of fatigue-tested pipe sample along with results of tensile test on new specimens are presented in Table 4-4 and Figure 4-22.

Table 4-4 Results of Tensile Test on HDPE Dogbone Specimen, Tensile Strength

Tensile Strength (psi)					
Specimen No.	**Section A**	**Section E**	**Section J**	**Section K**	**New**
1	3681	3611	3645	3659	3626
2	3662	3602	3627	3648	3536
3	3658	3561	3594	3637	3534
4	3597	3527	3568	3625	3519
5	3593	3493	3531	3569	3483
6	3487	3471	3496	3511	3424
Mean Value	3613	3544	3577	3608	3519
Standard Deviation	65	52	52	52	61

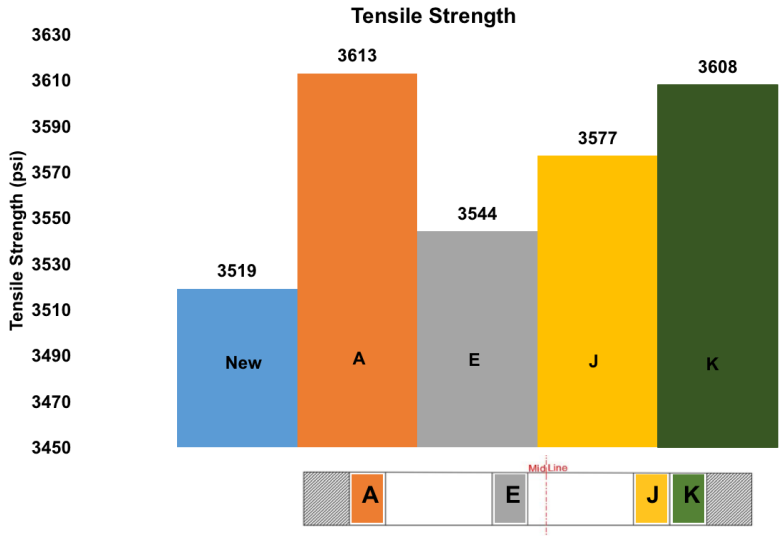

Figure 4-22 Tensile Strength of New and Fatigue-Tested Dogbone Specimens

As shown in Table 4-4, yield stress of specimens have increased compared to the new ones. For end sections, A and K, the increase is approximately 2.5%, and for sections E and J, it is roughly 1%.

Rupture Strain

Table 4-5 and Figure 4-23 present the rupture strain of different samples.

Table 4-5 Results of Tensile Test on HDPE Dogbone Specimens, Rupture Strain

Rupture Strain (%)					
Specimen No.	**Section A**	**Section E**	**Section J**	**Section K**	**New**
1	269	235	238	287	214
2	261	227	224	264	204
3	246	193	221	241	198
4	211	189	214	206	183
5	209	177	202	198	177
6	196	172	185	179	169
Mean Value	232	199	214	229	191
Standard Deviation	28	24	17	38	16

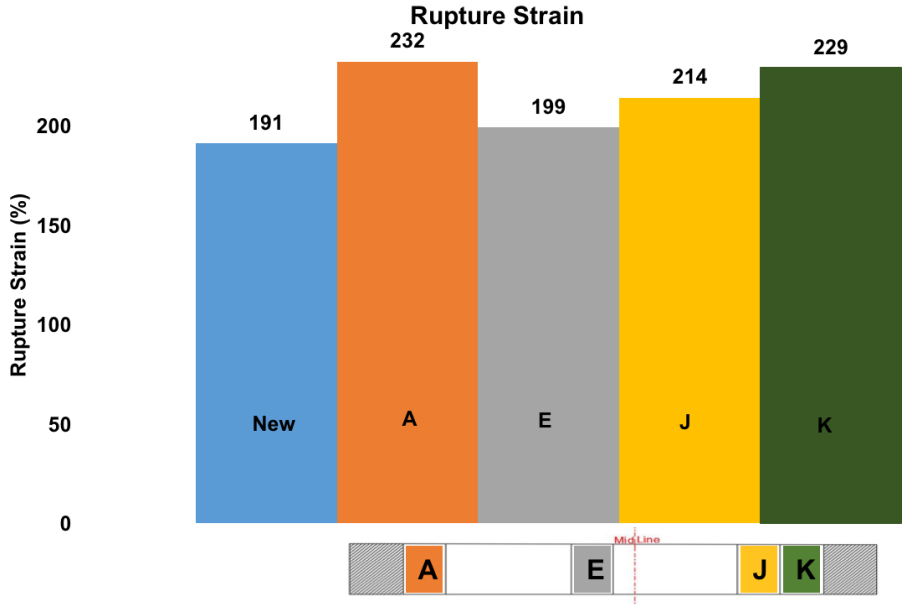

Figure 4-23 Ultimate Strain of New and Fatigue-Tested Dogbone Specimens

As shown in Figure 4-23, considering the mean value of each set of specimens, at two end sections (A and K) rupture strain has increased approximately 20% compared to the new specimens and for sections E and J increases in rupture strain are approximately 4% and 7% compared to the new ones.

Discussion

The results of tensile test showed the longitudinal location of the specimens in each segment has an almost considerable effect on the after fatigue mechanical properties of the material. Both end sections are somehow restricted in free expansion due to wooden support at the bottom of these parts and also, because of tight cap at both ends, while other segments can freely expand. HDPE is a semi-crystalline material which shows completely different behavior under different stress levels, strain rates and temperatures.

An important phenomenon that affects the tensile strength and yield stress of a semi-crystalline polymer is re-orientation of polymer chains. According to Juska et al. (1982) and Crist et al. (1989) the yield behavior of semi-crystalline polymers is associated with morphology transformation from original isotropic structure to re-oriented one. Transforming to re-oriented structure creates a stiffer structure. It means higher modulus of elasticity with increasing yield stress while decreasing yield strain simultaneously. To clarify forming this re-oriented structure, it should be considered that HDPE molecular structure includes two regions: an ordered crystalline and a random amorphous. The crystalline region contains packs of folded molecules (lamella), which are separated by the amorphous region. One vital factor which impacts deformation is the inter-crystalline polymer chains. Three types of inter-crystalline chains include Cilia which are suspended chains from the end of a crystalline chain, loose loops which are chains that begin and

end in the same lamella and tie molecules that are chains which begin and end in adjacent lamellae.

Applied tensile load to the face of the lamellae pull and deform the tie molecules. Tie molecules counted as reinforcing elements since they are intricately tangled. In this “mortar and brick” model, lamellae act as bricks and the tie molecules act as mortar which keeps the bricks together. Micro-fibrils, which present mainly in an oriented polymer, are connected to many tie molecules through the amorphous region and make a fibrous stiffness in the material. Therefore, increase in tensile strength and decrease in yield strain occurs. But then under applied stresses, the tie molecules get pulled to the point that they cannot withstand the applied stresses. It causes the lamellae to break up to smaller units and ductility after yield point (rupture strain) increases. Considering the effect of micro-cracks and strain accumulation in HDPE fatigue-tested specimens, it was expected to have less tensile strength, in samples cut from sections E and J comparing to sections A and K.

SCANNING ELECTRON MICROSCOPY (SEM)TEST

This test is a type of electron microscope that images a sample by scanning it with a high energy beam of electrons in a raster scan pattern. In electron microscopes, generation of electrons are by heating a tungsten filament to a temperature of about 2800°C (electron gun). Then electro-magnetic lenses focuses electron beam and the apertures in the column to a very small sharp point. The electron interacts with the atoms that make up the sample producing signals that contain information about the sample’s surface of topography, composition and other properties. Figure 4-24 shows parts of SEM, which generate electrons.

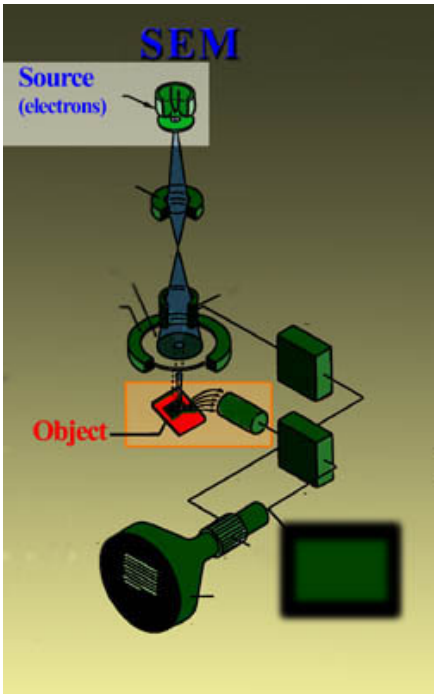

Figure 4-24 Source of Generation of Electrons in SEM, Hafner (2007)

Characteristics that can be viewed on SEM includes:

- Topography- The surface features of an object or “how it looks”, its texture;
- Morphology- The shape and size of the particles making up the object;
- Composition- The elements and compounds that the object is composed of and the relative amounts of them;
- Crystallographic Information- How the atoms are arranged in the object;
- There is a direct relation between all above features and material properties.

Components of SEM Instrumentation

All SEMs have essential below mentioned components:

- Gun or electron source
- Electron lenses
- Sample stage

- Signals' detector
- Display device

And it also requires, power supply, cooling and vacuum system and a stable floor free of any kind of vibrations. A schematic drawing of SEM instrumentation is shown in Figure 4-25.

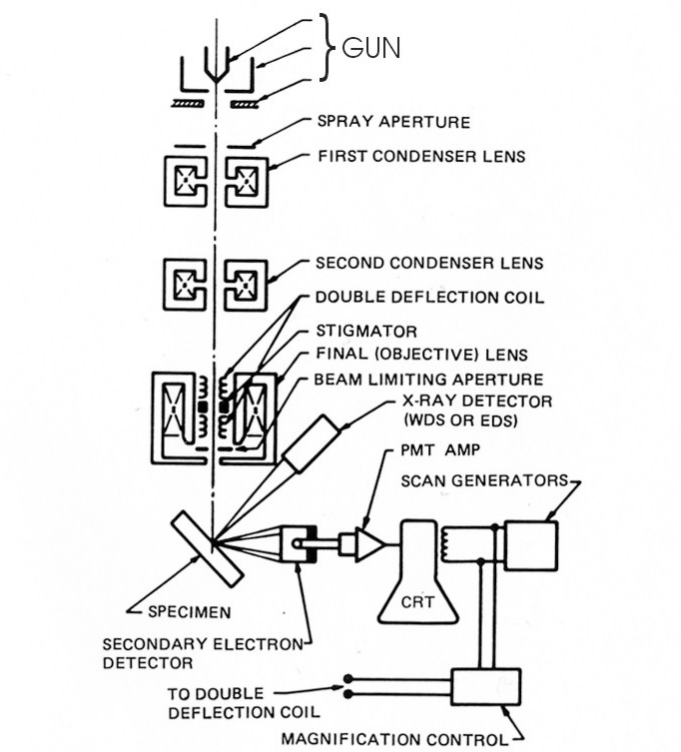

Figure 4-25 Schematic Drawing of SEM Instrumentation, Joy (1989)

Application

SEM is used to generate high-resolution images of different objects' shapes. It also can be used to show difference in chemical compositions by generating elemental map or detecting chemical analyses, identification of different phases based on mean atomic number (generally depending on relative density) and compositional maps according to difference in trace element "activators." The SEM is also widely used to identify phases

based on qualitative chemical analysis and/or crystalline structure. Very small features and objects, as tiny as 50 nm in size, can be measured exactly using the SEM. Rapid discrimination of phases in multiphase samples can be accomplished by backscattered electron images (BSE). SEMs equipped with diffracted backscattered electron detectors (EBSD) can be used to examine micro-fabric and crystallographic orientation in many materials.

Testing process

Rectangular specimens were cut from a new HDPE and HDPE fatigue tested pipe samples to compare the SEM test results. Figure 4-26 shows SEM samples.

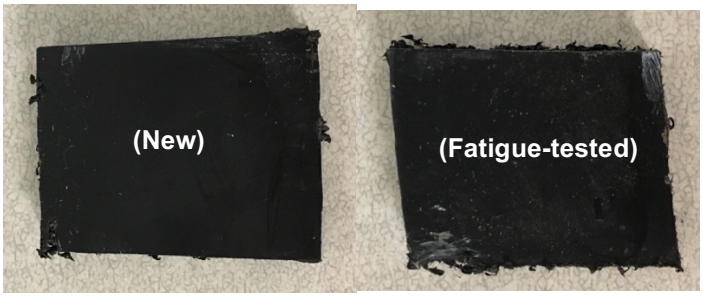

Figure 4-26 Rectangular Samples for SEM Test

The SEM test was performed with Hitachi S-3000N testing machine at material science and engineering lab at the University of Texas at Arlington, as shown in Figure 4-27.

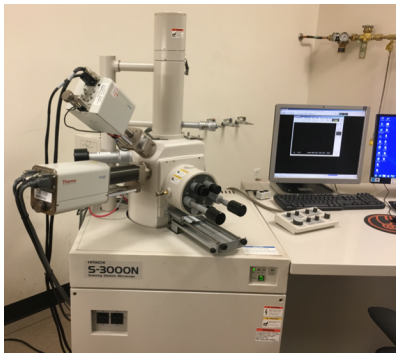

Figure 4-27 Hitachi S-3000N Testing Machine to Perform SEM Test

Surfaces of samples got carefully cleaned with alcoholic pads and glued to a metal cylinder to be mounted in the testing machine as shown in Figures 4-28 and 4-29.

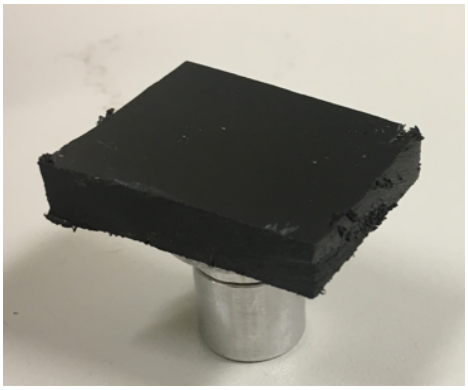

Figure 4-28 Preparing the Specimen to be Placed in the SEM Testing Machine

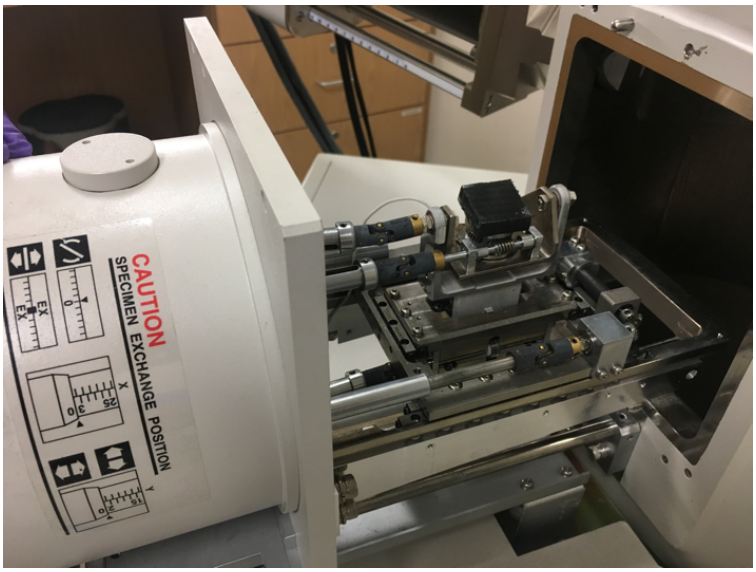

Figure 4-29 Placing the Specimen in the SEM Testing Machine

For the test the accelerating voltage was set at 25 kV. Accelerating voltage (kV) is the difference between filament and the anode's voltage which accelerates the electron beam towards the anode. Figure 4-30 shows the filament and anode in SEM testing machine. The accelerating voltage of a typical SEM ranges between 0 to 30kV.

In general, selection of acceleration voltage depends on the type of information which is required, the type of SEM testing machine available, material type (i.e., a highly

insulating ceramic materials versus a metal versus plastic), geometry (i.e., a thin film versus a bulk sample versus powder) and techniques used for preparation. Higher accelerating voltage causes electron beams penetrate deeper within the sample, depending on the density of the sample and its elemental composition, so results in higher signals and lower noise in the images.

However, higher accelerating voltages create a phenomenon called charging. In this phenomenon, the number of escaping electrons from the surface of the specimen is lower than the number of incident electrons, so it builds a negative charge at the hitting point of electron beam with specimen's surface. It means there is lack of an even flow of electrons emitted from the specimen's surface which leads some unusual effects on the image such as abnormal contrast, deformation and shift. If the specimen is coated appropriately with a metal, then the issue of charging would be minimized.

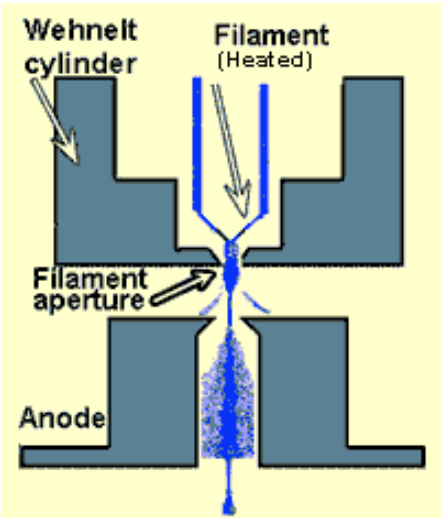

Figure 4-30 A Conventional SEM Source of Electrons with Thermionic Tungsten Filament, Hafner (2007)

SEM Topography Test

Surface topography test were performed on the specimens to compare surfaces of the new HDPE specimen and fatigue-tested HDPE specimen. Figure 4-31 shows how the topography test can be monitored on the computer connected to the testing machine.

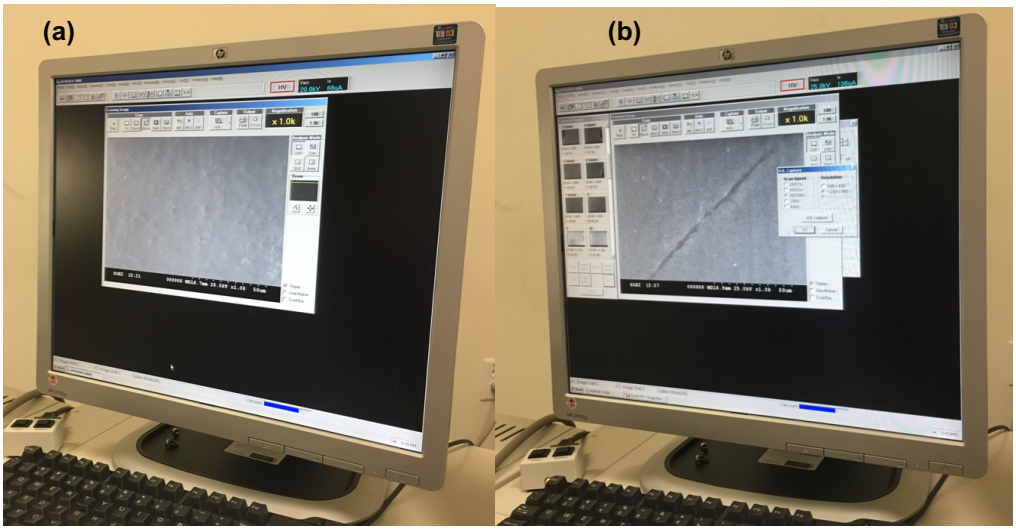

Figure 4-31 Monitoring Surface Topography of (a) New Specimen and (b) Fatigue-Tested Specimen

Results of surface topography showed that there are so many micro-cracks in the fatigue tested pipe comparing to the surface of a new pipe sample. Figures 4-32 and 4-33 illustrate the new and cracked surfaces of specimens, respectively.

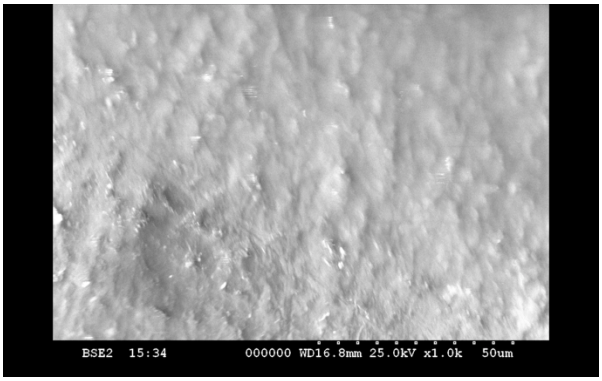

Figure 4-32 SEM Test Result of Surface of New HDPE Specimen

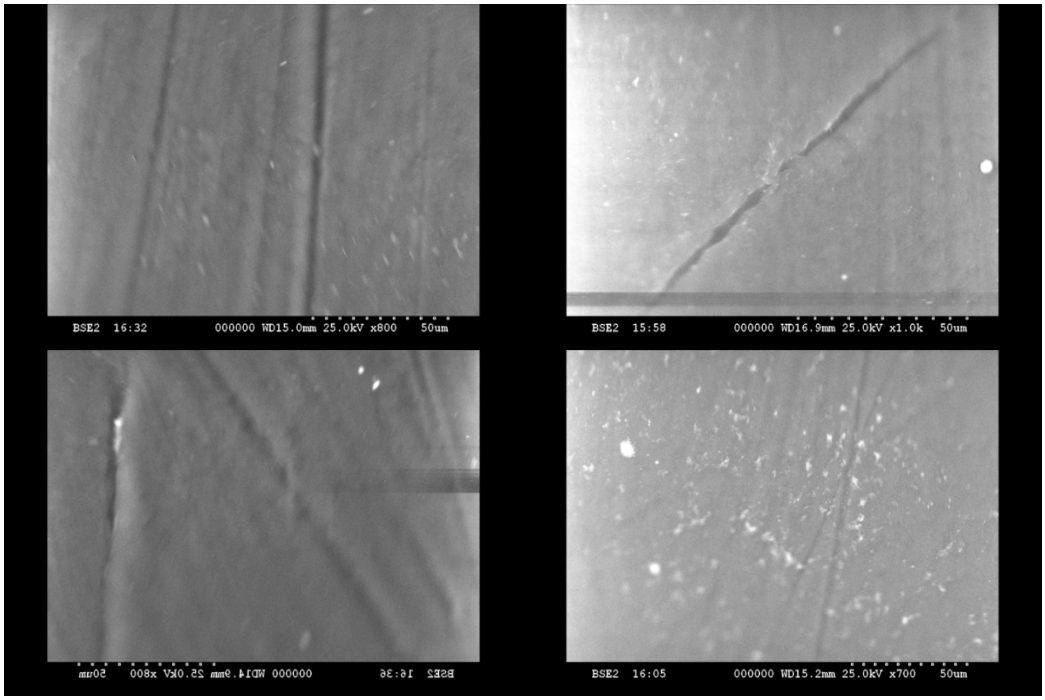

Figure 4-33 SEM Test Result of Surface of Fatigue-Tested HDPE Specimen Including Many Micro-cracks

Since HDPE is not electrically conductive, to have higher quality images, after performing SEM test on uncoated surfaces of specimens, the test was repeated with and metal-coated surfaces of samples. A thin layer of silver was applied on the surfaces of both specimens with CrC-100 Sputtering system. Figure 4-34 shows CrC-100 Sputtering system.

Figure 4-34 CrC-100 Sputtering System

Steps of operation procedure for this system are:

1. The specimen should be loaded on the sample chamber after venting.
2. Then the chamber should be closed.
3. Cooling water should be turned on.
4. Option “coat” should be selected, as illustrated in Figure 4-35.
5. Vacuum pump should be turned on, as shown in Figure 4-35.
6. When the pressure is below 0.001 millitorr, Argon gas should be turned on, as illustrated in Figure 4-35.
7. On three-way valve, as shown in Figure 4-36, gas should be selected and the pressure must be between 5 and 10 millitorr.
8. Finally, time should be set up and “process” turned on. When time is over, the process will be off automatically.

Figure 4-35 Process of Metal-Coating HDPE Specimens (Steps 4 to 6)

Figure 4-36 Process of Metal-Coating HDPE Specimens (Steps 7 and 8)

Figure 4-37 shows specimens after being silver-coated. Results SEM test of metal-coated specimens are illustrated in Figures 4-38 and 4-39 for new and fatigue-tested samples, respectively.

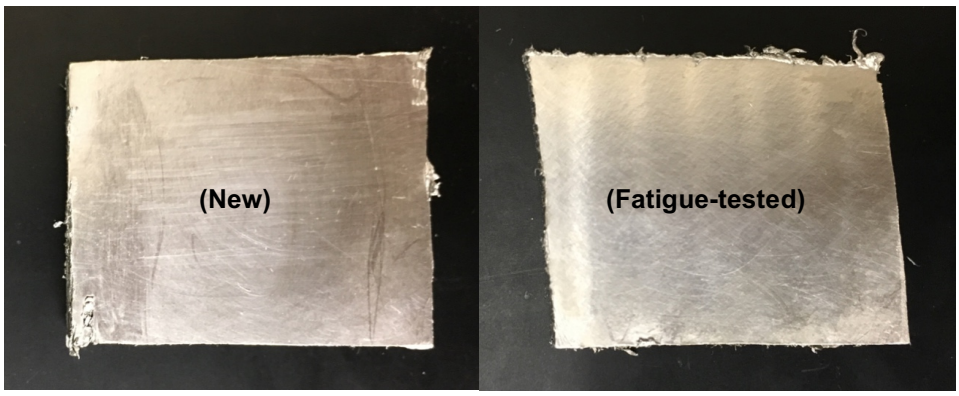

Figure 4-37 Silver-Coated HDPE Specimens for SEM Testing

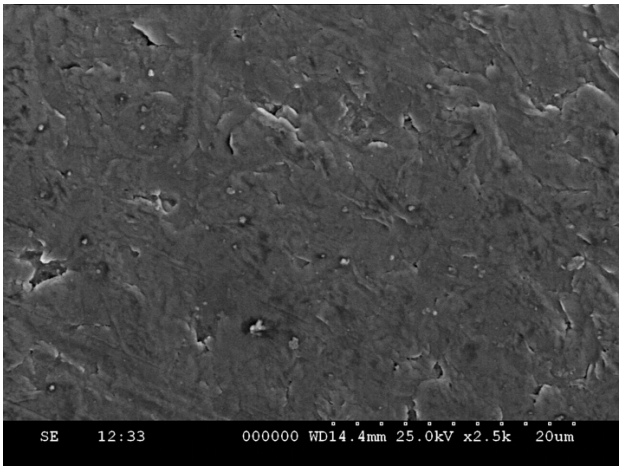

Figure 4-38 Surface of New HDPE Specimen after Being Silver-Coated

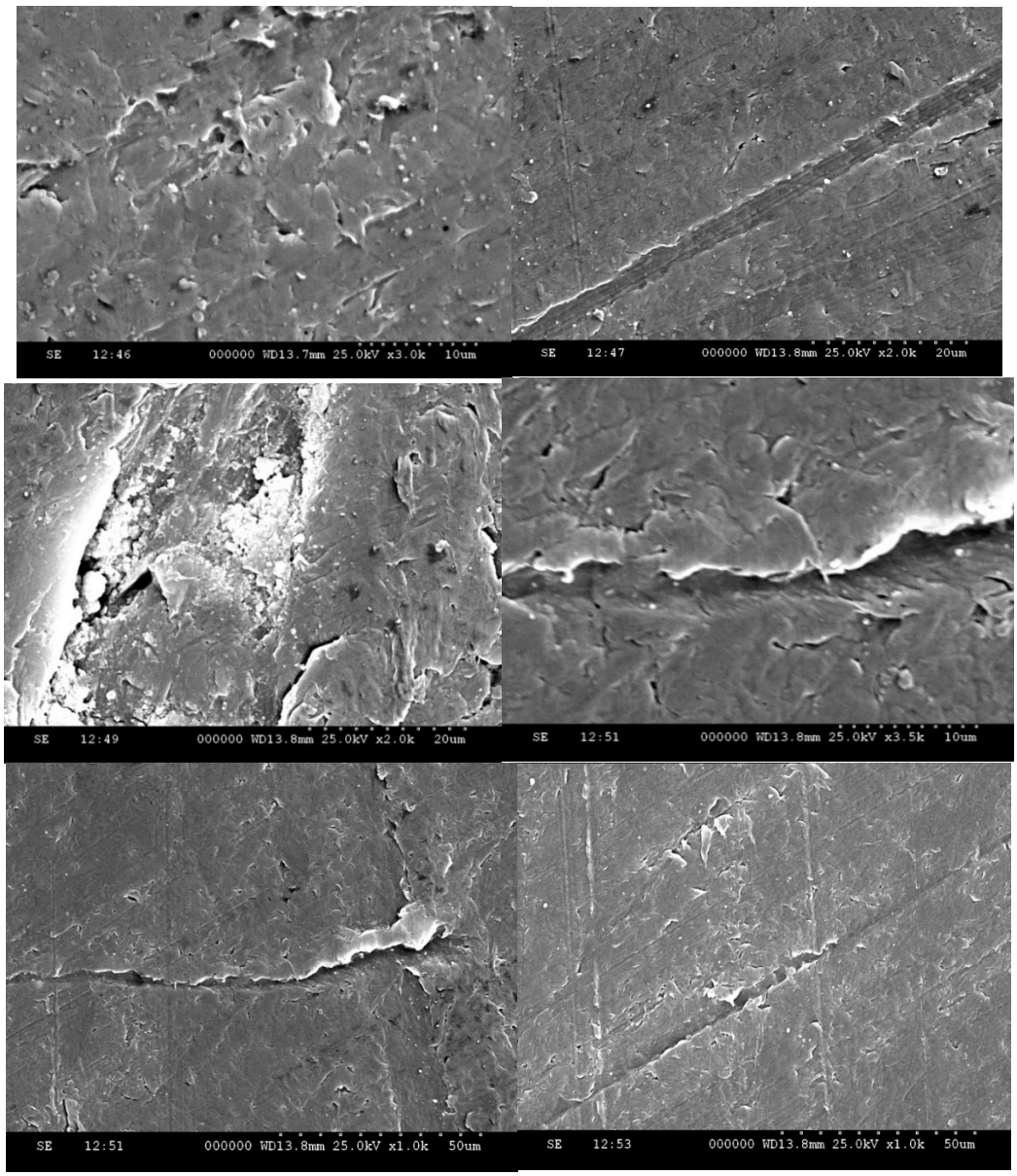

Figure 4-39 Micro-Cracks on the Surface of Fatigue-Tested HDPE

Specimen after Being Silver-Coated

SEM Composition Test Results

Scanning Electron Microscopy (SEM) composition test was performed on the specimens. Results of composition test on new HDPE sample showed it includes 100% carbon, as is shown in Figures 4-40 and 4-41.

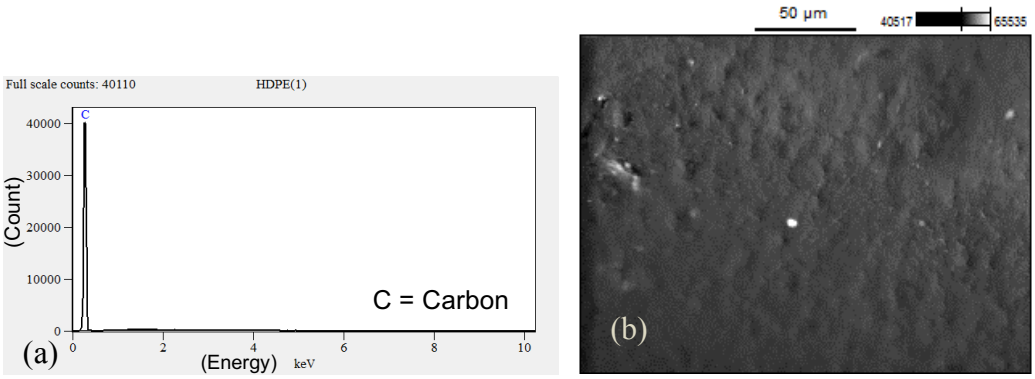

Figure 4-40 (a) Chemical Composition of New HDPE Specimen (b) Surface of New HDPE Specimen for Composition Analysis

Element Line	Int. Cps/nA	Z	A	F	ZAF	Weight %	Weight % Error	Norm. Wt.%	Norm. Wt.% Err	Atom %	Atom % Error
C K	37.169	1.000	1.001	1.000	1.001	100.00	± 0.26	100.00	± 0.26	100.00	± 0.26
Total						100.00		100.00		100.00	

Figure 4-41 Composition Analysis of New HDPE Specimen

Two different points on fatigue tested HDPE specimen were selected to perform composition analysis. Figure 4-42 illustrates the selected locations of un-cracked point and cracked point of fatigue-tested specimens for chemical composition test to be performed.

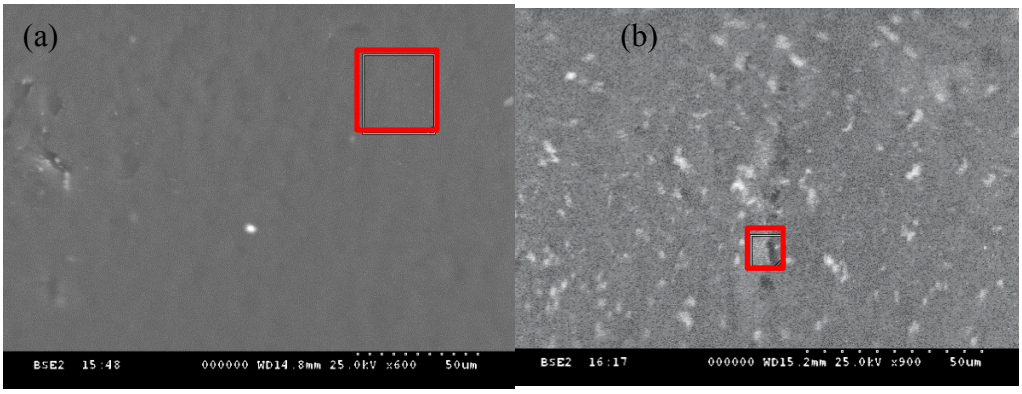

Figure 4-42 Selected Locations on (a) Un-cracked (b) Cracked Points of Fatigue-Tested HDPE Specimen

Figures 4-43, 4-44, 4-45 and 4-46 show results of SEM composition test on fatigue tested HDPE specimen, for un-cracked and cracked points. The results indicated that un-cracked point composition includes 100% of carbon while cracked point includes 98.5% of carbon and 1.5% of oxygen in its composition.

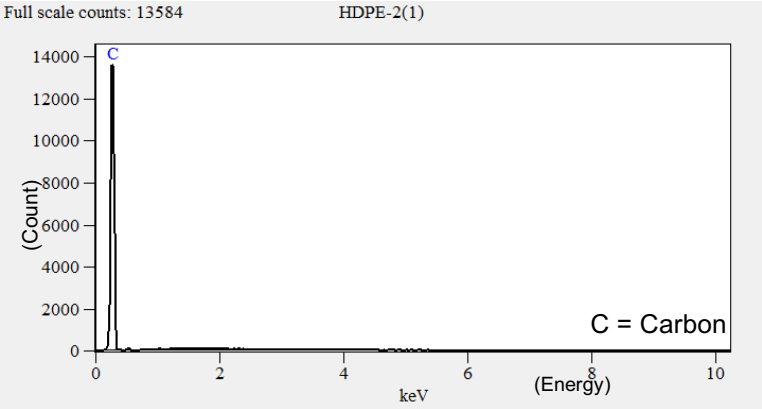

Figure 4-43 Chemical Composition of an Un-Cracked Point of Fatigue-Tested HDPE Specimen

Element Line	Int. Cps/nA	Z	A	F	ZAF	Weight %	Weight % Error	Norm. Wt.%	Norm. Wt.% Err	Atom %	Atom % Error
C K	13.379	1.000	1.001	1.000	1.001	100.00	± 0.33	100.00	± 0.33	100.00	± 0.33
Total						100.00		100.00		100.00	

Figure 4-44 Composition Analysis of an Un-Cracked Point of Fatigue-Tested HDPE Specimen

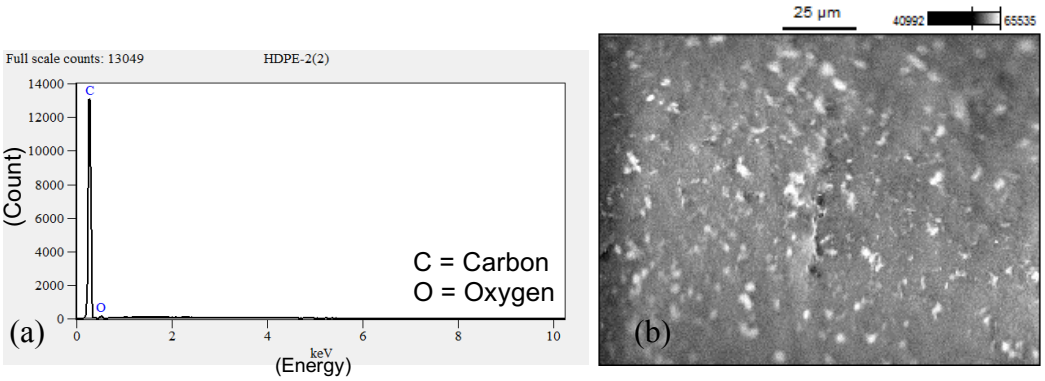

Figure 4-45 (a) Chemical Composition of a Cracked Point of Fatigue-Tested HDPE Specimen (b) Surface of Crack Selected for Composition Analysis

Element Line	Int. Cps/nA	Z	A	F	ZAF	Weight %	Weight % Error	Norm. Wt.%	Norm. Wt.% Err	Atom %	Atom % Error
C K	12.835	1.000	1.001	1.000	1.001	100.00	± 0.34	100.00	± 0.34	100.00	± 0.34
O K	0.000	1.052	12.562	1.000	13.216	0.00	---	0.00	---	0.00	± 0.00
Total						100.00		100.00		100.00	

Figure 4-46 Composition Analysis of a Cracked Point of Fatigue-Tested HDPE Specimen

Discussion

According to Donald and Dale (2009) HDPE pipe materials are heavily stabilized with antioxidant additives (some with additional UV additives) to last multiple years of continuous service in the field and, therefore, unless the antioxidants are consumed, it is not likely to get oxidized when exposed to air (or typical potable water) in cracked or un-cracked areas. Pipe extrusion is typically at higher temperature (370° F to 420° F) and, at this temperature HDPE is more vulnerable to oxidation than at ambient temperature (Donald and Dale; 2009). While under the protection of sufficient antioxidants, the

chance of oxidation is low but if the antioxidants in HDPE pipe are insufficient or depleted, oxygen can cause chain scission for polyethylene backbone and results in weakened physical properties due to molecular structure changes, i.e., creation of impurity and defection in the pipe.

In the SEM topography many micro-cracks were observed in the inner surface of the pipe after being fatigue tested. Defects such as impurities, i.e., air bubbles or imperfections, caused cracks to initiate. In the SEM test imperfections were observed at the inner surface of the pipe wall which emerges that crack initiation most likely occurs at these defects at the inner surface and then propagate through the wall in a longitudinal direction. This longitudinal cracking demonstrates that the driving force is oriented circumferentially (hoop stress).

Failure mode in the pipe is the actual procedure of pipe failure, not the failure mechanism. Failure mode depends on the material of the pipe and its diameter, e.g., in smaller diameter pipes which have relatively low water pressure and smaller moments of inertia, longitudinal bending derives circumferential failure and larger diameter pipes because of having higher internal water pressure and larger moment of inertia, mainly longitudinal cracking and shearing at the bell occur. In this study, the HDPE pipe with 16-in diameter classified as large diameter pipes and longitudinal cracking was expected, as the SEM results also proved existence of longitudinal cracks in the inner surface of HDPE fatigue-tested pipe.

CHAPTER SUMMARY

PE4710 pipe with 15-ft long and 16-in. diameter (DR 17) successfully passed two million cycles of internal water pressure. After performing fatigue test, dogbone specimens type III, based on ASTM D638, were cut from the pipe to perform tensile test. Results of tensile tests indicated that circumferential location of HDPE specimens does

not have any effect on the mechanical properties of samples while longitudinal location have an almost considerable impact on yield strain, tensile strength and rupture strain. According to the test results, tensile strength and rupture strain of fatigue-tested specimens were increased comparing to the new ones but yield strain were considerably reduced. Also, longitudinal cracks were observed in SEM test of the specimens cut from fatigue-tested pipe sample.

Chapter 5 FINITE ELEMENT MODELING

INTRODUCTION

Previous chapter presented information about the experimental study and results and discussion. In this chapter a brief description about Finite Element Modeling (FEM) part of the study has been given. Detailed information about the different aspects of this study, including the geometry of models, mechanical properties of materials and modeling details are presented. Also, since this study is a numerical study, it is highly essential to ensure the accuracy of modeling results. Therefore, the results of tensile test are used to verify the material properties used in the study. For this research FE modeling software ABAQUS 6.14-3 was used.

The results presented in this chapter is based on a theoretical Finite Element Analysis (FEA) model that while was verified with material tensile test, but was not verified with real conditions with actual fatigue cycles that are commonly determined by physical testing. These results are based on capability of the ABAQUS software (version 6.14-3) at the time of study, so this dissertation developed a preliminary programing code to be used along with ABAQUS software to perform cyclic analysis. Since actual fatigue testing of HDPE pipe is time consuming, the suggested FEA model was developed to simulate actual testing, but it is preliminary and did not agree with actual cyclic test results presented by physical testing at JANA Lab, UTA-Arlington/CUIRE and the UK Water Industry Research (UKWIR). The FEA model developed with this dissertation would need to be further developed, studied and validated to properly evaluate the fatigue resistance of HDPE material.

THE FINITE ELEMENT METHOD

In the finite element method, the structure body of interest can be subdivided into many discrete shapes which are called elements. The stiffness finite element method is usually used in stress analysis problems. This approach is outlined below for the two dimensional case.

Figure 5-1 shows an isoperimetric continuum element for two dimensional plane stress or plane strain problems, together with local and global coordinate axes. The local coordinates vary from -1 to +1 over the element area.

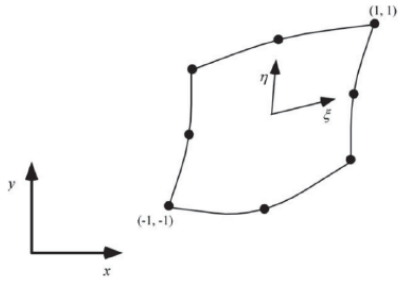

Figure 5-1 The Local Coordinates, Lapidus et al. (1982)

Consider one of points on the element at (ξ, η), the global coordinates of this point can be written as Equations 5-1 and 5-2.

$$X = \sum_{i=1}^{n} N_i(\xi, \eta) \qquad \text{Equation 5-1}$$

$$Y = \sum_{i=1}^{n} N_i(\xi, \eta) y_i \qquad \text{Equation 5-2}$$

Where n is the number of nodes in the elements and N_i is the shape functions corresponding to the node i, whose coordinates are (xi,yi) in the global system and (ξ_i, η_i) in the parametric system.

The displacements within an element can be written as Equation 5-3 and 5-4.

$$u = \sum_{i=1}^{n} N_i(\xi, \eta) u_i \qquad \text{Equation 5-3}$$

$$v = \sum_{i=1}^{n} N_i(\xi, \eta) v_i \qquad \text{Equation 5-4}$$

Where (u_i,v_i) are the nodal displacement for x and y directions. The strain matrix at (x,y) can be written as Equation 5-5.

$$\begin{Bmatrix} \varepsilon_x \\ \varepsilon_y \\ \gamma_{xy} \end{Bmatrix} = [B] \begin{Bmatrix} u_i \\ v_i \end{Bmatrix} \quad \text{Equation 5-5}$$

Where:

$$[B] = \begin{Bmatrix} \frac{\partial N_i}{\partial x} & 0 \\ 0 & \frac{\partial N_i}{\partial y} \\ \frac{\partial N_i}{\partial y} & \frac{\partial N_i}{\partial x} \end{Bmatrix}$$

and

$$\begin{Bmatrix} \frac{\partial N_i}{\partial x} \\ \frac{\partial N_i}{\partial y} \end{Bmatrix} = [J]^{-1} \begin{Bmatrix} \frac{\partial N_i}{\partial \xi} \\ \frac{\partial N_i}{\partial \eta} \end{Bmatrix} \quad \text{Equation 5-6}$$

Where J is the Jacobian matrix and can be written as Equation 5-7.

$$[J] = \begin{bmatrix} \frac{\partial x}{\partial \xi} & \frac{\partial y}{\partial \xi} \\ \frac{\partial x}{\partial \eta} & \frac{\partial y}{\partial \xi} \end{bmatrix} \quad \text{Equation 5-7}$$

The stress matrix can be written as Equation 5-8.

$$\{\sigma\} = [D]\{\varepsilon\} \quad \text{Equation 5-8}$$

$[D]$ is stress-strain matrix.

The stresses and strains can be calculated at several Gauss points or integration points within each element. The global force, displacement, and stiffness matrices are related and can be written as Equation 5-9.

$$[K][u] = [F] \quad \text{Equation 5-9}$$

$[K]$ is the element stiffness matrix and can be written as Equation 5-10.

$$[K] = \int_{-1}^{1}\int_{-1}^{1}[B]^T\,[D][B]\,det|J|d\xi d\eta$$ Equation 5-10

ABAQUS Simulation

ABAQUS software does not have any fixed units for the input parameters and the unit should be set by the user. In this study, the following units, presented in Table 5-1, are used in the software.

Table 5-1 Units to be Used for FE Modeling with ABAQUS

Parameter	**Unit**
Density	lb./in.^{3}
Force	lb.
Length	in.
Stress	Psi
Time	S

All material properties and parameters such as elastic, plastic, young's modulus and damage values have been obtained from the tensile test of dogbone shape HDPE specimen.

The properties have been used to model the tensile test to validate the material properties definition. After validation, 15-ft long pipe with 16-in. outer diameter and DR 17 was modeled to analyze different cyclic loadings. 3D solid part model is chosen to analysis the specimen. The following key points have been used in the model:

- The material property is considered as isotropic and homogeneous.
- In the part section, 3D is chosen as the modeling space; deformable and solid is chosen in the corresponding section.
- Young's modulus, plasticity and damage parameters should be obtained from the true stress-strain curve.

MATERIAL PROPERTIES FOR ABAQUS SIMULATION

Different material properties should be defined in ABAQUS to model the material correctly.

Density is volumetric mass density of a substance described as mass per unit volume and can be calculated by Equation 5-11.

$$Density = \frac{Mass}{Volume}$$ Equation 5-11

Young's Modulus: Young's modulus, E, can be calculated by dividing the tensile stress by the extensional strain in the elastic (initial, linear) portion of the stress–strain curve as presented in Equation 5-12.

$$Young's\ Modulus = \frac{Tensile\ Stress}{Strain}$$ Equation 5-12

In the ABAQUS simulation model, only values form true stress-strain curve can be accepted. Some modification for engineering stress-strain curve should be done to match the numerical simulation requirement. True stress is the stress determined by the instantaneous load acting on the instantaneous cross-sectional area true stress is related to engineering stress as mentioned in Equations 4-4 and 4-5.

Poisson's ratio: is the negative ratio of transverse to axial strain. When a material is compressed in one direction it usually tends to expand in the other two directions perpendicular or parallel to the direction of flow.

Plasticity: In physics and engineering, plasticity is the propensity of a material to undergo permanent deformation under load when compressed. In ABAQUS model the plasticity value should be obtained from the true stress-strain curve and followed the Equation 5-13.

$$\varepsilon_{Plastic\ True} = \varepsilon_{True} - (\frac{\sigma_{True}}{E})$$ Equation 5-13

Fracture at strain: The logarithmic strain where the specimen breaks and it can be obtained from the true stress-strain curve.

Damage Evolution: The evolution of damage variable with the relative plastic displacement can be specified in tabular, linear, or exponential form and linear form is

chosen in this study. In linear form, the damage variable increases according to the Equation 5-14.

$$\dot{d} = \frac{\dot{L_\varepsilon^{pl}}}{\bar{u}_f^{pl}} = \frac{\dot{\bar{u}_f^{pl}}}{\bar{u}_f^{pl}} \qquad \text{Equation 5-14}$$

The plastic displacement at failure can be computed as Equation 5-15.

$$\bar{u}_f^{pl} = \frac{2G_f}{\sigma_{y0}} \qquad \text{Equation 5-15}$$

Where G_f is the fracture energy per unit, σ_{y0} is the fracture stress and *L* is the characteristic length of the element.

NONLINEAR ALGORITHMS

Nonlinearities in analysis always present in the structural mechanics problems. Three general types of nonlinearities are material, geometric, and contact nonlinearities.

In the material nonlinearities, the constitutive equation which relates stress and strain rates is nonlinear. Materials behave linearly until they reach to a certain point, which is called elastic limit, after this point the behavior is nonlinear. There are different nonlinear material models for different types of material.

In geometrical nonlinearity, the relationship between strain and displacement is not linear. Large rotation, large strain, and large displacement are various types of geometric nonlinearities. Geometric nonlinearity is solved by using Lagrangian and Eulerian techniques. In Lagrangian method, material and mesh points deform and translate together due to their attachment. In Eulerian technique, during analysis mesh points stay in their initial position and material nodes will move independent of the mesh nodes. The later formulation is suitable for liquid materials.

Changing boundary conditions of the problem creates contact nonlinearity. Also it can be created when the load path is going through the contact of two surfaces. In

contact nonlinearity two constraints are applied; displacement constraint and force constraint. Two surfaces of the contact should not penetrate each other which is known as displacement constraint, and load or force should not keep the two surfaces together, which is called force constraint.

HARDENING

Loading, unloading, and reloading cycles of yield of an elastic-perfectly plastic material are the same. Yield strength is varied in different load cycles, in a material with hardening properties. Therefore, previous loading cycles has a significant role in the behavior of the material and the elastic region of it. Three major hardening theories of materials consist of isotropic hardening, kinematic hardening, and mixed hardening (Dezfooli; 2013).

In isotropic hardening theory it is assumed that the hardening is the same in all directions. As shown in Figure 5-2 the yield surface will expand symmetrically about its origin. Figure 5-3 shows the effect of isotropic hardening on stress-strain curve.

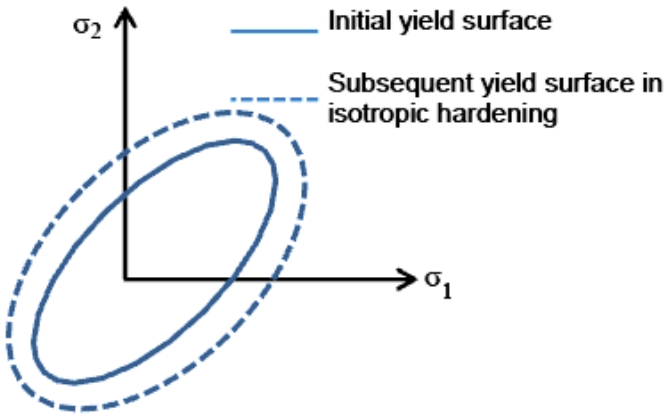

Figure 5-2 Yield Surface in Isotropic Hardening Model, Dezfooli (2013)

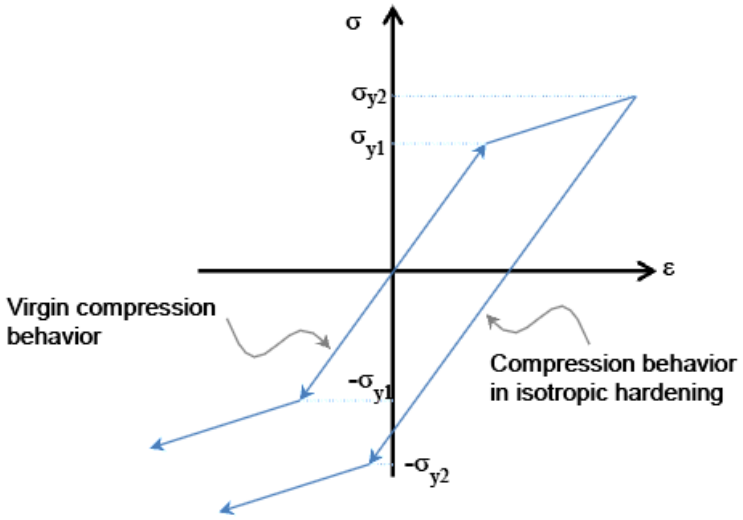

Figure 5-3 Stress-Strain Curve of Isotropic Hardening Model, Dezfooli (2013)

Another hardening theory which includes the Bauschinger effect in cyclic loading of metals is kinematic hardening. In kinematic hardening theory, the hardening in one direction increases while the hardening in other directions decreases equally (Dezfooli; 2013). Figure 5-4 shows the effect of kinematic hardening model on yield surface. Figure 5-5 illustrates the effect of kinematic hardening on stress-strain curve.

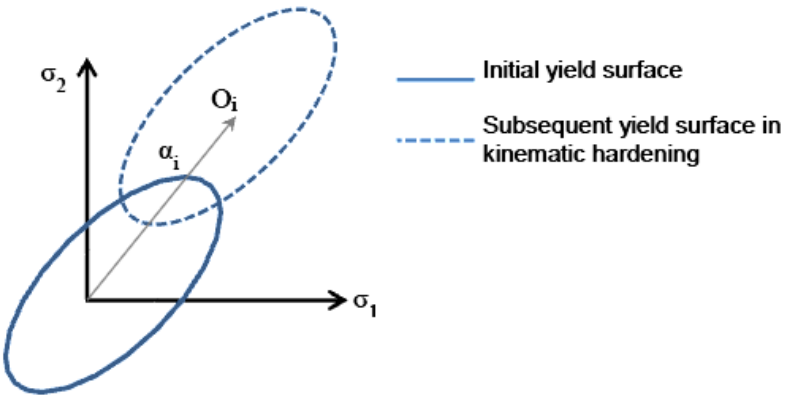

Figure 5-4 Yield Surface of Kinematic Hardening Model, Dezfooli (2013)

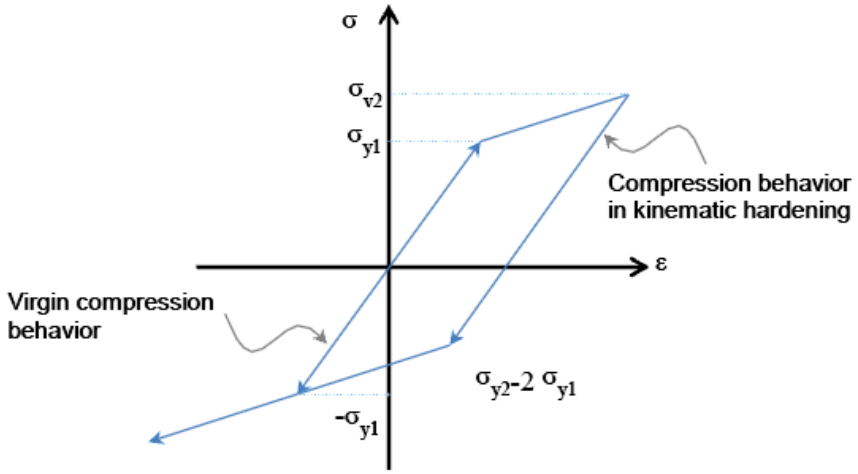

Figure 5-5 Stress-Strain Curve of Kinematic Hardening Model, Dezfooli (2013)

A combination of the isotropic and kinematic hardening creates the mixed formulation. A weighted average of plastic strain increment of the either models will be calculated.

NUMERICAL METHODS OF FATIGUE LIFE PREDICTION

Initiation, growth, and propagation of micro-cracks and voids in the material degenerate mechanical properties of material. According to Warhadpande (2010) damage variable of a one-dimensional structure, can be calculated as Equation 5-16.

$$D = \frac{S_D}{S}$$ Equation 5-16

Where S is total cross sectional area and SD is total micro-cracks and cavities area.

By strain equivalence theory after damage initiation, Lemaitre (1992) obtained the true stress of material. So, in one-dimensional stress state, the constitutive relation of material can be defined as Equation 5-17.

$$\varepsilon = \frac{\tilde{\sigma}}{E_0} = \frac{\sigma}{E_0(1-D)}$$ Equation 5-17

Where $\tilde{\sigma}$, E_0 and ε are damaged material's true stress, the initial modulus of elasticity of material, and the elastic strain, respectively.

For three-dimensional isotropic damage material constitutive relation is presented in Equation 5-18.

$$\sigma_{ij} = C_{ijkl}(1 - D)\varepsilon_{kl} \quad \text{Equation 5-18}$$

Where D = 0 presents undamaged material and D = 1 is a completely failed material. According to Xiao (1998) and Bomidi (2012) damage evolution model can be written as Equation 5-19.

$$\frac{dD}{dN} = \frac{\bar{B}}{q(1-D)^{2q}}(\sigma_{eqM}^{2q} - \sigma_{eqm}^{2q}) \quad \text{Equation 5-19}$$

Where $\bar{B}$ and q are material constants, σ_{eqM} is the maximum equivalent stress (MISES), and σ_{eqm} is the minimum equivalent stress.

These nonlinear equations should be solved with increment variable of damage parameter to calculate the stress and damage field of the model. In the increment step of damage parameter, $C_{ijkl}(1 - D)$ is a constant matrix. So, the damaged material would be considered as a "new" material (undamaged). For the linear elastic materials maximum equivalent stress can be calculated as Equation 5-20.

$$\sigma_{eqm} = R\sigma_{eqM} \quad \text{Equation 5-20}$$

Here R is the ratio of stress of fatigue loads and during the damage process it is a constant. So, Equation 5-19 can be written as Equation 5-21.

$$\frac{dD}{dN} = \frac{\bar{B}\,(1-R^{2q})}{q(1-D)^{2q}}(\sigma_{eqM}^{2q}) \quad \text{Equation 5-21}$$

Where in $\bar{B}$ and q are the material constants. Equation 5-21 can be modified as Equation 5-22.

$$\frac{dD}{dN} = \frac{(\sigma_{eqM}^{2q})}{B(1-D)^{2q}} \quad \text{Equation 5-22}$$

Since R (stress ratio) is constant during damage process of the model, $B = \frac{q}{\bar{B}(1-R^{2q})}$ is also constant. So, the model would have less fitting parameters and finite element programs would be capable of analyzing it.

Therefore, the model of damage evolution can be employed to predict the lifetime of specimen, using equations of geometry, equilibrium, constitutive relation, and boundary conditions, combined with damage and stress which are known parameters.

According to Wang et al. (2016) damage mechanics-finite element method can be used to predict the fatigue life and simulate damage field of material. In this method, during the analytical process the damage increment of dangerous point remains constant. The steps of this process include:

1. After developing FE model, the values of damage are assumed to be zero the first loading step.
2. According to the stress field, damage evolution is calculated. Then, maximum damaged element is selected as the dangerous point of the structure. During every loading step the status of the dangerous point should be checked in terms of damage value. When the dangerous point is failed, another dangerous point should be re-estimated for the model.
3. For i_{th} modeling cycle ($i \geq 2$), life increment is calculated according to Equation 5-16.

$$\Delta N_i = \frac{B(1-D_{i-1})}{\sigma_{eqM}^{2q}} \Delta D \qquad \text{Equation 5-23}$$

The value of total life is updated as

$$N_i = \sum_0^{j-i} \Delta N_j \qquad \text{Equation 5-24}$$

4. The damage increment of gauss points of other elements is obtained on the basis of life increment:

$$\Delta D_i(x) = \frac{(\sigma_{i-1}(x))_{eqM}^{2q}}{B(1-D_{i-1}(x))^{2q}} \Delta N_i$$ Equation 5-25

The damage values of gauss integral points of each element are

$$D(x)_i = \sum_0^{j=i} \Delta D(x)_j$$ Equation 5-26

5. With the new damage field, the stress field is updated until the components lose efficacy or ΔN_i is infinitesimally smaller than ΔN_{i-1}.

CONVERGENCE DIFFICULTIES

Different convergence problems may occur during modeling and analyzing. There are several methods to solve the problems considering the definition of mesh, boundary condition and loads. Some common solutions for convergence problem are mentioned in this part. Sometimes ABAQUS cannot analyze the problem in some points and it is required to divide the increments into smaller steps. In these cases, in the time step definition in ABAQUS, the minimum time increment should be defined lower than the default values and thus, the maximum number of increments should be increased. Apart from solving the convergence problem, it also leads to more accurate results. However, it needs high computational capacity and is time consuming.

In parts including contacts, convergence problems occur due to distortion of elements with less stiff material. In some cases, due to local instabilities such as surface wrinkling, material instability or local buckling, the results cannot converge in aforementioned zones. Therefore, it is recommended to specify automatic stabilization, which can be introduced in time steps. Automatic stabilization can be defined by either specifying a dissipated energy fraction or specifying a damping factor. According to Esfahani and Nilforoush (2012), this stabilization, if a relatively small amount is used, does not interfere with the material behavior and thus, it is an appropriate manner to overcome such this problem. The most effective way of handling convergence problems

is to increase the tolerances and the number of iterations (Esfahani and Nilforoush; 2012). Parameters, which are recommended to change in step module, are:

- R_n^{α}: A convergence criterion for the ratio of the largest residual to the corresponding average flux norm for convergence (Habbitt; 2010). The default value is 0.005 and it should be increased to solve convergence problem.
- I_0: the number of equilibrium iterations without severe discontinuities after which the check is made whether the residuals are increasing in two consecutive iterations (Habbitt; 2010). Default value is 4 and it can be increased up to 3-4 times the default value.
- I_R: the number of consecutive equilibrium iteration without severe discontinuities at which the logarithmic rate of convergence check begins (Habbitt; 2010). The default value is 8 and it can be increased up to 3-4 times the default value.
- I_A: the maximum number of cutbacks, allowed for an increment (Habbitt; 2010). The default value is 4 and it can be increased up to 3-4 times the default value.

DOGBONE SPECIMEN TENSILE SIMULATION

Results of tensile test performed on HDPE dogbone specimens used to validate material properties in ABAQUS. Uniaxial tensile test was performed based on ASTM D638. Non-linear analysis was performed by ABAQUS 6-14.3.

Geometry

Dogbone shaped specimens were made based on ASTM D638, type III specimens. The dimensions of dogbone specimen type III were illustrated in Figure 4-13. Dogbone shape specimen was modeled as 3-D solid. The section was partitioned in different locations in order to use different sizes of mesh wherever required. Figure 5-6 illustrates 3-D model of HDPE dogbone sample.

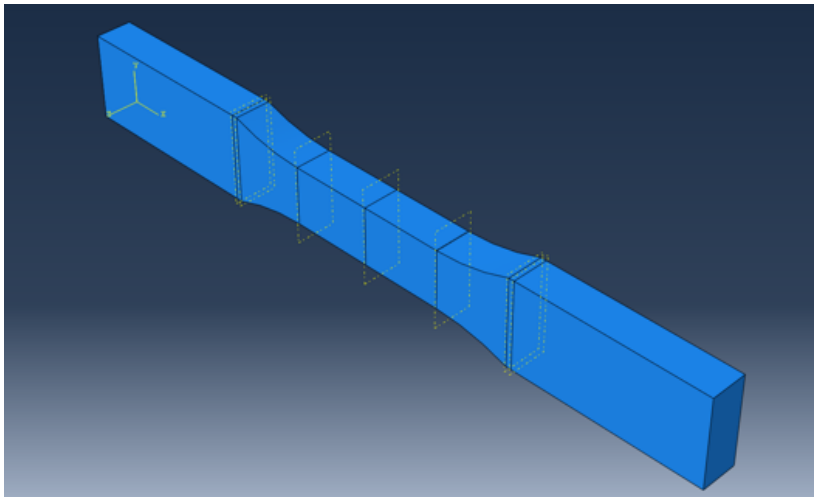

Figure 5-6 3-D Model of HDPE Dogbone Specimen

Material Properties

Elastic and plastic behavior of HDPE should be defined in ABAQUS in order to model the material correctly. Input value for defining elastic part of PE4710 material model is presented in Table 5-2.

Table 5-2 Input Values to Define Elastic Behavior of PE4710 Material

Parameter	Value	Unit
Density	0.0343	lb./in.^{3}
Elastic Modulus	100,000	psi
Poisson's ratio	0.4	-

Plastic behavior is defined using plastic part of true stress-strain curve of HDPE. True stress-strain curve was calculated based on nominal stress-strain curve of HDPE (results of uniaxial tensile test). Equations 4-4 and 4-5 was used to convert nominal stress-strain curve to true stress strain curve. Then Equation 5-13 was used to define the plastic part. Figure 5-7 shows the true stress-strain curve comparing to the nominal stress-strain curve and Figure 5-8 illustrates the input value of stress-strain as plastic behavior of PE4710 in ABAQUS.

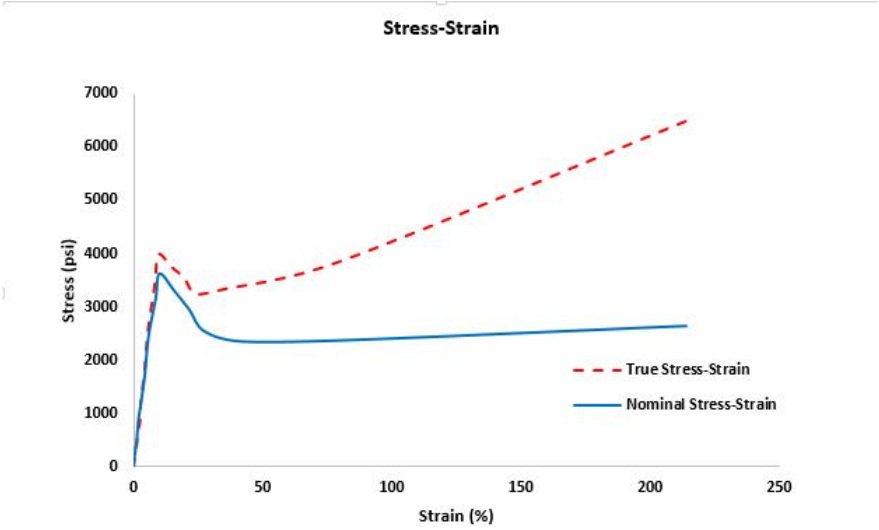

Figure 5-7 True Stress-Strain and Nominal Stress-Strain Curves of HDPE

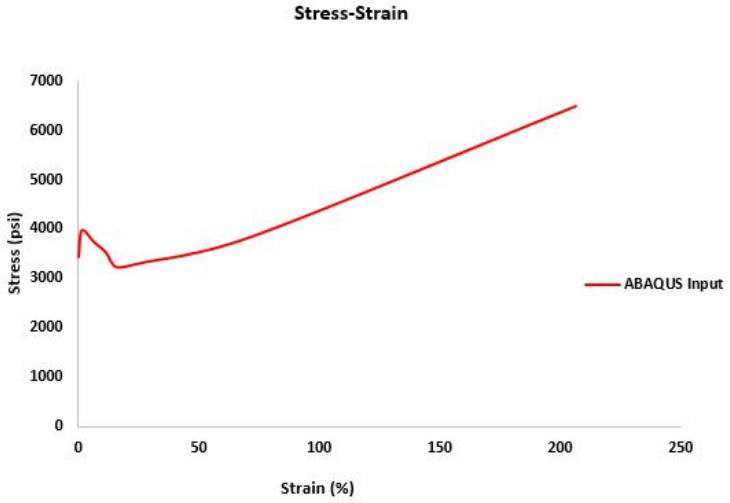

Figure 5-8 Plastic Part of True Stress-Strain Curve

Boundary Conditions

Dogbone specimen is assumed to be fixed at the bottom and free at the top, as it really was in the testing machine. Therefore, U_x, U_y, U_z and U_{rx}, U_{ry} and U_{rz} are closed. U_x,

U_y and U_z are translation in direction of X, Y and Z axes, as shown in Figure 5-9. U_{rx}, U_{ry} and U_{rz} are rotation about X, Y and Z axes as shown in Figure 5-10.

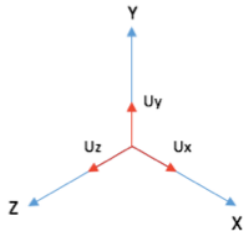

Figure 5-9 Definition of U_x, U_y and U_z in ABAQUS Software

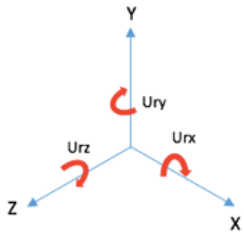

Figure 5-10 Definition of U_{rx}, U_{ry} and U_{rz} in ABAQUS Software

Loading

Distributed load has been applied to the top surface of the specimen to pull it upward. Figure 5-11 shows the applied load on the top surface of the specimen.

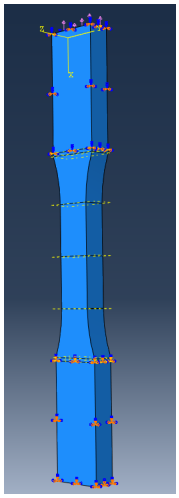

Figure 5-11 Applied Load on the Top Surface of Dogbone Specimen

Meshing

For meshing the whole specimen C3D8 elements was used. C3D8 is a three dimensional element with 8 nodes as is illustrated in Figure 5-12. Mesh size is 0.06-in. at thicker parts of top and bottom and 0.05-in. at the thinner middle part of the specimen. Meshed specimen is shown in Figure 5-13.

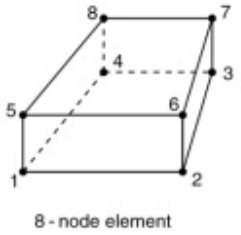

Figure 5-12 C3D8 Element Used to Mesh Dogbone Specimen

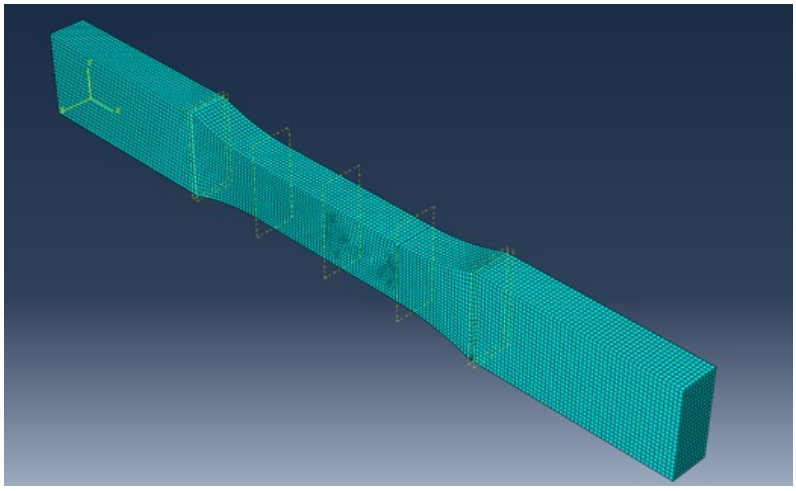

Figure 5-13 Meshed Dogbone Specimen

Analysis and Results

After non-linear analysis of the model, stress-strain curve of FE model was compared with stress-strain curve of experiment and the results show a good agreement between graphs. Figure 5-14 shows the contouring of strain distribution in HDPE

dogbone specimen after analysis. Stress-strain curves of FE results and experiment are illustrated in Figure 5-15.

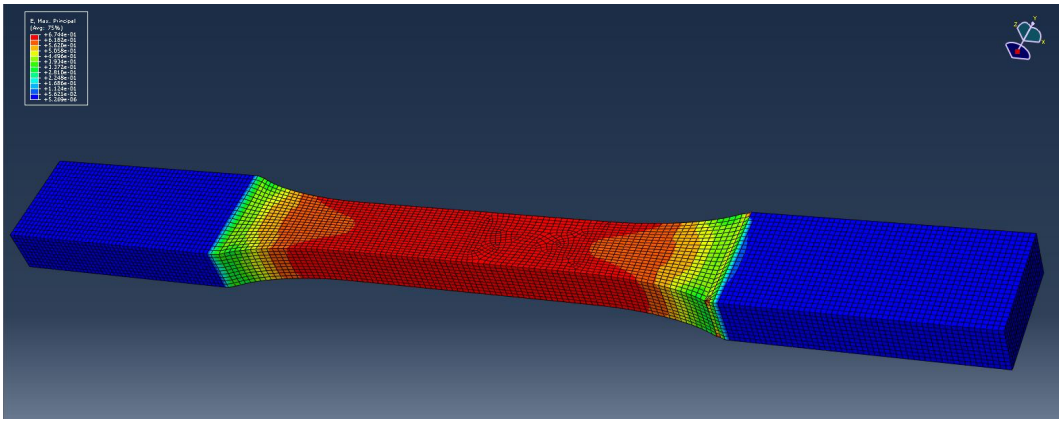

Figure 5-14 HDPE Dogbone Specimen after FE Analysis

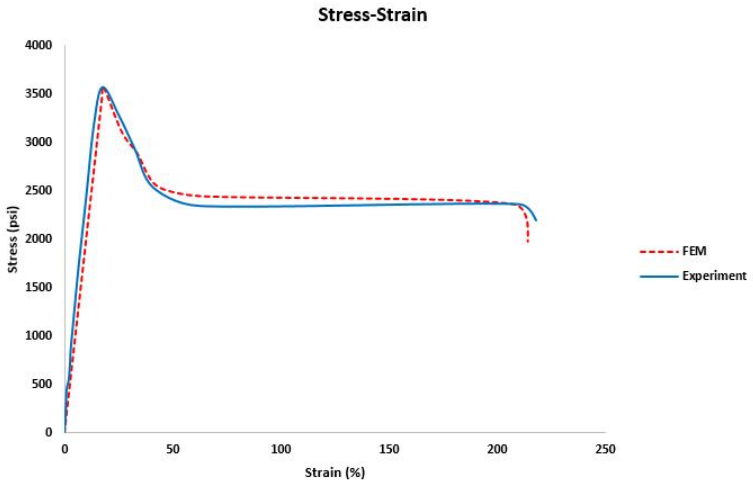

Figure 5-15 Stress-Strain Curve of HDPE Specimen, FE Modeling and Experiment

MODELING OF HDPE PIPE SAMPLE

After verifying material properties using tensile test data, the PE4710 pipe sample was modeled. The purpose of modeling was to evaluate the performance of pipe under cyclic loading (fatigue) to develop a new equation to draw S-N curve of PE4710.

Geometry

3-D solid section was used to model PE4710 pipe sample with a 15-ft long and 16-in. diameter (DR 17). This model is shown in Figure 5-16.

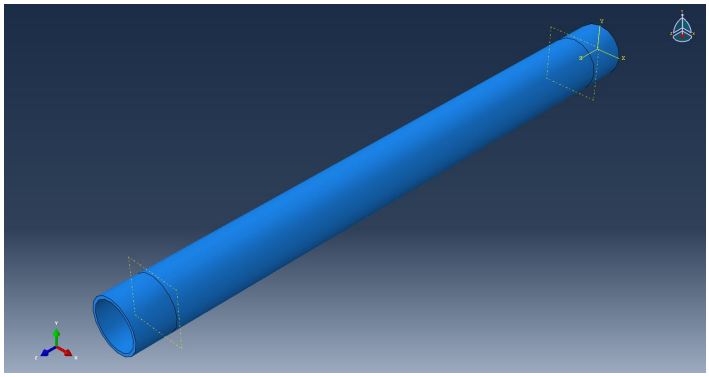

Figure 5-16 3-D Model of HDPE Pipe Sample

Material Properties

Defined material properties for PE4710 to model material behavior is the same as dogbone shaped specimen. Subroutine USDFLD in ABAQUS is used to define the damage in ABABQUS and using the Python language the fatigue process of PE4710 is simulated. According to ABAQUS manual, “USDFLD is utilized to define the values of field variables directly at the integration points of elements. The field variable values can be functions of element variables such as stress or strain.”

The damage mechanics-finite element method is used in ABAQUS, according to proposed model of Wang et al. (2016). Python and Fortran are used for coding to implement the built-in functions, such as post-process of stress, and results of damage field analysis. The modeling includes these steps:

1. Coding with the Python language, finite element model is built in ABAQUS while the initial damage field value is set to zero.
2. Using SDVINI subroutine, the damage field is imported to USDFLD subroutine. Then, the structural stress would be analyzed.

3. After distribution of stress of the inner structure, results are read using Python to find the dangerous points of the specimen. Then considering the damage increment and output the file including status of damage of the model, life increment and damage values of other gauss integral points are calculated.
4. Finally, a new dangerous point is selected when the value of damage in dangerous point reaches to the critical state. This step is repeated until the complete efficacy loss of component.

Boundary Conditions

Both sides of the pipe in the real test had a tight cap to keep it close while preventing any movement. So, in this FE model it was assumed that two cap exists on both sides of the pipe and they got fixed to prevent movement in X, Y and Z directions.

Loading

Internal water pressure was applied to the inner surface of pipe as cyclic internal pressure. Model with different cyclic loadings were analyzed to check the total number of cycles for each scenario. Loading pattern assumed to be saw-tooth, as was really applied to the fatigue test on HDPE pipe. Loading pattern for the performed fatigue test was shown in Figure 4-6. Table 5-3 shows different applied stresses considered for this study.

Table 5-3 Different Scenarios for FE Analysis

Case No.	P_{min} (psi)	P_{max} (psi)	$\sigma_{amplitude}$ (psi)
I	125	188	252
II	125	250	500
III	125	300	700
IV	125	350	900
V	125	400	1,100

Meshing

Element type used is C3D8 (shown in Figure 5-12). Sensitivity analysis was performed on the model with mesh sizes of 0.2 in., 0.4 in. and 0.6 in. The results are

shown in Figure 5-17. Mesh size 0.4 in. is selected, since, as shown in Figure 5-17, larger mesh size did not provide accurate results and smaller mesh size had the same results as mesh size 0.4 in., while requiring more time for analysis. Swept mesh was assigned due to the round shape of pipe. Figure 5-18 shows meshing of pipe.

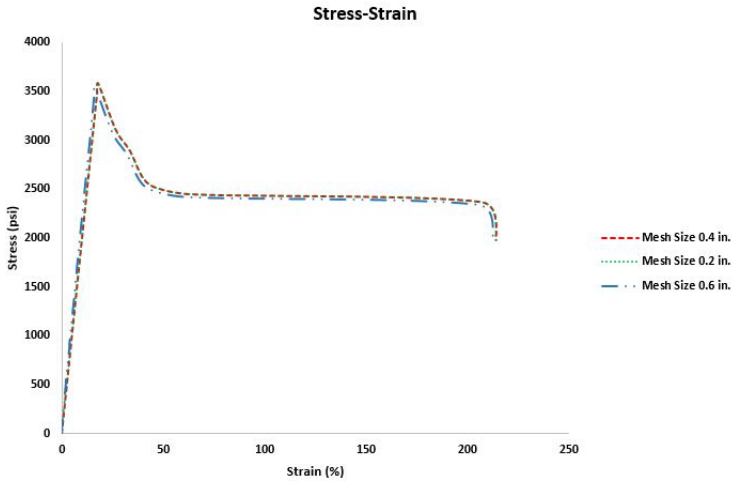

Figure 5-17 Stress-Strain curves of Mesh Sensitivity Analysis

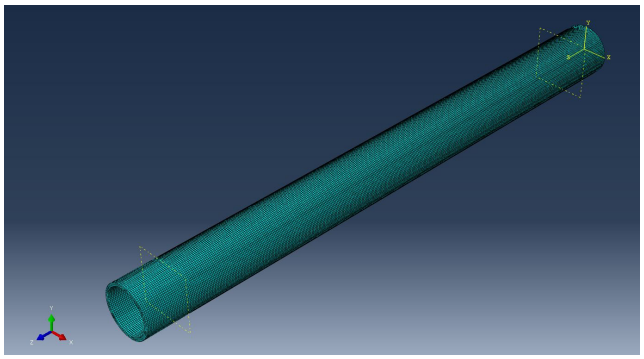

Figure 5-18 Meshing of 3-D Pipe Model

Results

Figure 5-19 shows contouring of maximum principal stress for HDPE pipe after analyzing. After analysis, the number of cycles to failure of each scenario was derived. The results are shown in Table 5-4.

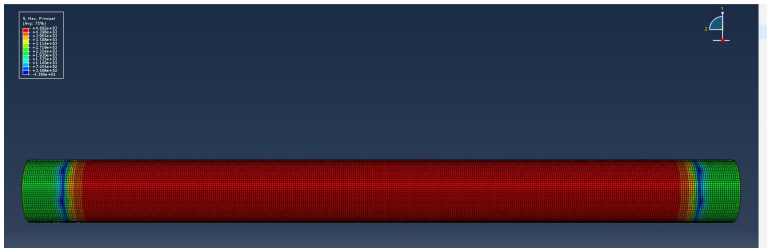

Figure 5-19 HDPE Pipe after FE Analysis

Table 5-4 Results of FE Analysis of Cycle Number of each Case

Case No.	$\sigma_{amplitude}$ (psi)	Number of Cycles
I	252	6,654,321
II	500	387,416
III	700	37,638
IV	900	10,302
V	1,100	2,873

S-N CURVE

S-N Curve is a graph of the magnitude of stress vs. the number of cycles to failure for a given material. Using this curve, fatigue life of the material can be estimated considering the applied stress. It was first developed by the German scientist August Wöhler while investigating of a train crash in 1842 in Versailles, France (Frank et al.; 2009).

In this study S-N curve of PE4710 was drawn using Equation 5-27 suggested in technical report of Electric Power Research Institute (EPRI) (2013) for PE4710 and Equation 5-28 based on Petroff (2013).

$$S = \frac{8420}{N^{0.12}}\ (psi) \qquad \text{Equation 5-27}$$

Where S is the stress amplitude (half range) and N is total number of cycles to failure.

$$N = 10^{\frac{1.708 - Log\frac{Peak\ Stress}{145}}{0.101}} \qquad \text{Equation 5-28}$$

Where N is total number of cycles and peak stress is calculated based on Equation 5-29.

$$Peak\ Stress = \left(P_{Pumping} + P_{Surge}\right) * \frac{(DR-1)}{2} \qquad \text{Equation 5-29}$$

Figures 5-20 and 5-21 illustrate S-N curve of PE4710 based on EPRI (2013) and Petroff (2013) equations, respectively. According to Petroff (2013), fatigue tested pipe in this study will fail after 7, 313, 515 cycles. In the pipe fatigue design 1,000,000 cycles are equal to approximately 50 years.

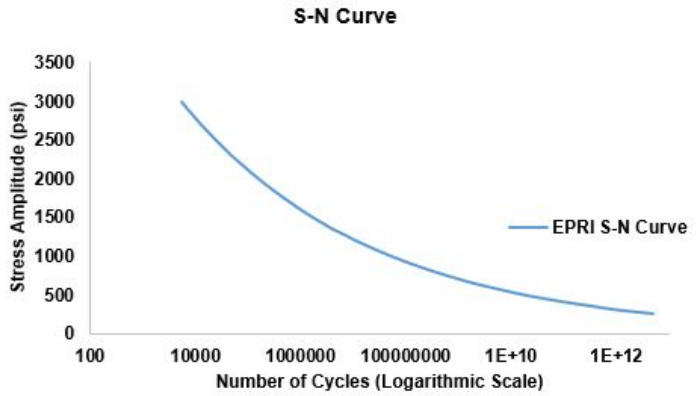

Figure 5-20 S-N Curve of PE4710 Based on EPRI (2013)

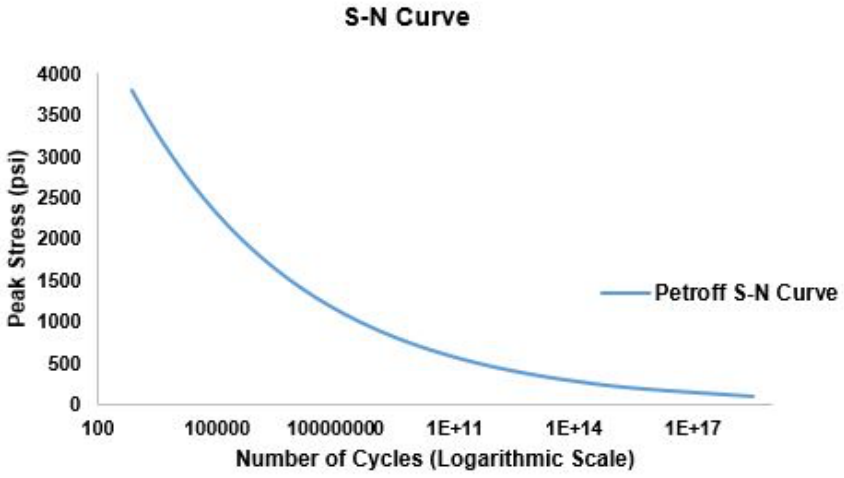

Figure 5-21 S-N Curve of PE4710 Based on Petroff (2013)

New S-N Curve

A new equation was developed to draw S-N curve of HDPE using the outcomes of ABAQUS. For developing the new equation, linear regression was applied on FE outcomes. Equation 5-30 was obtained as shown in Figure 5-22.

$$S = 5048.3\ N^{-0.191}$$ Equation 5-30

Where S is stress amplitude (half range) and N is total number of cycles. Two constants of 5048.3 and 0.191 depend on the material type.

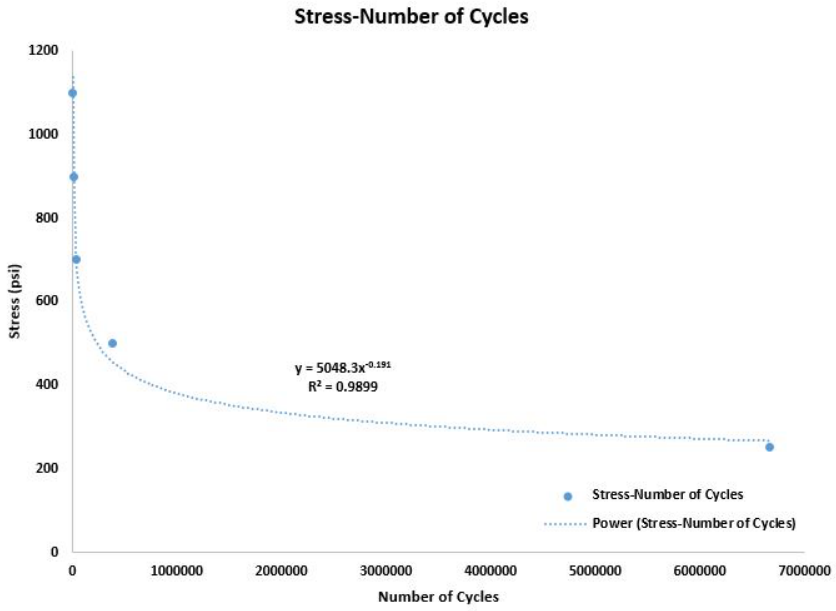

Figure 5-22 Proposed Equation for Stress to Number of Cycles Using FE Outcome

Equation 5-30 can be rewritten as Equation 5-31.

$$S = \frac{5048.3}{N^{0.191}}$$ Equation 5-31

Using Equation 5-31, S-N curve for PE4710 would be as illustrated in Figure 5-23. Figure 5-24 illustrates EPRI (2013) S-N curve and the new proposed S-N curve for PE4710. According to the Equation 5-31, the PE4710 pipe in this study, can withstand

6,545,379 cycles of internal water pressure of 125 psi to 188 psi which is much less than suggested equation by Petroff (2013).

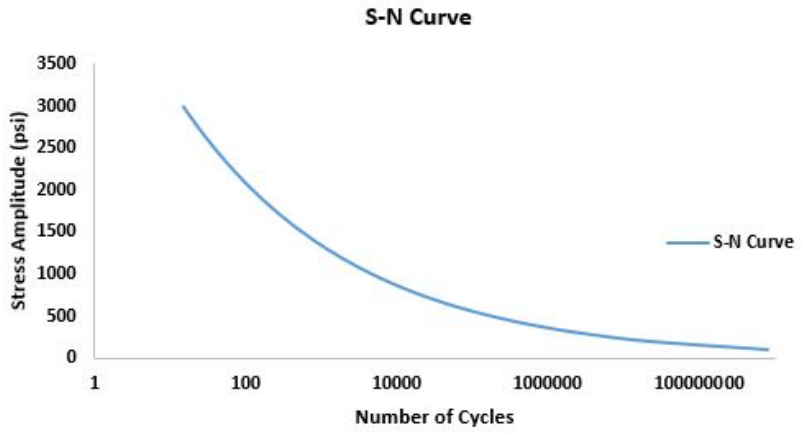

Figure 5-23 New Developed S-N Curve

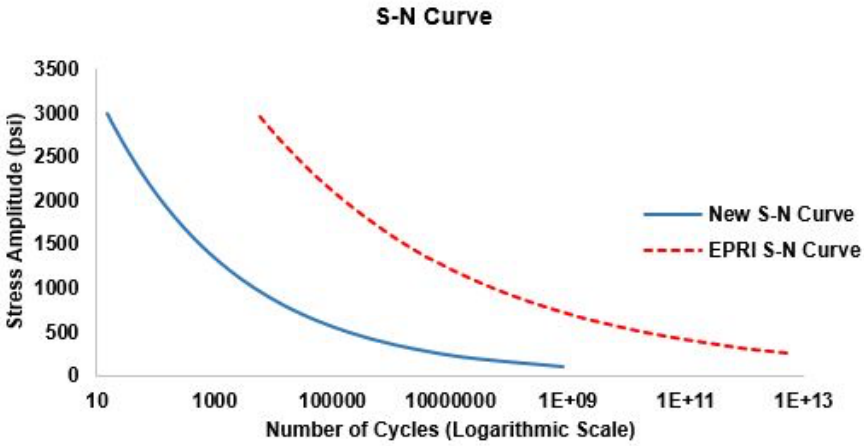

Figure 5-24 Comparison of New and EPRI S-N Curves of PE4710

CHAPTER SUMMARY

This chapter presented results of FE study. FE results showed that predicted FE results of total number of cycles that PE4710 material can withstand before failure is much less than the predicted fatigue life with current equation. More numerical studies are required to confirm if Petroff (2013) overestimates fatigue life of the PE4710 pipe or

limited ability of the developed code and software to analyze tens of millions of cycles of loading on the defined material (fatigue analysis) leads to failure of material before reaching to its actual final capacity.

Using FE analysis results, a new equation was developed to predict cycle numbers of PE4710 for different applied stress levels. A new S-N curve was developed in this dissertation to predict fatigue life of PE4710 material. According to this S-N curve, the fatigue tested pipe could withstand approximately 6,545,379 cycles of 125 psi to 188 psi before failure.

As mentioned in this chapter, the FE results presented in this dissertation are based on FE model verified only with material tensile test and not with actual fatigue cycles testing. Since actual fatigue testing of HDPE pipe is time consuming, the suggested FEA model was developed to simulate actual testing. These results are based on a capability of ABAQUS 6.14-3 and with future versions of FE modeling software, more accurate FE models would be developed to analyze billions of cycles of loading on different materials.

Chapter 6 CONCLUSIONS AND RECOMMENDATIONS FOR FUTURE STUDY

CONCLUSIONS

One of the major challenge faced by drinking water infrastructure in the North America is delivering potable water efficiently with minimum loss to end users through a durable and reliable water transmission and distribution pipe material. Frequent pressure surges in a piping system may lead to fatigue failure. Therefore, evaluation of the fatigue life of pipes is of a great importance. Application of HDPE pipes has been increased recently and more studies on the long-term performance of these pipes are required.

Two million cycles of internal water pressure from 125 psi to 188 psi with additional 50,000 cycles up to 250 psi were performed at CUIRE Laboratory on a 15-ft long and 16-in. diameter (DR 17) PE4710 pipe sample. Several specimens were taken from this fatigue tested pipe sample to determine material properties and compare with a new pipe sample from the same manufacturer. These dogbone-shaped specimens were tensile tested according to ASTM D-638. Additionally, Scanning Electron Microscopy (SEM) tests were performed on both new and fatigue tested specimens. Results of tensile tests were used to validate material properties in FE analysis. Then, FE analysis were utilized to simulate the number of cycles that PE4710 pipe sample can withstand under different stress amplitudes before failure. Using above physical testing and FEA, the following results were obtained:

- After approximately two million cycles, PE4710 became stiffer, as compared with the new pipe, the higher tensile strength and lower yield strain were observed for the fatigue-tested dogbone specimens. The tensile strength increased in average by approximately 2%, and the yield strain decreased in average by approximately 20%. Rupture strain showed about 15% increase compared to new specimens.

- Circumferential location of samples in each segment did not have any impacts on the mechanical properties after the fatigue, but longitudinal location impacted the results. End sections of the fatigue tested pipe sample showed higher rupture strain, yield strain and tensile strength. This phenomenon is due to free expansion of mid sections compared to the end sections of the pipe sample, which led to initiate micro-cracks in those areas.
- Longitudinal cracks observed in the pipe sample were an indication that the driving force is in circumferential direction. These cracks usually initiate at the location of defections or impurities, e.g., air bubbles.
- S-N curve of PE4710 derived with this dissertation indicated that current fatigue life design equations may overestimate the expected life of the pipe under fatigue. More numerical studies are required to confirm if current equations overestimate fatigue life of the PE4710 pipe or limited ability of the developed FE model to analyze tens of millions of cycles of loading on the pipe leads to failure of material before reaching to its actual final capacity.

RECOMMENDATIONS FOR FUTURE STUDIES

Recommendations for future research can be summarized as following:

- More cyclic loading tests on PE4710 are needed to validate maximum number of cycles that a pipe sample can withstand. According to experimental and numerical results of this dissertation, it is anticipated that current PE4710 water pipes can withstand several million cycles without failure in surge pressures up to 1.5 times pipe's pressure class, but more research is needed to determine fatigue strength in other pressure classes.

- It is recommended that repair spots, tapping points, electro fusion joints, mechanical joints and connections be added to the pipe sample to verify their resistance to cyclic loadings.
- The experimental fatigue test described in this dissertation was performed in a soil box without any soil cover. Impact of pipe embedment and soil cover should be investigated to realistically simulate actual service conditions.
- It is suggested to perform fatigue test on different lengths of large diameter pipe, to check the effect of longitudinal location in degradation of mechanical properties.
- Cyclic testing should be conducted for different pipe diameters and different resin types.
- Due to time and resource limitations, this dissertation conducted FE models to predict fatigue failure of PE4710 pipe sample of 15-ft long and DR 17 under five different stress amplitudes. It is recommended that future researchers develop more accurate FE model and consider other stress amplitudes and surge pressures on different pipe sizes and configurations.

Appendix A

EXPERIMENTAL STUDY

Table A-1 Dogbone Samples Dimensions and Environmental Condition of Tests

Sample ID	Dimensions Width (in)*Thickness (in)	Temperature (º F)	Humidity (%)
0-A	0.754 * 0.500	76	45
45-A	0.754 * 0.500	76	47
90-A	0.750 * 0.500	76	44
135-A	0.755 * 0.500	76	43
180-A	0.750 * 0.500	76	44
225-A	0.755 * 0.500	76	47
270-A	0.754 * 0.500	76	44
315-A	0.750 * 0.500	76	43
0-K	0.748 * 0.504	76	44
45-K	0.752 * 0.500	76	47
90-K	0.756 * 0.500	76	44
135-K	0.750 * 0.500	76	43
180-K	0.753 * 0.500	76	44
225-K	0.753 * 0.500	76	47
270-K	0.750 * 0.500	76	44
315-K	0.756 * 0.500	76	43
0-E	0.762*0.556	74	42
45-E	0.762*0.555	74	42
90-E	0.760*0.558	74	42
135-E	0.759*0.562	74	42
180-E	0.759*0.555	74	42
225-E	0.775*0.518	74	42
270-E	0.765*0.540	74	42
315-E	0.763*0.520	74	42
0-J	0.757*0.570	74	43
45-J	0.753*0.585	74	43
90-J	0.764*0.550	74	43
135-J	0.762*0.523	74	43
180-J	0.762*0.540	74	43
225-J	0.758*0.534	74	43
270-J	0.752*0.530	74	43
315-J	0.767*0.559	74	43
N-1	0.764*0.559	73	44
N-2	0.765*0.518	73	44
N-3	0.762*0.567	73	44
N-4	0.767*0.593	73	44
N-5	0.762*0.588	73	44
N-6	0.763*0.559	73	44

Figure A-1 Reciprocating Saw to Cut the Pipe and Cutting Process

Figure A-2 Different sets of Dogbone Shape Samples

Figure A-3 Measuring Distance Between two Grips to Set Gage Length

Figure A-4 Pulling Out the Sample

References

ABAQUS Analysis User's Manual, 2014.

Allison, S., Pinnock, P., Ward, I., 1966. Cold Drawing of Polyethylene Terephthalate, Journal of Polymer Science, vol. 7, no. 1, pp. 66-69.

Alvarado-Contreras, J., 2007. Micromechanical Modelling of Polyethylene, PhD Thesis, Department of Civil Engineering, University of Waterloo, Waterloo, Ontario, Canada.

Ambrose, M., Burn, S., DeSilva, D., and Rahilly, M., 2008. Life Cycle Analysis of Water Networks, Plastics Pipe XIV: Plastics Pipes Conferences Association, Budapest, Hungary.

American Society for Testing and Materials, 2014. ASTM D638-14, Standard Test Method for Tensile Properties of Plastics. West Conshohocken, PA: American Society for Testing and Materials.

American Water Work Association, 1994. Minimizing Earthquake Damage, A Guide for Water Utilities, Denver, Co.

American Water Works Association, 2002. PVC Pipe: Design and Installation - M23, U.S.A.

American Water Works Association, 2006. PE Pipe: Design and Installation - Manual of Water Supply Practices, M55, 1st Edition., USA.

American Water Works Association, C900-07, 2006. AWWA Standard for Polyvinyl Chloride (PVC) Pressure Pipe and Fabricated Fittings, 4 in. Through 12 in. (100 mm Through 300 mm), for Water Transmission and Distribution.

American Water Works Association, C906-07, 2006. AWWA Standard for Polyethylene (PE) Pressure Pipe and Fittings, 4 in. (100 mm) Through 63 in. (1,600 mm), for Water Distribution and Transmission.

American Work Water Association, 2007. AWWA C906-07 Polyethylene (PE) Pressure Pipe and Fittings 4 in. (100 mm) Through 63 in. (1,600 mm) for Water Distribution and Transmission. Denver, CO.

American Water Works Association, C901-08, 2008. AWWA Standard for Polyethylene (PE) Pressure Pipe and Tubing, 1/2 in. (13 mm) through 3 in. (76 mm), for Water Service.

American Water Works Association, C905-10, 2009. AWWA Standard for Polyvinyl Chloride (PVC) Pressure Pipe and Fabricated Fittings, 14 in. Through 48 in. (350 mm Through 1,200 mm).

ASCE, 2013. Report Card for America's Infrastructure. Rep. No. 978-0-7844-1037-0, American Society of Civil Engineers (ASCE), Reston, VA.

Austin, R. G., 2011. Detailed Water Quality Modeling of Pressurized Pipe Systems and its Effect on the Security of Municipal Water Distribution Networks. PhD Dissertation, University of Arizona, Tucson, AZ.

Balika, W., Pinter, G., Lang, R., 2007. Systematic Investigations of Fatigue Crack Growth Behavior of a PE-HD Pipe Grade in Through-Thickness Direction, Journal of Applied Polymer Science, vol. 103, pp. 1745-1758.

Bao, Y., Wierzbicki, T., 2004. On Fracture Locus in the Equivalent Strain and Stress Triaxiality Space. International Journal of Mechanical Sciences, vol. 46, pp 81–98.

Barenblatt, G., 1959. On the Equilibrium Cracks due to Brittle Fracture. Straight Line Cracks in Flat Plates. Journal of Applied Mathematics and Mechanics, vol. 23, p. 434.

Barsoum I., Faleskog, J., 2007. Rupture Mechanisms in Combined Tension and Shear Experiments. International Journal of Solids and Structures, vol. 44(6), pp.1768–1786.

Bell, K., Cave, S., 2011. Comparison of Environmental Impact of Plastic, Paper and Cloth Bags, Northern Island Assembly, Research and Library Service Briefing Note.

Bhatnagar, A., Broutman, L., 1985. Effect of Annealing and Heat Fusion on Residual Stresses in Polyethylene Pipe, Annual Technical Conference, Society of Plastics Engineers, Brookfield Center, CT, USA, pp. 545-549.

Bhave, R., Gupta. R., 2006. Analysis of Water Distribution Networks. Alpha Science International Ltd., Oxford, U.K.

Bomidi, J., Weinzapfel, N., Wang, C., Sadeghi, F., 2012. Experimental and Numerical Investigation of Fatigue of Thin Tensile Specimen, International Journal of Fatigue, vol. 44, pp. 116–130.

Bonds, R., 2000. Ductile Iron Pipe Versus HDPE Pipe, Ductile Iron Pipe Research Association, Birmingham, Alabama.

Bowman, J., 1988. The Fatigue Behavior of Medium Density Polyethylene Pipe Systems, Plastics Pipes VII: p. 14.

Bowman, J., 1990. The Fatigue Response of Polyvinyl Chloride and Polyethylene Pipe Systems, American Society for Testing and Materials: Philadelphia, PA. p. 21.

Brochard, F., de Gennes, P., 1986. Polymer-polymer Inter Diffusion, Europhysics Letters, vol. 1, no. 5, pp. 221-224.

Brostow, W., Corneliussen, D., 1986. Failure of Plastics, Hanser Publishers, New York.

Callister W., 2007. Materials Science and Engineering: An introduction. New Jersey, John Wiley and Sons.

Cech, T.V., 2005. Principles of Water Resources: History, Development, Management, and Policy. 2nd Edition. John Wiley & Sons, Inc., New York.

Cheng, J., 2008, Mechanical and Chemical Properties of High Density Polyethylene: Effects of Microstructure on Creep Characteristics, Doctorate's dissertation, University of Waterloo, Waterloo, Ontario, Canada.

Cheng, J., Polak, M., Penlidis, A., 2011. Influence of Micro-molecular Structure on Environmental Stress Cracking Resistance of High Density Polyethylene, In Tunneling and Underground Space Technology, Volume 26, Issue 4, pp. 582-593, ISSN 0886-7798.

De Gennes, P., 1971. Reptation of a Polymer Chain in the Presence of Fixed Obstacles, Journal of Chemical Physics, vol. 55, no. 2, pp. 572-579.

De Gennes, P., 1975. Reptation of stars, Journal de Physique, vol. 36, pp. 1199-1203.

Dezfooli, M., 2013. Staged Construction Modeling of Large Diameter Steel Pipes Using 3-D Nonlinear Finite Element Analysis, PhD Dissertation, University of Texas at Arlington.

Djebli, A., Aid, A., Bendouba, M., Talha, A., Benseddiq, N., Benguediab, M., Zengah, S., 2014. Uniaxial Fatigue of HDPE-100 Pipe – Experimental Analysis, *Engineering,* Technology & Applied Science Research vol. 4, no. 2, pp. 600-604

Divyashree, D., 2014. An Investigation of Durability and Reliability of HDPE Pipe for Large Diameter Water Transmission Applications, Master's Thesis, University of Texas at Arlington.

Divyashree, D., Najafi, M., Sever, F., 2015. Development of a Testing Protocol for Fatigue Testing of Large Diameter HDPE Pipes, ASCE Pipeline Conference 2015, Baltimore, Maryland.

Doi, M., Edwards, S., 1986. The Theory of Polymer Dynamics, Clarendon Press, Oxford.

Doi, M., Kuzuu, N., 1980. Nonlinear Elasticity of Rod-like Macromolecules in Condensed State, Journal of Polymer Science, Polymer Physics Edition, vol. 18, no. 3, pp. 409-419.

Dolan, T., Richart, F., Work, C., 1949. Influence of Fluctuations in Stress Amplitude on the Fatigue of Metals, ASTM Proc., vol. 49.

Donald, E., Dale, B., 2009. Oxidative Degradation of High Density Polyethylene Pipes from Exposure to Drinking Water Disinfectant's. Engineering Systems Inc. ESI File No.:29261A, 3851 Exchange Avenue, Aurora, Illinois 60504.

Donald, E., Dale, B., 2011. Field Failure Mechanisms in HDPE Potable Water Pipe. Proceeding of Annual Technical Conference (ANTEC) Journal.

Dougdale, D., 1960. Yielding of Steel Sheet Containing Silts. Journal of Mechanics and Physics of Solids, vol. 8, pp. 100-104.

Electric Power Research Institute (EPRI), 2013, Creep and Fatigue Properties of PE4710 Cell Classification 445574C High Density Polyethylene Pipe Material, Final Technical Report.

Elvers, B., Hawkins, S., Schulz, G., 1992. Ullman's Encyclopedia of Industrial Chemistry, 5th Edition, VCH Publishers, New York.

Esfahani, M., Nilforoush, R., 2012. Numerical Evaluation of Structural Behavior of the Simply Supported FRP-RC Beams, Master's Thesis, Royal Institute of Technology, Stockholm, Sweden.

Favier, V., Giroud, T., Strijko, E., Hiver, J., M., G'Sell, C., Hellinckx, S., Goldberg, A., 2002. Slow Crack Propagation in Polyethylene under Fatigue at Controlled Stress Intensity. Journal of Polymer Science, vol. 43, pp.1375–1382.

Ferry, J., 1980. Viscoelastic Properties of Polymers, 3rd Edition, Wiley, New York.

Fischer, E., 1957. Step and Spiral Crystal Growth of Polymers, Zeitschrift fuer Naturforschung, vol. 12a, pp. 753-754.

Fleming, K., Gullik, R., Dugandzic, J., Lechevallier, M., 2006. Susceptibility of Potable Water Distribution Systems to Negative Pressure Transients, State of New Jersey: Trenton, NJ. P. 6.

Flory, P., Yoon, D., 1978. Molecular Morphology in Semi-crystalline Polymers, Nature, vol. 272, no. 16, pp. 226-229.

Folkman, S., 2013. Water Main Break Rates in the USA and Canada: A Comprehensive Study. Utah State University, Logan, UT.

Frank, A., Pinter, G. and Lang, R., 2009. Prediction of the Remaining Lifetime of Polyethylene Pipes After up to 30 Years in Use. Society of Plastic Engineers. Annual Technical Conference (ANTEC) Proceedings.

Geil, P., 1964. Polymer Deformation – Annealing of Drawn Polyethylene Single Crystals and Fibers, Journal of Polymer Science Part A-General Papers, vol. 2, no. 9, pp. 3835-3855.

Graessley, W., Bhuiyan, A., Droescher, M., Neuse, E., 1982. Synthesis and Degradation Rheology and Extrusion, Advances in Polymer Science, vol. 47, p. 145.

Haager, M., Pinter, G., and Lang, R., 2006. Ranking of PE-HD Pipe Grades by Fatigue Crack Growth Performance, Plastics Pipes XIII: Washington. P. 11.

Hafner, B., 2007, Scanning Electron Microscopy Primer, Journal of Characterization Facility, University of Minnesota-Twin Cities, April 2007.

Hay, I., Keller, A., 1965. Polymer Deformation in Terms of Spherulites, Kolloid-Zeitschrift and Zeitschrift fur Polymere, vol. 204, no. 1-2, pp. 43-74.

Heywood, R., 1962. Designing against Fatigue, Chapman & Hall, Ltd., London.

Hibbitt, K., 2010. ABAQUS User's Manual. Pawtucket, 6th Edition.

Hizoum, K., Belouettar, S., 2011. Uniaxial Tensile Cyclic Behavior of High Density Polyethylene: Experimental and Modeling, International Journal of Solids and Structures, March 2011.

Hodgkinson, J., 2000. Mechanical Testing of Advanced Fiber Composites, Cambridge: Woodhead Publishing, Ltd., pp. 132–133.

Hosoda, S., Nomura, H., Gotoh, Y., Kihara, H., 1990. Degree of Branch Inclusion into the Lamellar Crystal for Various Ethylene/a-olefin Copolymers, Journal of Polymer Science, vol. 31, pp. 1999-2005.

Hsuan, Y., McGrath, T., 1999. HDPE Pipe: Recommended Material Specifications and Design Requirements, NCHRP Report 429, Transportation Research Board, National Academy Press, Washington, D.C., pp. 33-34.

Hsuan, Y., Zhang, J., 2005. Stress Crack Resistance of Corrugated HDPE Pipes in Different Test Environments, Transportation Research Board (TRB) Annual Meeting, Washington D.C.

Hu, Y., 2003. Correlation of Fatigue and Creep Crack Growth in Polyvinyl Chloride, Journal of Materials Science, vol. 38, pp. 633-642.

IGN 4-37-02, 1999. Design Against Surge and Fatigue Conditions for Thermoplastic Pipes. UK Water Industry. p. 12.

Irwin, G., 1957. Analysis of Stresses and Strains Near the End of a Crack Traversing a Plate, Journal of Applied Mechanics, vol. 24, pp. 361–364.

Jafari, N., Stark, T., Rowe, R., 2014. Service life of HDPE Geo-membranes Subjected to Elevated Temperature. Journal of Hazardous, Toxic, and Radioactive Waste, vol. 18, no. 1, pp. 16-26.

Jeffrey, J., Moser, A., Folkman, S., 2004. Guidelines for Fatigue Failure in PVC Pipe, Plastics Pipes XII, Milan, Italy.

Jeremy, A., 1990. The Fatigue Response of Polyvinyl Chloride and Polyethylene Pipe Systems, Buczala, G.S. and Cassady, M.J. Editors. American Society for Testing and Materials: Philadelphia, PA.

Joy, D., 1989, Low Voltage Scanning Electron Microscopy, Hitachi Instrument News, July 1989.

Jung, B., Boulos, P., Altman, T., 2011. Optimal Transient Network Design: A Multi Objective Approach. p.10.

Kanninen, M., Popelar, C., 1985. Advanced Fracture Mechanics, Oxford Engineering Science Series.

Kasakevich, M., L., Moet, A., 1990. Comparative Crack Layer Analysis of Fatigue and Creep Crack Propagation in High Density Polyethylene. Journal of Polymer Science, vol. 31, no. 3, pp. 435–439.

Kawai, M., Itoh, N., 2014. A Failure-mode Based Anisomorphic Constant Life Diagram for a Unidirectional Carbon/epoxy Laminate under Off-axis Fatigue Loading at Room Temperature. Journal of Composite Materials. vol. 48, no. 5, pp. 571–592.

Keith, D., Padden, F., 1959. The Optical Behavior of Spherulites in Crystalline Polymers-1- Calculation of Theoretical Extinction Patterns in Spherulites with Twisting Crystalline Orientation, Journal of Polymer Science, vol. 39, no. 135, pp. 101-122.

Keith, D., Padden, F., 1959. The Optical Behavior of Spherulites in Crystalline Polymers-2- The Growth and Structure of the Spherulites, Journal of Polymer Science, vol. 39, no. 135, pp. 123-138.

Keller, A., 1957. A Note on Single Crystals in Polymers - Evidence for A Folded Chain Configuration, Philosophical Magazine, vol. 2, no. 21, pp. 1171-1175.

Keller, A., 1959. Investigations on Banded Spherulites, Journal of Polymer Science, vol. 39, pp. 151-173.

Kfouri, A., 1996. Crack Extension under Mixed-mode Loading in an Anisotropic Mode Asymmetric Material in Respect of Resistance to Fracture. Fatigue & Fracture of Engineering Materials & Structures, vol. 19, no. 1, pp. 27–38.

Khelif, R., Chateauneuf, A., Chaoui, K., 2008. Statistical Analysis of HDPE Fatigue Life Time, Meccanica, DOI 10.1007/s11012-008-9133-7, Springer Science and Business Media.

Kiass, N., Khelif, R., Boulanouar, L., Chaoui, K., 2005. An Experimental Approach to Mechanical Properties Variability through HDPE Pipe Wall. Journal of Applied Polymer Science, vol. 97, pp. 272–281.

Kitagawa, M., Qui, J., Nishida, K., Yoneyama, T., 1992. Cyclic Stress Strain Curves at Finite Strains under High Pressures in Crystalline Polymers, Journal of Material Science, vol. 27, p. 1449.

Koerner, R., 2012. Designing with Geosynthetics, 6th Edition, vol.1, Prentice Hall.

Lapidus, L., Pinder, G., 1982. Numerical Solution of Partial Differential Equations in Science and Engineering. John Wiley & Sons, New York.

Larson, R., 1999. The Structure and Rheology of Complex Fluids, Oxford University Press, New York.

Lemaitre, J., 1992. A Course on Damage Mechanics, Springer, Berlin, Germany.

Li, S., Qi, K., 2014. The Mechanical and Fracture Property of HDPE-Experiment Result Combined with Simulation, Master's Thesis, Department of Mechanical Engineering Blekinge Institute of Technology Karlskrona, Sweden.

Liang, X., 2007. Ductile Fracture Modelling-Theory, Experimental Investigation and Numerical verification, Massachusetts Institute of Technology.

Lin, L., Argon, A., 1994. Structure and Plastic Deformation of Polyethylene, Journal of Materials Science, vol. 29, pp. 294-323.

Liu, H., 2003. Pipeline Engineering, Lewis Publishers, Boca Raton, FL.

Lu, X., Brown, N., 1986. The Relationship of the Initiation Stage to the Rate of Slow Crack Growth in Linear Polyethylene. Journal of Materials Science, vol. 21, pp. 2423-2429.

Lu, X., Brown, N., 1990. The Ductile-Brittle Transition in a Polyethylene Copolymer. Journal of Materials Science, vol. 25, pp. 29-34.

Lu, X., Qian, R., Brown, N., 1995. The Effect of Crystallinity on Fracture and Yielding of Polyethylene, Journal of Polymer Science, vol. 36, no. 22, pp. 4239-4244.

Lustiger, A., Markham, R., 1983. Importance of Tie Molecules in Preventing Polyethylene Fracture under Long-term Loading Conditions, Journal of Polymer Science, vol. 24, pp. 1647-1654.

Malchev P., De Vos, G., Norder, B., Picken, S., Gotsis, A., 2007. Evolution of the Morphology and the Mechanical Properties of Ternary PE/PA6/GF Composites During Annealing, Journal of Polymer Science, vol. 48, no. 21, pp. 6294–303.

Mamoun, M., 2006. Development of an Accelerated SCG Test Method for Polyethylene (PE) Pipe and Correlation with Elevated Temperature Hydrostatic Stress Rupture Test Method ASTM D 1598. Plastics Pipe Institute, Hydrostatic Stress Board: Des Plaines, IL.

Marshall, G., Brogden, s., Shepherd, M., 1998. Evaluation of Surge and Fatigue Resistance of Polyvinyl Chloride and Polyethylene Pipeline Materials for Use in the UK Water Industry, Plastics Rubber and Composites Processing and Applications, vol. 27, no. 10, pp. 483-488.

Mays, L., 2000. Water Distribution Systems Handbook, McGraw Hill Companies, Inc. Two Penn Plaza New York, NY.

McPherson, D., Haeckler, C., 2011. Answering the Question: Is a Surge Analysis Required? ASCE Pipelines 2011, Seattle, WA.

Menard, K., 1999. Dynamic Mechanical Analysis: A Practical Introduction, CRC Press, New York.

Meyers, M., Kumar, K., 1998. Mechanical Behaviors of Materials, Prentice Hall, ISBN 978-0-13-262817-4.

Molent, L., Jones, R., Barter, S., Pitt, S., 2006. Recent Developments in Fatigue Crack Growth Assessment. International Journal of Fatigue, vol. 28, no. 12, pp.1759–1768.

Moore I., Zhang, C., 1995. The Proceedings of the Annual Conference of the Canadian Society for Civil Engineering, p. 565.

Najafi, M., 2010. Trenchless Technology Piping: Installation and Inspection, McGraw-Hill, New York.

Najafi, M., 2013. Trenchless Technology Planning, Equipment and Methods, McGraw-Hill, New York.

Najafi, M., Gokhale, S., 2005. Trenchless Technology: Pipeline and Utility Design, Construction and Renewal, McGraw-Hill, New York, USA.

National Research Council Canada (NRC), 2003. Deterioration and Inspection of Water Distribution Systems a Best Practice by the National Guide to Sustainable Municipal Infrastructure. issue no. 1.

Nicholson, J., 2017. The Chemistry of Polymers, 5th Edition, The Royal Society of Chemistry, ISBN 978-1-78262-832-3.

Oliphant, K., Conrad, M., Bryce, W., 2012. Fatigue of Plastic Water Pipe: A Technical Review with Recommendations for PE4710 Pipe Design Fatigue, Jana Laboratories Inc., Aurora, Ontario, Canada.

Ong, S., Gaunt, J., Feng, M., Cheng, C., Esteve-Agelet, L., Hurburgh, C., 2008. Impact of Hydrocarbons on PE/PVC Pipes and Pipe Gaskets, AWWA Water Research Foundation, Denver, Co.

Park, K., Patel, H., Stivala, S., Plochocki, A., 1987. Extrusion Process for Polyethylene Pipe: Dependence of Morphology on the Process parameters, Advances in Polymer Technology, vol. 7, no. 2, pp. 201-207.

Parsons, M., Stepanov, E., Hiltner, A., Baer, E., 2000. Correlation of Fatigue and Creep Slow Crack Growth in a Medium Density Polyethylene Pipe Material. Journal of Material Science, vol. 35, pp. 2659–2674.

Paul, D., Max, P., David, C., Rajendra, K., Steven, J., Pamela, L., Elizabeth, A., Ashish, M., Bill B., Wolfe A., 2005. A Comparative Study of Multimodal vs. Bimodal Polyethylene Pipe Resins for PE-100 Application. Polymer Engineering and Science, Technical conference, pp. 1203-1213.

Peacock A., 2000. Handbook of Polyethylene: Structures, Properties and Applications. New York, Marcel Dekker Inc.

Peterlin, A., 1965. Crystalline Character in Polymers, Journal of Polymer Science Part C-Polymer Symposium, no. 9, pp. 61-89.

Petroff, L., 2013. Occasional and Recurring Surge Design Considerations for HDPE pipe. ASCE Pipelines 2013, pp. 161-170.

Pinter, G., Haager, M., Balika, W., Lang RW, 2006. Cyclic Crack Growth Tests with CRB Specimens for the Evaluation of the Long-term Performance of PE Pipe Grades, Journal of Polymer testing, pp. 23-34.

Plastic Pipe Institute, 2007. TN-41/2007-High Performance PE Materials for Water Piping Applications. Technical report on Municipal and industrial division.

Plastics Industry Pipe Associations of Australia Limited, 2010. Industry Guidelines: Polyethylene Pressure Pipes Design for Dynamic Stresses, vol. 5, no. 1, p. 10.

Plastics Pipe Institute, 2009. PPI Comments on Permeation of Water Pipes and on the AWWA-RF Report on Hydrocarbons.

Polyethylene Water Service Pipe and Tube Installation Guide, The Plastic Pipe and Fittings Association (PPFA), Illinois, available at

Popelar, C., Popelar, C. H., Kenner, V., 1990. Viscoelastic Material Characterization and Modeling for Polyethylene. Journal of Polymer Engineering and Science, vol. 30, pp. 577–586.

PPI Handbook of Polyethylene Pipe, 2008. The Plastics Pipe Institute, 2nd Edition, Irving, Texas, USA.

Pugno, N., Ciavarella M., Cornetti, P., Carpinteri, A., 2006. A Generalized Paris' law for Fatigue Crack Growth. Journal of Mechanics and Physics of Solids, vol. 54, pp.1333–1349.

Reynolds, P., Lawrence, C., 1993. Mechanisms of Deformation in the Fatigue of Polyethylene Pipe, Journal of Materials Science, vol. 28, pp. 2277-2282.

Rubeiz, C., 2004. Case Studies on the Use of HDPE Pipe for Municipal and Industrial Projects in North America. Pipeline Engineering and Construction, ASCE, pp. 1-10.

Rubeiz, C., 2009. Performance of Pipes during Earthquakes. Pipeline Conference 2009, pp. 1205-1215.

Schapery, R., 1975. A Theory of Crack Initiation and Growth in Viscoelastic Media. International Journal of Fracture, vol. 11, no. 1, pp. 141-159.

Scheirs, J., 2000. Compositional and Failure Analysis of Polymers: A practical approach, John Wiley & Sons, Ltd, Chichester, West Sussex, England.

Scheirs, J., Böhm, L., Boot, J., Leevers, P., 1996. PE100 Resins for Pipe Applications: Continuing the Development into the 21st Century, Trends in Polymer Science, vol. 4, no. 12, pp. 408-415.

Schijve, J., 2005. Statistical Distribution Functions and Fatigue of Structures. International Journal of Fatigue, vol. 27, pp. 1031–1039.

Sines, George, Waisman, S., 1959. Metal Fatigue, Chap. 12, Estimation of Fatigue Life with Particular Emphasis on Cumulative Damage, by Milton A. Miner, McGraw-Hill Book Company, New York.

Storm, T., Rasmussen, S., 2011. 100+ Years of Plastic. Leo Baekeland and Beyond, American Chemical Society, Printed by Oxford University Press, Inc., History of Polyethylene.

Strebel, J., Moet, A., 1992. Determining Fracture Toughness of Polyethylene from Fatigue, Journal of Materials Science, vol. 27, pp. 2981-2988.

Szpak, E., Rice, F., 1977. Strength of Polyethylene Piping - New Insights. Engineering Digest, Parts I and II.

Till, P., 1957. The Growth of Single Crystals of Linear Polyethylene, Journal of Polymer Science, vol. 24, no. 106, pp. 301-306.

Vibien, P., Chung, S., Fong, S., Oliphant, K., 2009. Long-Term Performance of Polyethylene Piping Materials in Potable Water Applications. Jana Laboratories Inc.

Vinson, H., 1981. Response of PVC Pipe to Large, Repetitive Pressure Surges. International Conference on Underground Plastic Pipe. New Orleans, LA: American Society of Civil Engineers.

Wallace, Floyd Associates Inc., 1984. Metropolitan District Commission Water Supply Study and Environmental Impact Report – 2020. Task 18.20: A History of the Development of the Metropolitan District Commission Water Supply System Submitted to Metropolitan District Commission.

Wang, M., Fei, Q., Zhang, P., 2016. A Modified Fatigue Damage Model for High-Cycle Fatigue Life Prediction, Advances in Materials Science and Engineering, vol. 2016, Article ID 2193684, doi:10.1155/2016/2193684.

Ward, A., Lu, X., Brown, N., 1990. Accelerated Test for Evaluating Slow Crack Growth of Polyethylene Copolymers in Igepal and Air, Journal of Polymer Engineering and Science, vol. 30, no. 18, pp. 1175–1179.

Ward, L., Lu, X., Huang, Y., Brown, N., 1991. The Mechanism of Slow Crack Growth in Polyethylene by an Environmental Stress Cracking Agent, Polymer, vol. 32, no. 12, pp. 2172-2178.

Ward, M., 1971. Mechanical Properties of Solid Polymers, Wiley-Interscience, Toronto.

Wetzel, B., Rosso, P., Haupert, F., Friedrich, K., 2006. Epoxy Nano-composites – Fracture and Toughening Mechanisms. Journal of Engineering Fracture Mechanics 2006; vol. 73, no. 16, pp. 2375–98.

Xiao, Y., Li, S., Gao, Z., 1998. A Continuum Damage Mechanics Model for High Cycle Fatigue, International Journal of Fatigue, vol. 20, no. 7, pp. 503–508.

Yau, J., Wang, S., Corten, H., 1980. A Mixed-mode Crack Analysis of Isotropic Solids Using Conservation Laws of Elasticity, ASME Journal of Applied Mechanics, vol. 47, pp. 335-341.

Zhang, C., Moore, I., 1997. Nonlinear Mechanical Response of High Density Polyethylene. Part II: Uniaxial Constitutive Modeling, Journal of Polymer Engineering and Science, vol. 37, pp. 414–420.

Zhang, X., Jia, C., 2005. The Microstructural Characteristics of the Deformed Nanocrystalline Cobalt, Journal of Material Science and Engineering, pp. 418:77–80.

Zheng, L., Zhu, H., Kong, X., Seibi, A., 2012. Combined Effect of Temperature and Soil Load on Buried HDPE Pipe. Advanced Materials Research, vol. 452-453, pp. 1169-1173.

Zhou, Y., Brown, N., 1992. The Mechanism of Fatigue Failure in a Polyethylene Copolymer, Journal of Polymer Science, vol. 30, pp. 477-487.

Zhou, Y., Lu, X., Zhou, Z., Brown, N., 1996. The Relative Influence of Molecular Structure on Brittle Fracture by Fatigue and under Constant Loads in Polyethylene, Journal of Polymer Engineering and Science, vol. 36, no. 16, pp. 2101–2107.

Biographical Information

Marjan Shahrokh Esfahani graduated with a Bachelor of Science in Civil Engineering from University of Science and Culture, Tehran, IRAN, in 2007. After graduation she moved to Stockholm, SWEDEN, in 2009, to complete her Master's degree in Infrastructure Engineering at the Royal Institute of Technology. Then she moved to the US and started her Ph.D. program in Civil Engineering at the University of Texas at Arlington (UTA) in 2012. During her time in UTA, Marjan worked as Teaching Assistant (TA) for several courses such as Structural Analysis, Concrete design and Statics. Also, she worked as a Graduate Research Assistant (GRA) in several projects, such as "Evaluation of a New PVC Pipe" and "Evaluation of the Performance of Synthetic Fiber Concrete Hollow Columns." She foresees a bright and successful future in the construction industry, especially in the pipeline and infrastructure area.